Vetenskapsrådet

Swedish Foundation for Strategic Research

Materials Platform

European Commission

NordForsk

Carl Tryggers Stiftelse för Vetenskaplig Forskning

Energy & Quantum Materials

Sustainable Materials Research & Technologies — SMaRT

SwedNess

Prof. Martin Månsson

Director of Studies - SwedNess

Division of Materials & Nano Physics
Department of Applied Physics
KTH Royal Institute of Technology
Stockholm, Sweden

Research

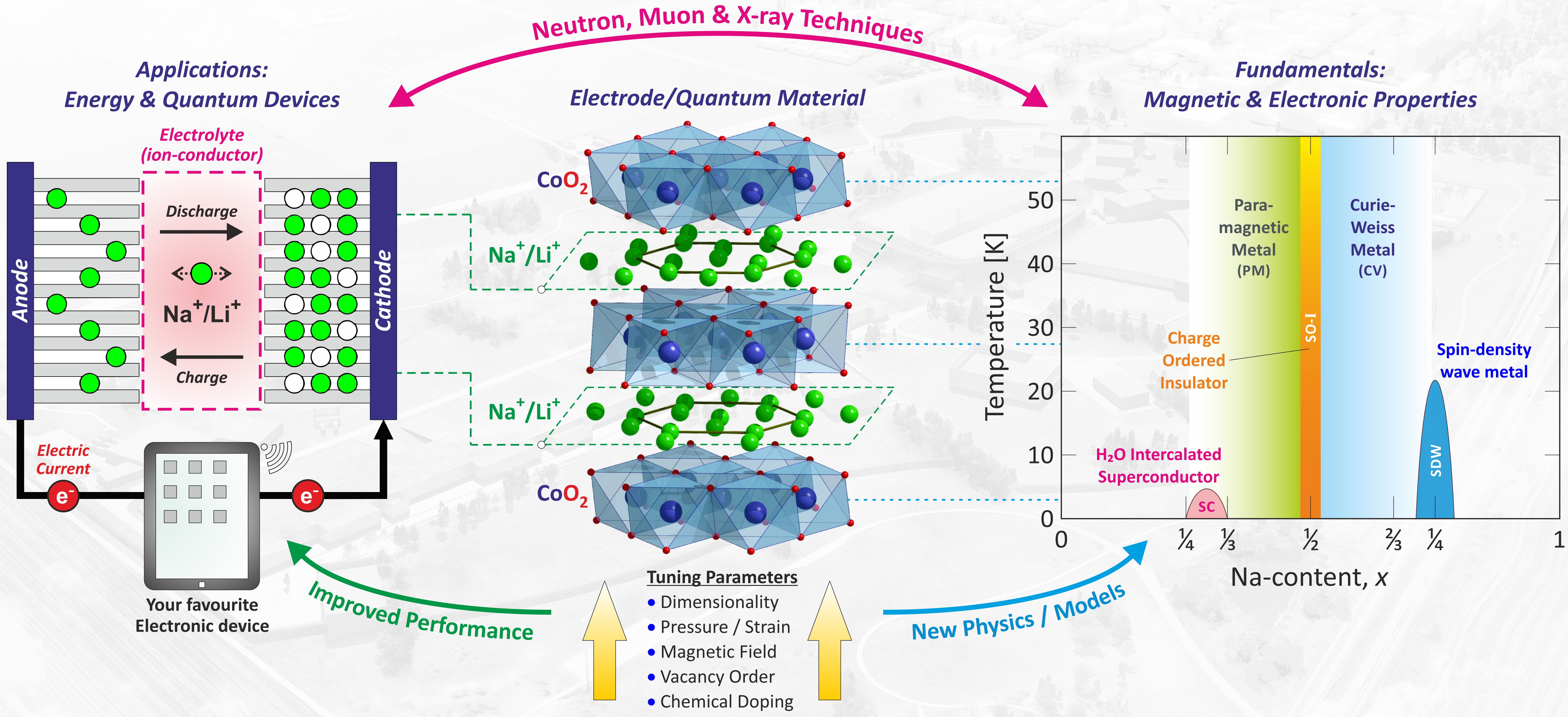

As. Professor Martin Månsson - KTH Royal Institute of Technology - condmat@kth.se

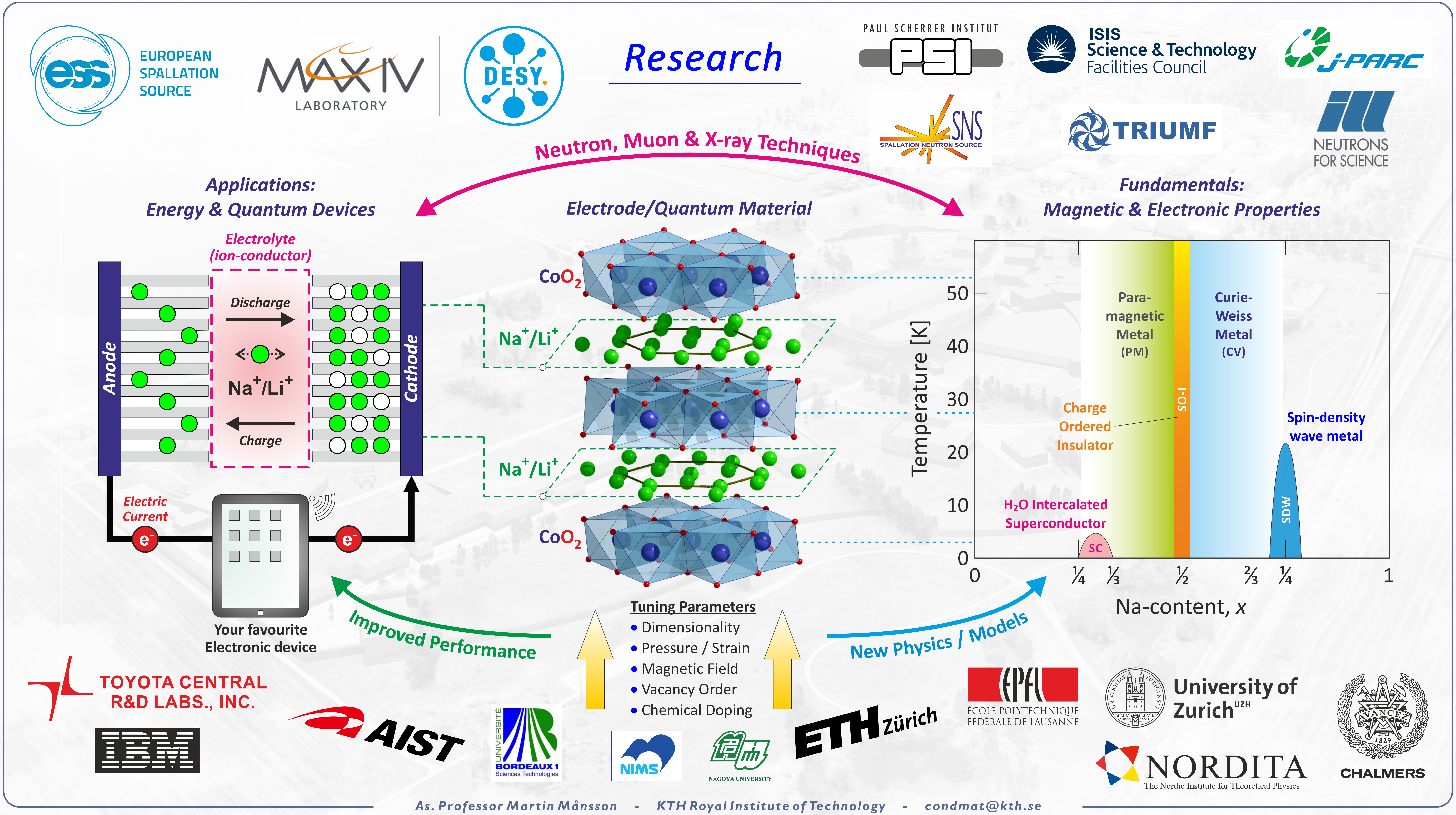

EUROPEAN SPALLATION SOURCE
MAX IV LABORATORY
DESY.
Research
PAUL SCHERRER INSTITUT PSI
ISIS Science & Technology Facilities Council
J-PARC
SNS SPALLATION NEUTRON SOURCE
TRIUMF
NEUTRONS FOR SCIENCE
Neutron, Muon & X-ray Techniques
Applications:
Energy & Quantum Devices
Electrode/Quantum Material
Fundamentals:
Magnetic & Electronic Properties
Electrolyte (ion-conductor)
Discharge
Na+/Li+
Charge
Anode
Cathode
Electric Current
e-
e-
Your favourite Electronic device
CoO2
Na+/Li+
Na+/Li+
CoO2
Temperature [K]
50
40
30
20
10
0
Para-magnetic Metal (PM)
Curie-Weiss Metal (CV)
CO-I
Charge Ordered Insulator
Spin-density wave metal
H2O Intercalated Superconductor
SC
SDW
0
¼
⅓
½
⅔
¾
1
Na-content, x
Improved Performance
Tuning Parameters
Dimensionality
Pressure / Strain
Magnetic Field
Vacancy Order
Chemical Doping
New Physics / Models
TOYOTA CENTRAL R&D LABS., INC.
IBM
AIST
UNIVERSITÉ BORDEAUX 1 Sciences Technologies
NIMS
NAGOYA UNIVERSITY
ETH Zürich
EPFL ÉCOLE POLYTECHNIQUE FÉDÉRALE DE LAUSANNE
University of Zurich UZH
NORDITA The Nordic Institute for Theoretical Physics
CHALMERS
As. Professor Martin Månsson - KTH Royal Institute of Technology - condmat@kth.se

Introduction to
Muon Spin Rotation/Relaxation (μ^+SR)

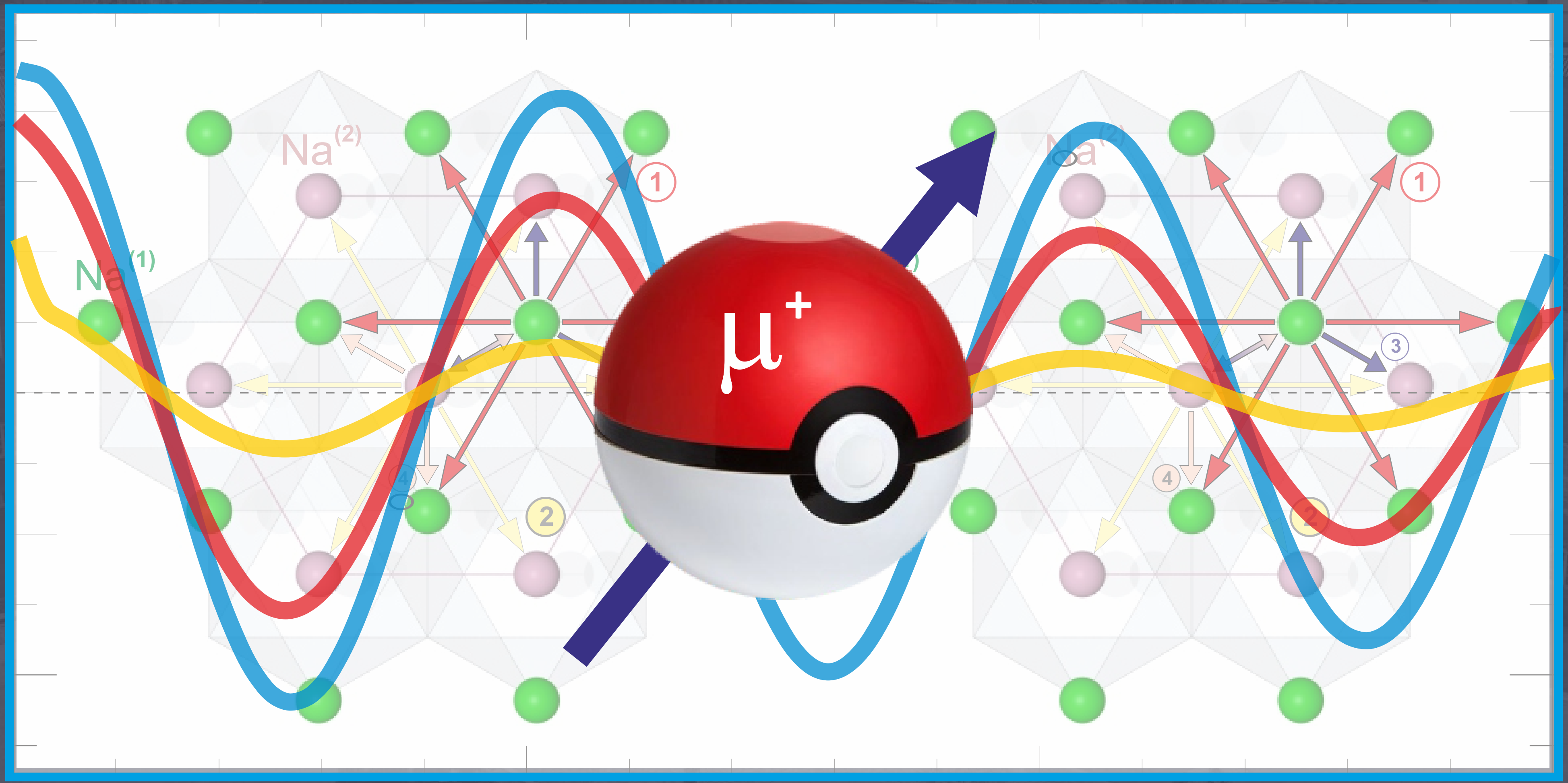

Prof. Martin Månsson

Department of Applied Physics
KTH Royal Institute of Technology
Stockholm, Sweden

What is a Muon?

What is a Muon?

μ

What is a Muon?

μ

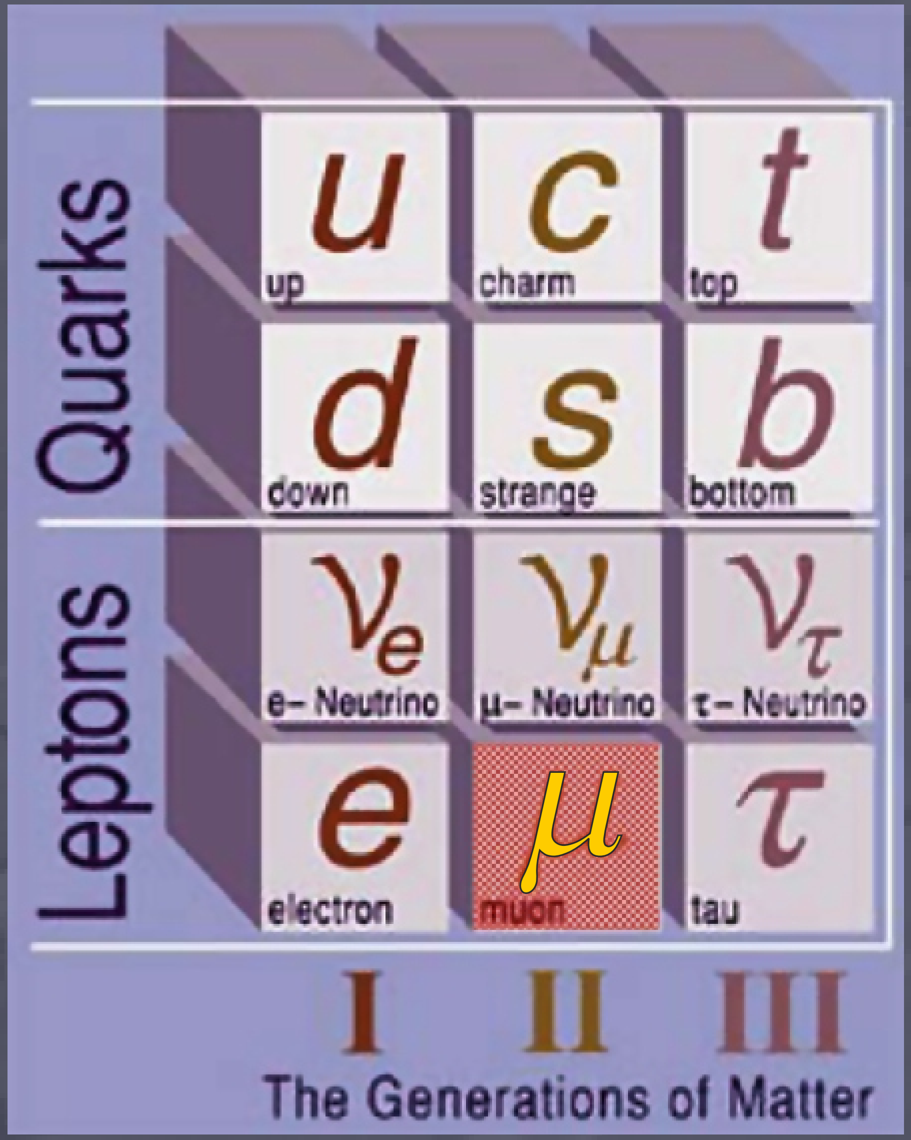

Muon Properties

mass	200 x e- (105.6 MeV/c^2) 1/9 x p+
charge	e- or e+ (μ^- or μ^+)
spin	1/2
lifetime	2.2 μs (half life)
Magn. Moment	3.18 x μ_{proton}
gyromagnetic ratio	$\gamma/2\pi$ = 135.5 MHz/T

Magn. Moment

Angular Momentum

$$\mu = \gamma J$$

What is a Muon?

μSR
- **μ**: muon
- **S**: spin
- **R**: otation / elaxation / esonance

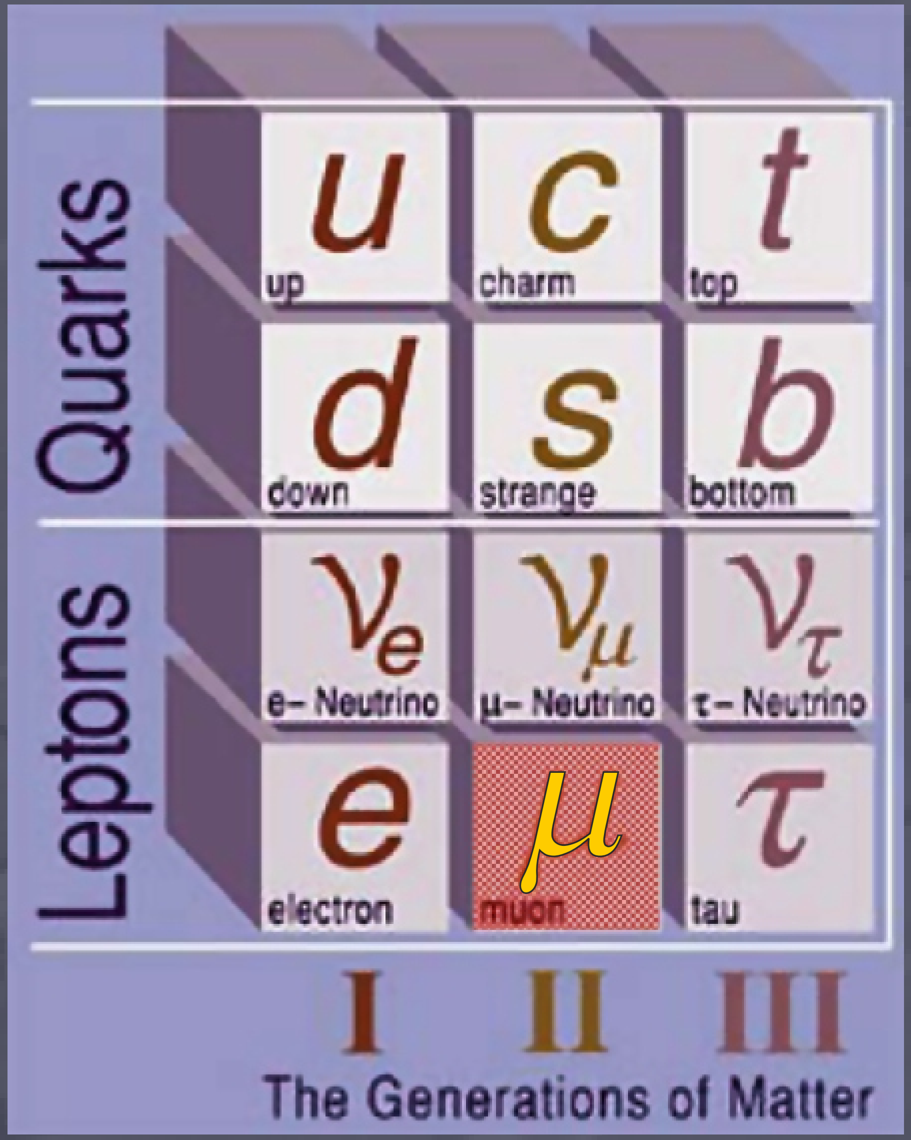

Muon Properties

mass	200 x e- (105.6 MeV/c^2) 1/9 x p+
charge	e- or e+ (μ^- or μ^+)
spin	1/2
lifetime	2.2 μs (half life)
Magn. Moment	3.18 x μ_{proton}
gyromagnetic ratio	$\gamma/2\pi$ = 135.5 MHz/T

μ

Magn. Moment → $\mu = \gamma J$ ← Angular Momentum

→ **Spin-precession frequency (Larmor)**

Cosmic Muons - “Space Particles & Pyramids”

- μ discovered 1936 by Anderson & Neddermeyer who studied cosmic radiations

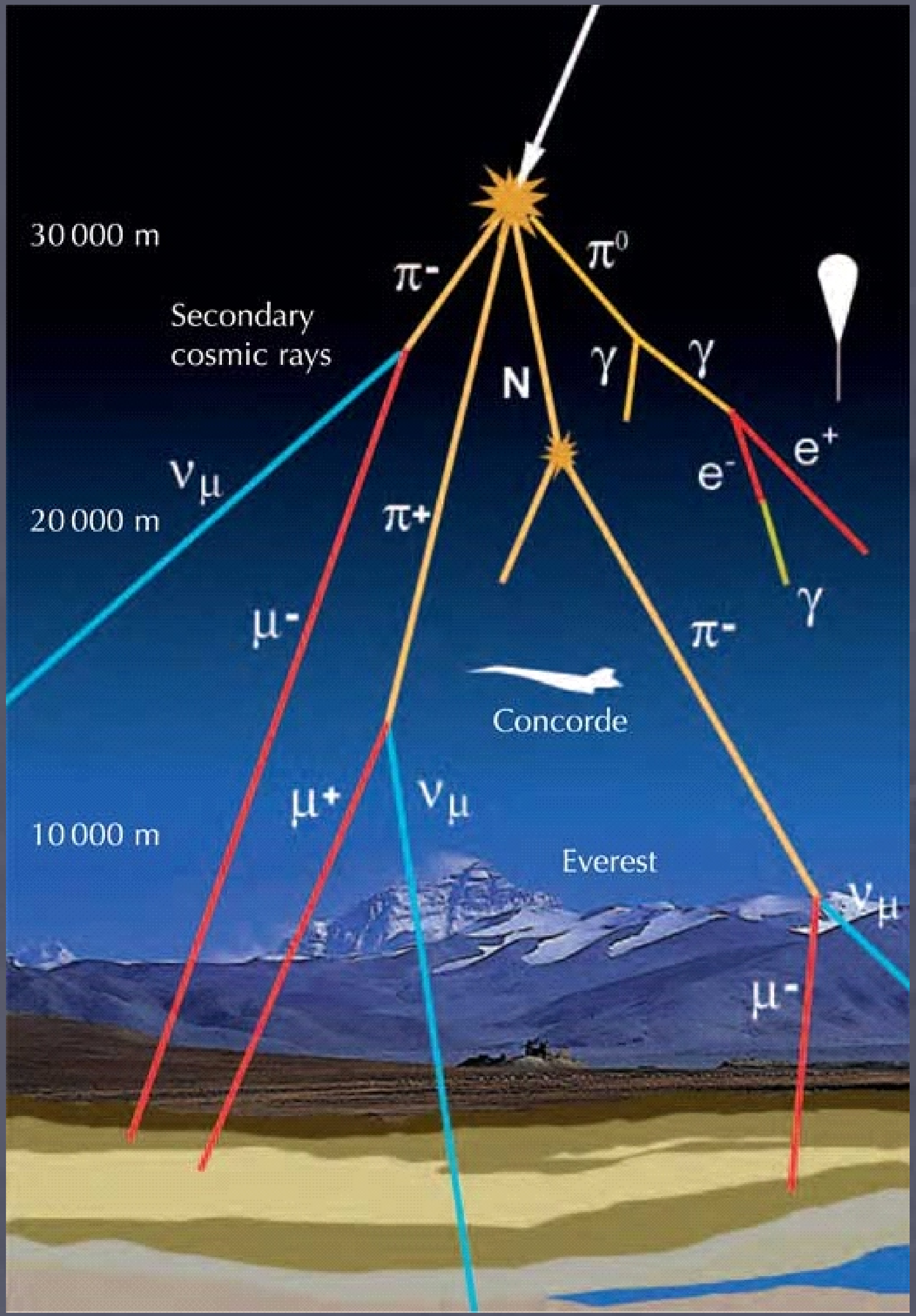


Khufu’s Pyramid (Cheops)

Cosmic Muons - "Space Particles & Pyramids"

- μ discovered 1936 by Anderson & Neddermeyer who studied cosmic radiations

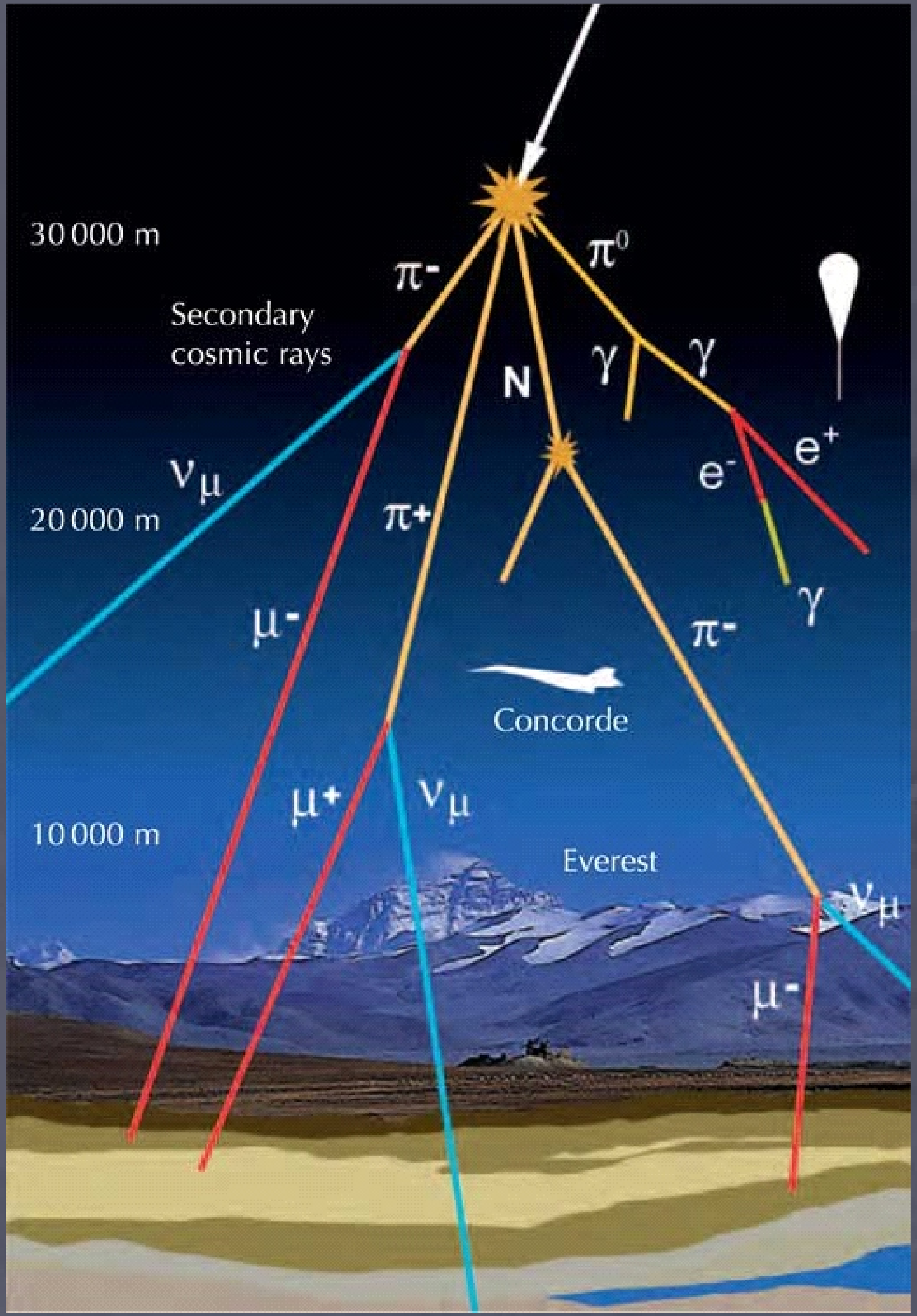

μ μ μ μ μ

Muon Detector

Cosmic Muons - "Space Particles & Pyramids"

Morishima, *et al.* Nature 552 386 (2017)

- μ discovered 1936 by Anderson & Neddermeyer who studied cosmic radiations

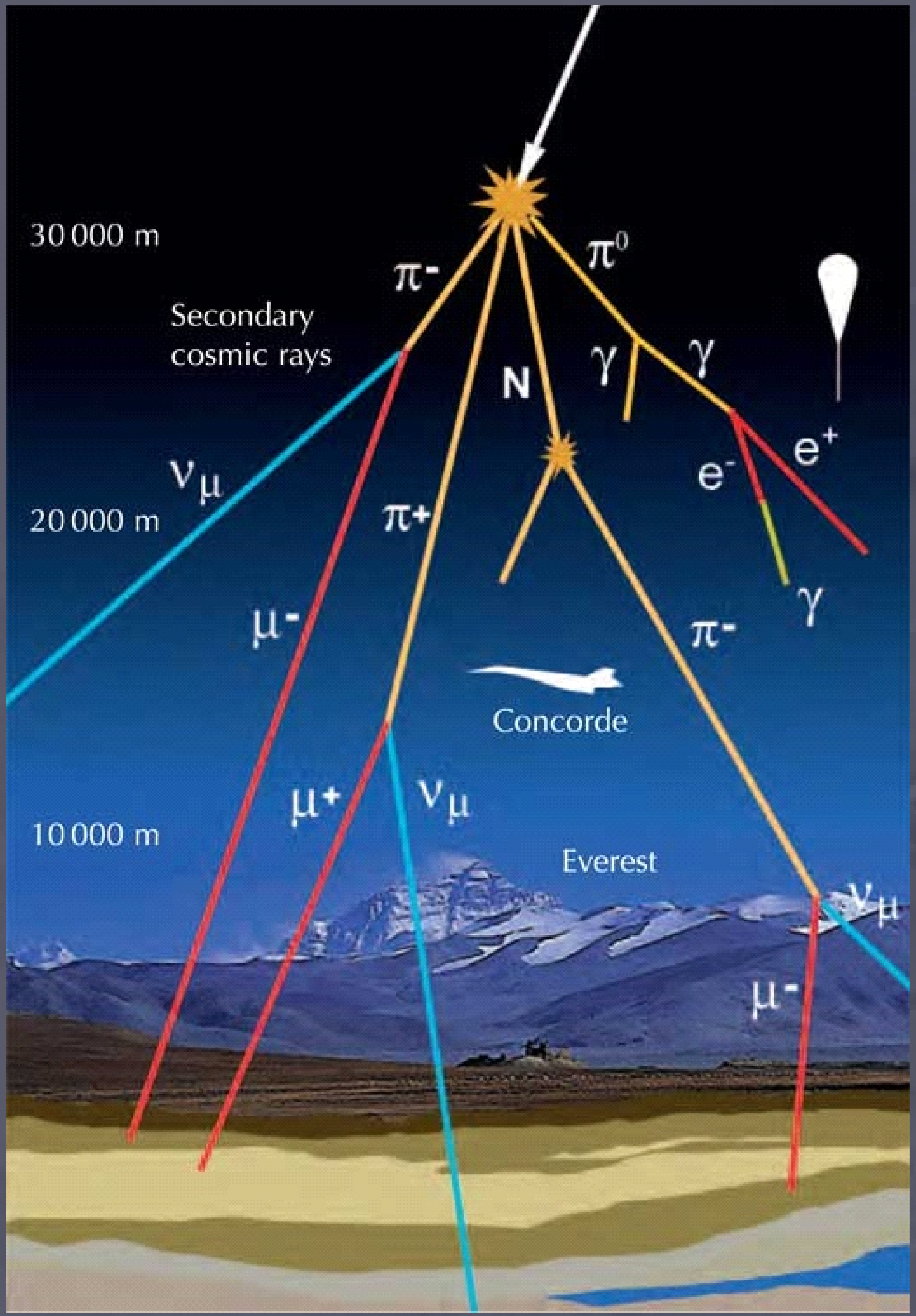

μ μ μ μ μ

Imaging / Tomography

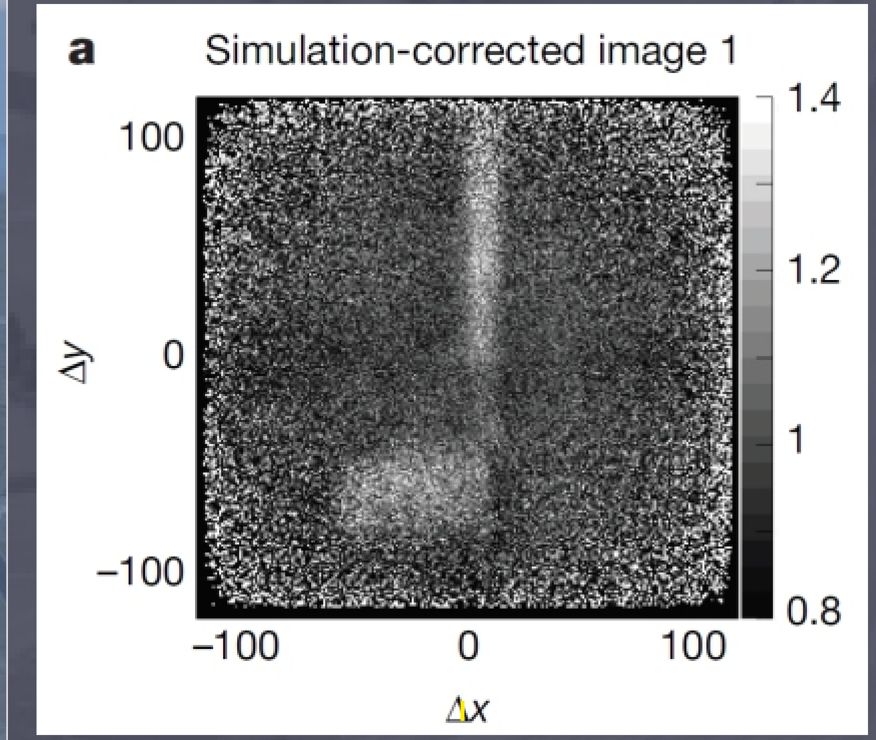

Muon Detector

Neutrons vs. Muons

n^o

μ^+

Neutrons vs. Muons

n^o

μ^+

Neutrons vs. Muons

n^o

- Mass ~ 1 u
- Charge = 0
- *S* = 1/2
- Life-time ~ 800 s
- γ = 29.16 MHz/T
- "Long-range"

μ^+

- Mass ~ 1/9 u
- Charge = +/-
- *S* = 1/2
- Life-time ~ 2.2 μs
- γ = 135.54 MHz/T
- "Local / short-range"

Muon Production

High-energy proton (500 eV)

Production Target (Carbon Nuclei)

Neutrino (ν_μ)

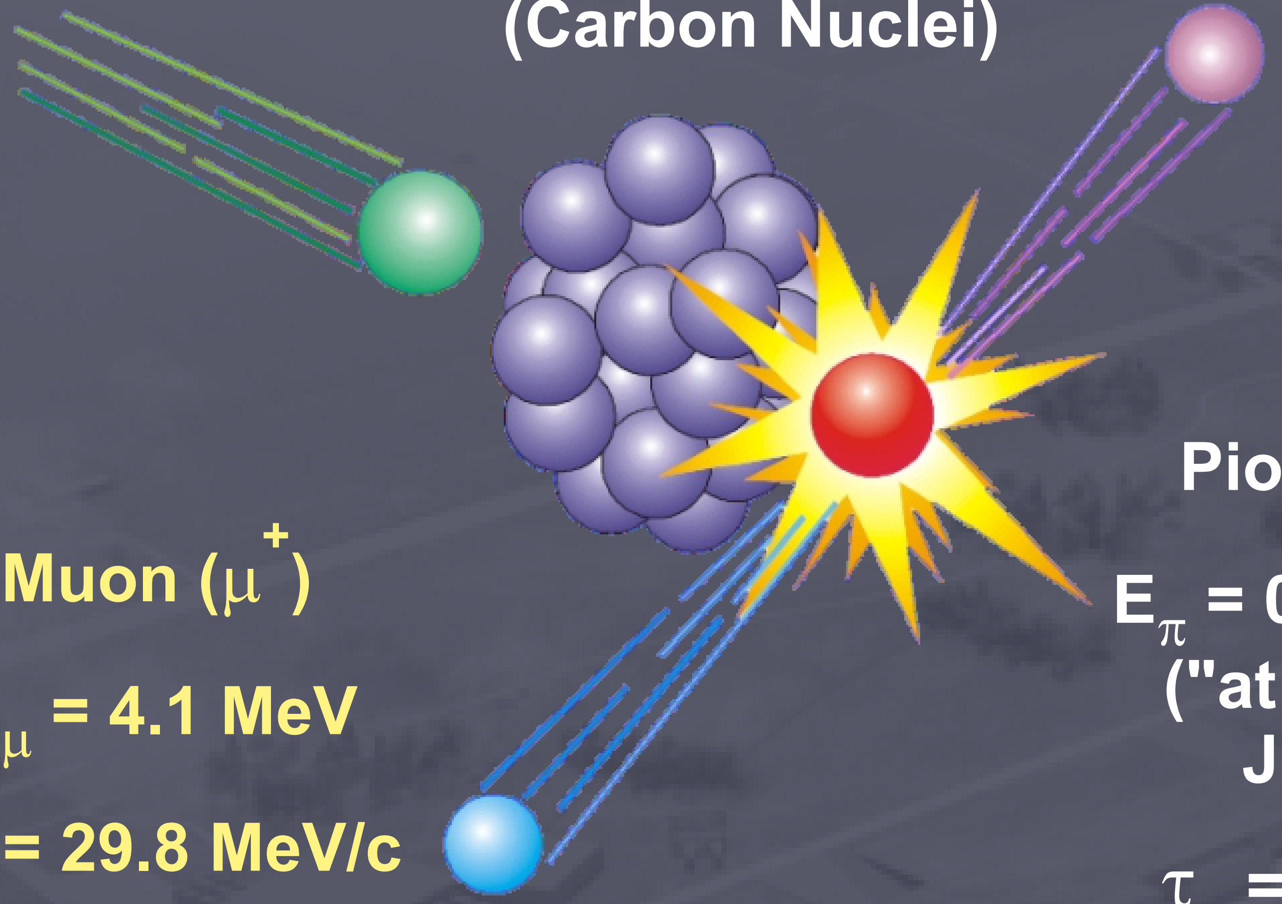

Muon (μ^+)

E_μ = 4.1 MeV

p_μ = 29.8 MeV/c

τ_μ = 2.2 μs

Pion (π^+)

E_π = 0, p_π = 0
("at rest")
J = 0

τ_π = 26 ns

- **Parity violation** (weak interaction decay) gives only left-handed neutrinos $\Rightarrow$

Muons are 'born' 100% spin polarized with their spin (s_μ) & momenta (p_μ) opposite.

Pion initially at rest

Conservation of linear and angular momentum

Muon and Neutrino are emitted with equal and opposite momenta (p) and also equal and opposite spin !!!

ESSENTIAL for µSR

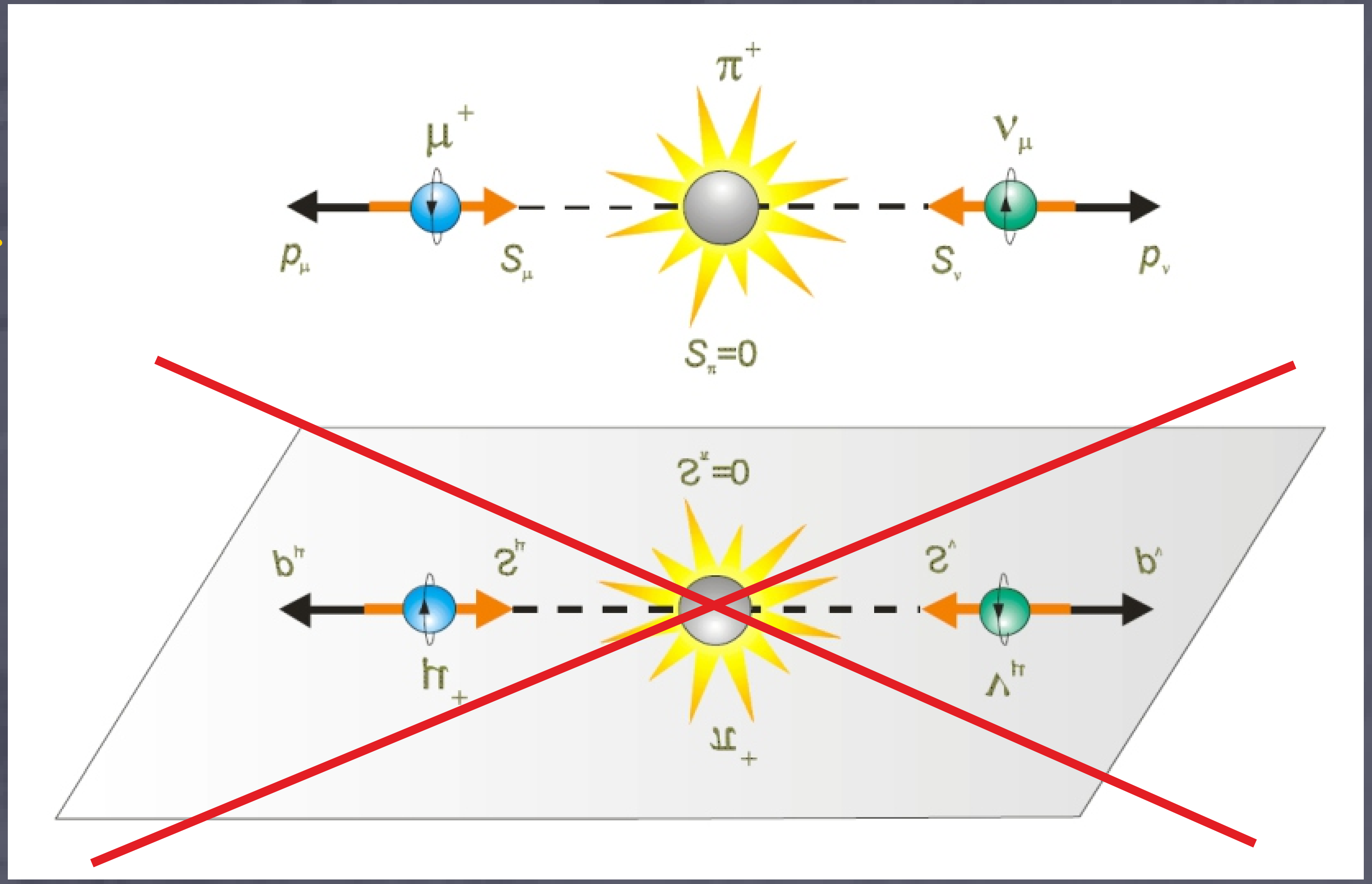

Muon Decay (death of the muon)

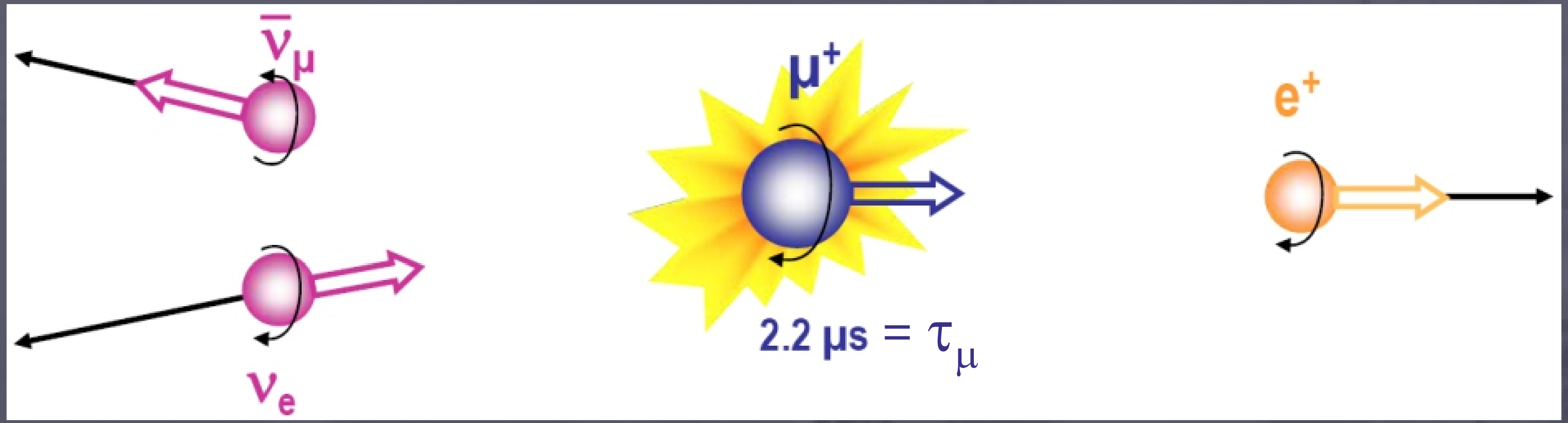

- The Muons decay into neutrino/antineutrino and a **positron** by exponential decay:
  $N(t) = B + N_0 \exp(t/\tau_\mu)$ with half-life $\tau_\mu = 2.2\ \mu s$

- **Parity violation**: the positron is emitted anisotropically and with a maximum probability in the direction of the muon spin. The angular distribution of emitted positrons:

$$W(E,\theta) \sim 1 + a(E) * \cos\theta$$

When all positron energies are sampled with equal probability ("real life") **a = 1/3** i.e. it is **twice as probable** that the positron is along as opposite the **muon spin direction**.

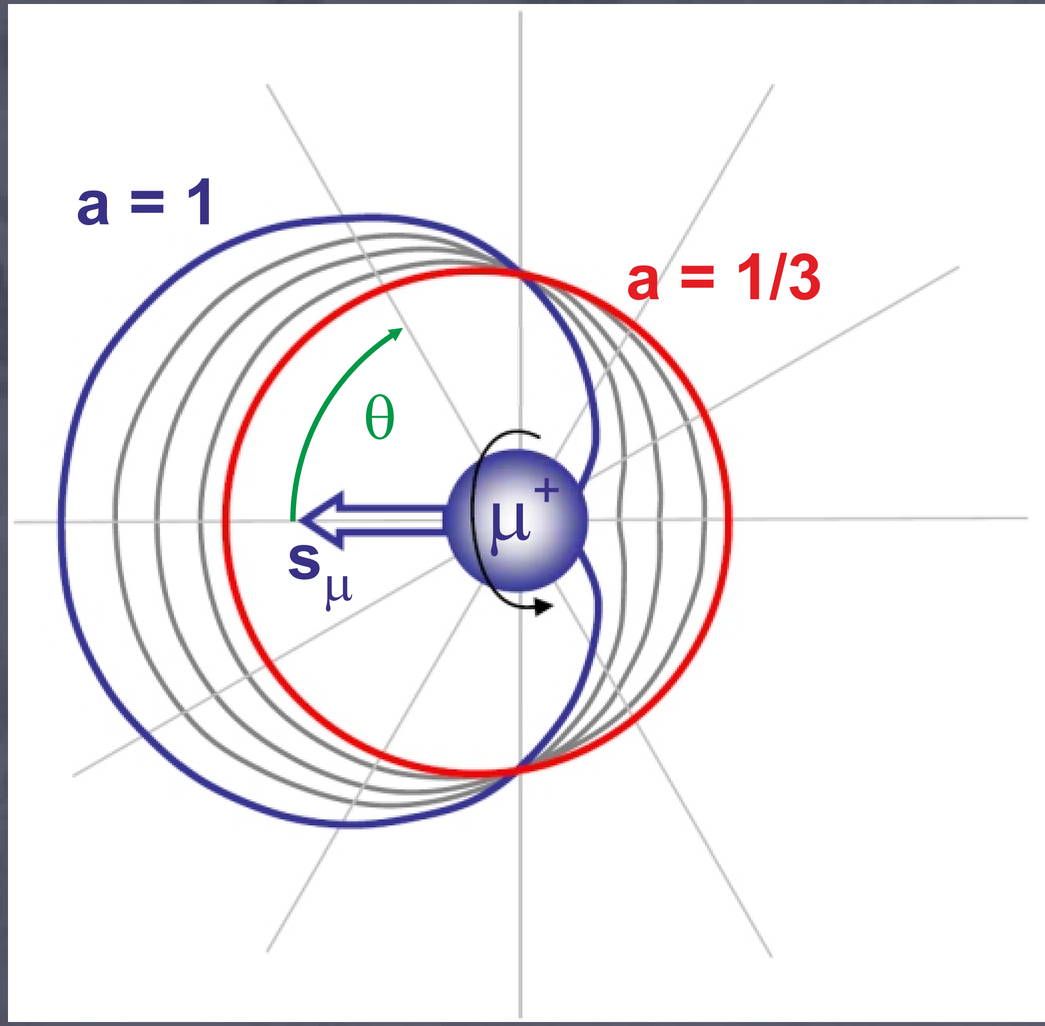

The spatial (asymmetric) positron emission as a function of time, "directly gives you the time evolution of the muon spin direction !!!

The μ^+SR Experiment

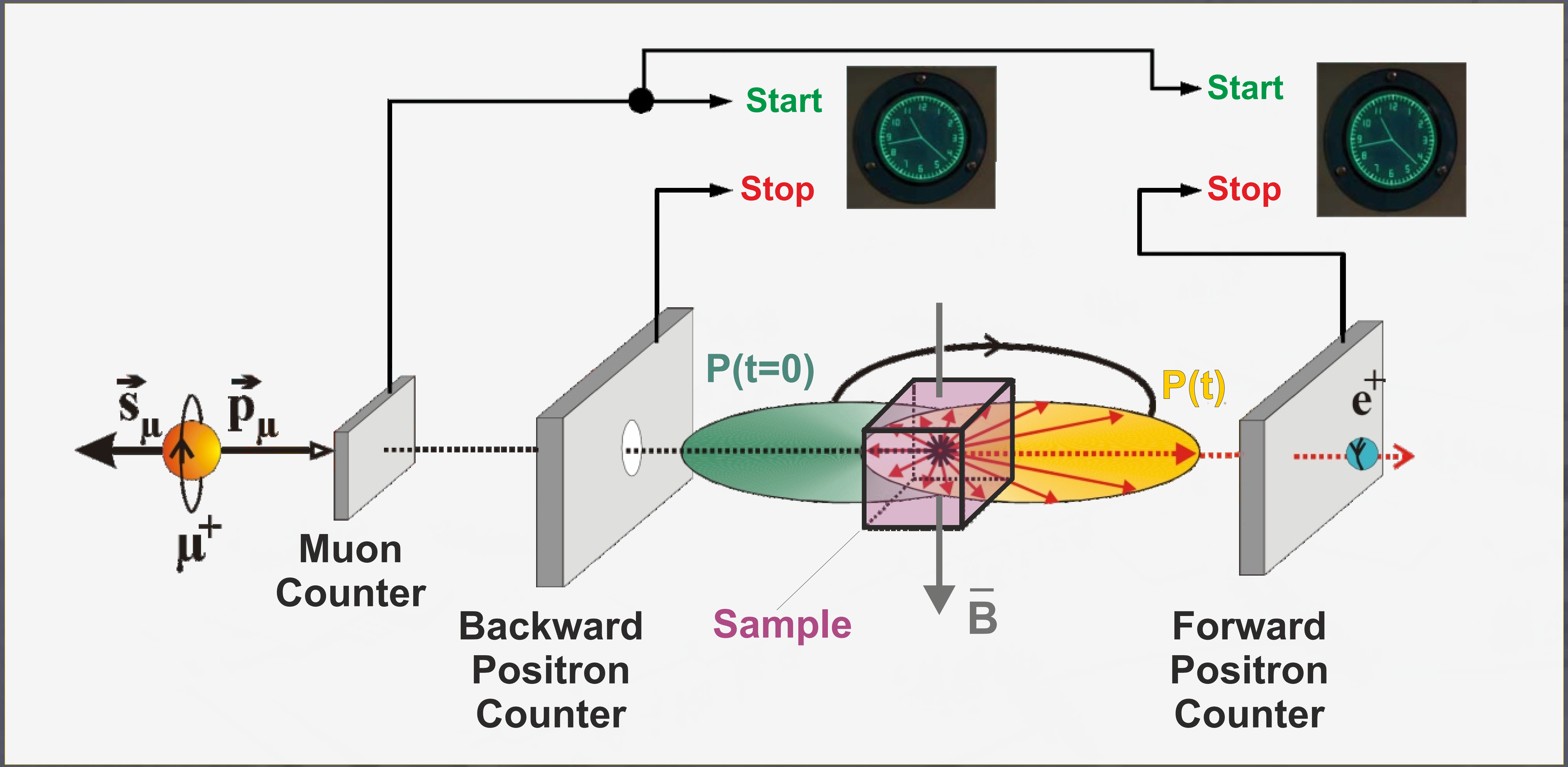

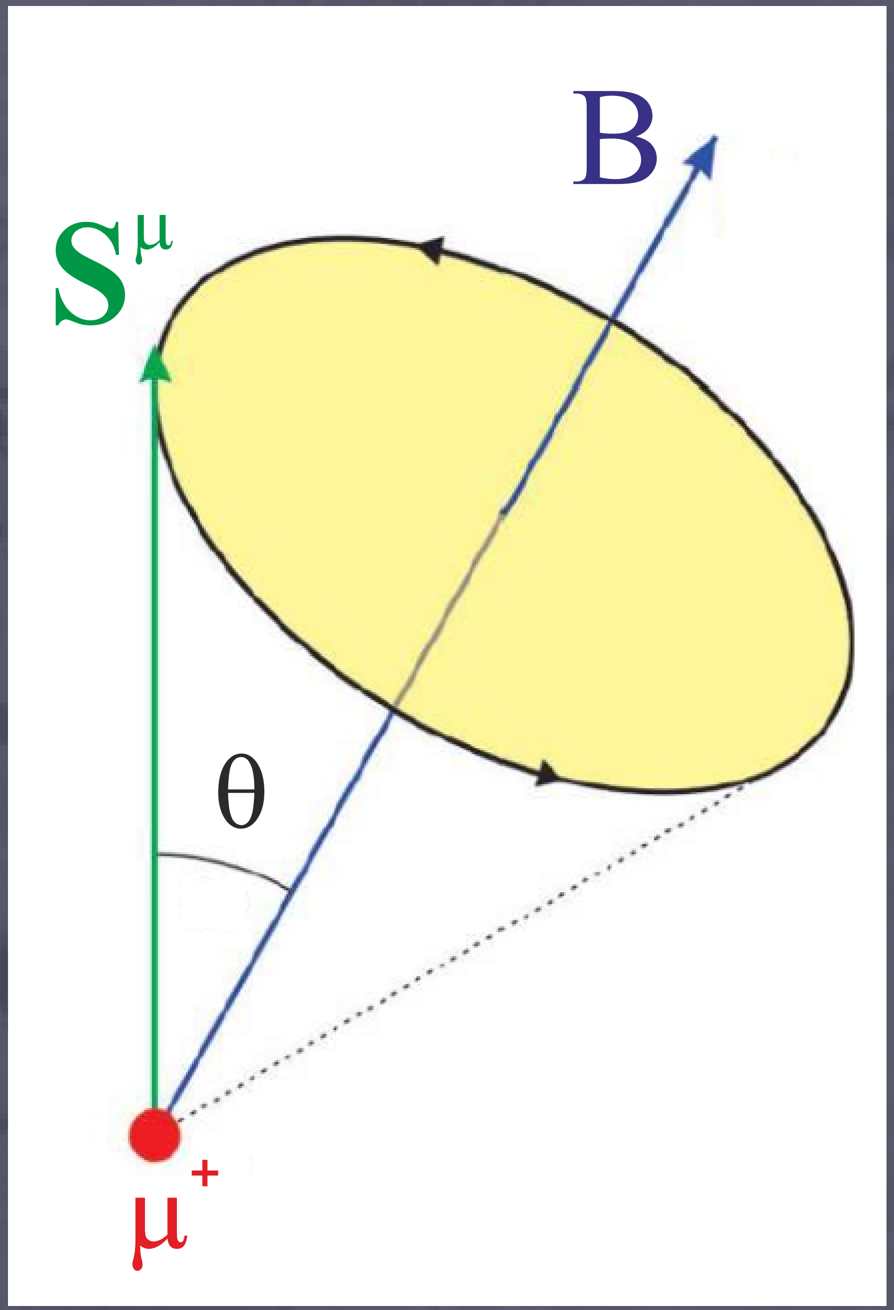

Any magnetic field (B) not parallel to S_μ gives muon (Larmor) precession with a frequency:

$$\omega = \gamma_\mu \cdot B$$

giving the magnetic field (B). Data analyzed in time domain (Asymmetry) or by Fourier Transform.

Forward / Backward Asymmetry Plot (= μSR data or time-spectrum)

If muons are implanted in an "inert" material (no magnetic moments) the polarization of the muon is unaffected. Hence, the positron is ~twice as probable to be ejected and detected in the "Backward" positron detector as in the "Forward". We only see the unaffected exponential muon decay with τ_μ = 2.2 μs.

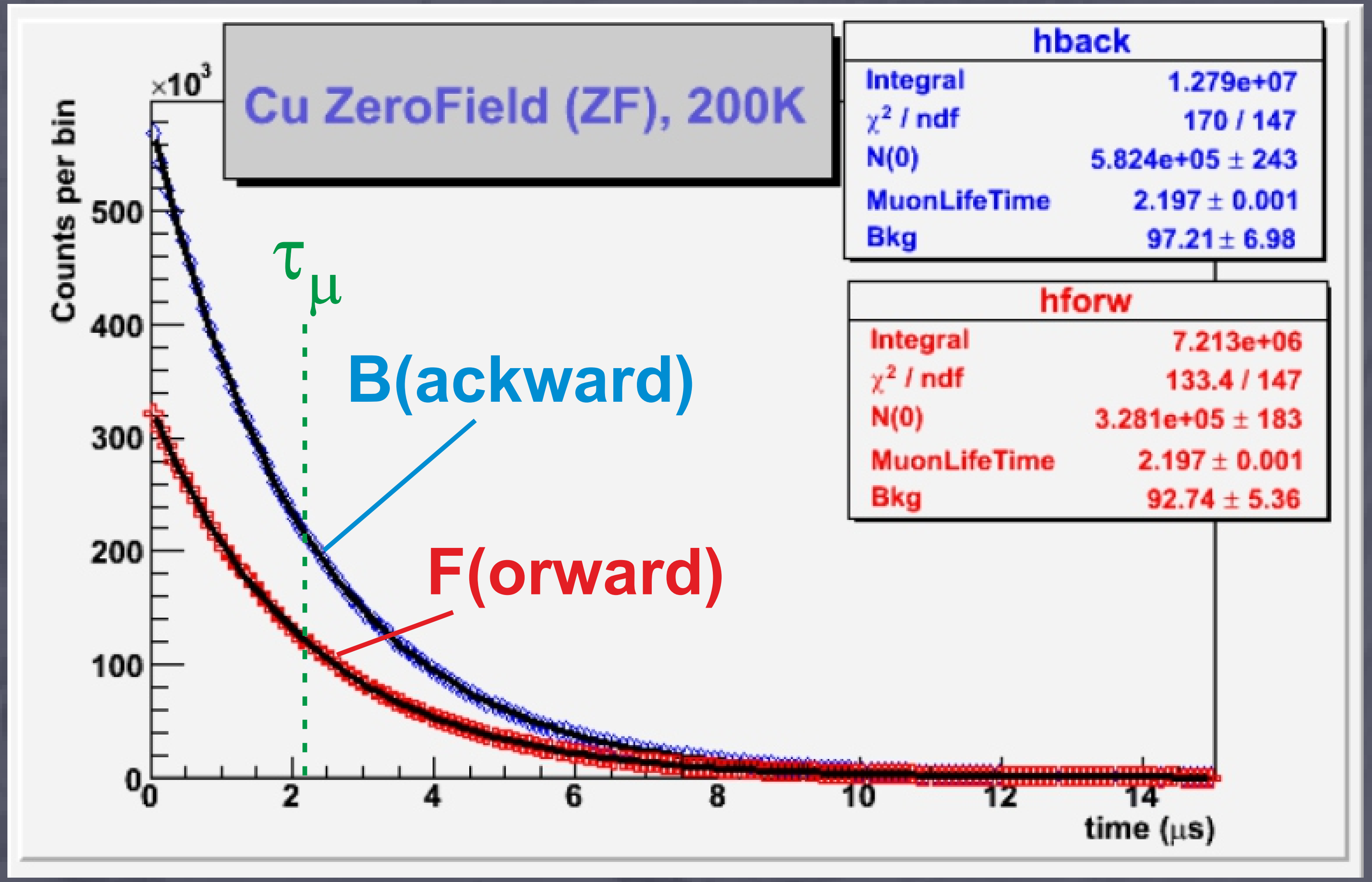

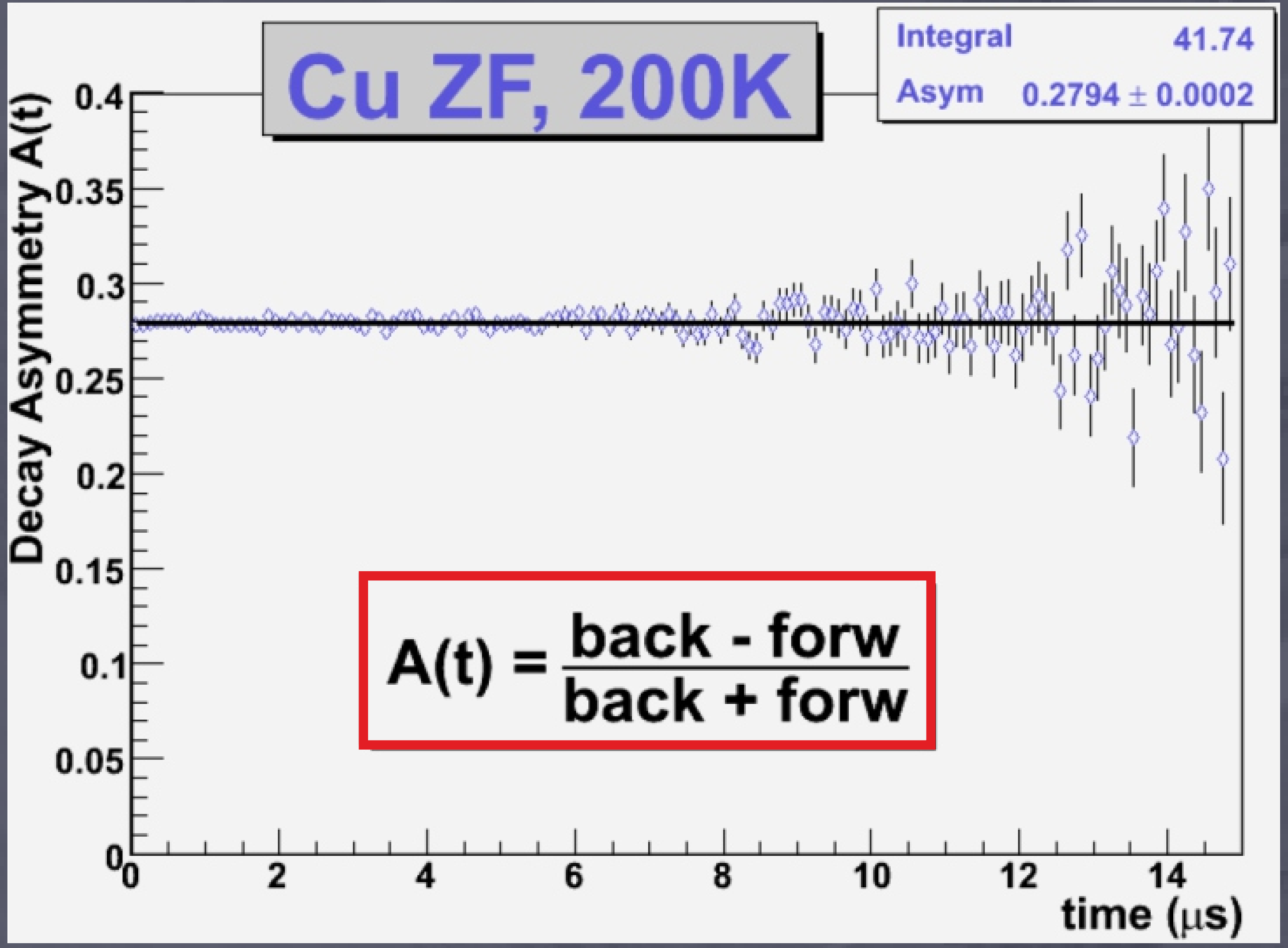

In most practical cases the data from a μSR experiment is displayed as the normalized asymmetry A(t) between Forward and Backward positron counters. Here we see time-independent A(t) close to (small polarization loss in beamline) the theorethical value of 1/3.

Rotating the Muon Spin

Internal or external field (not // to S_μ)

⇓

Precession of the muon spin

⇓

Probability for Backward or forward positron emission is changing with time (Asym. always biggest at t = 0)

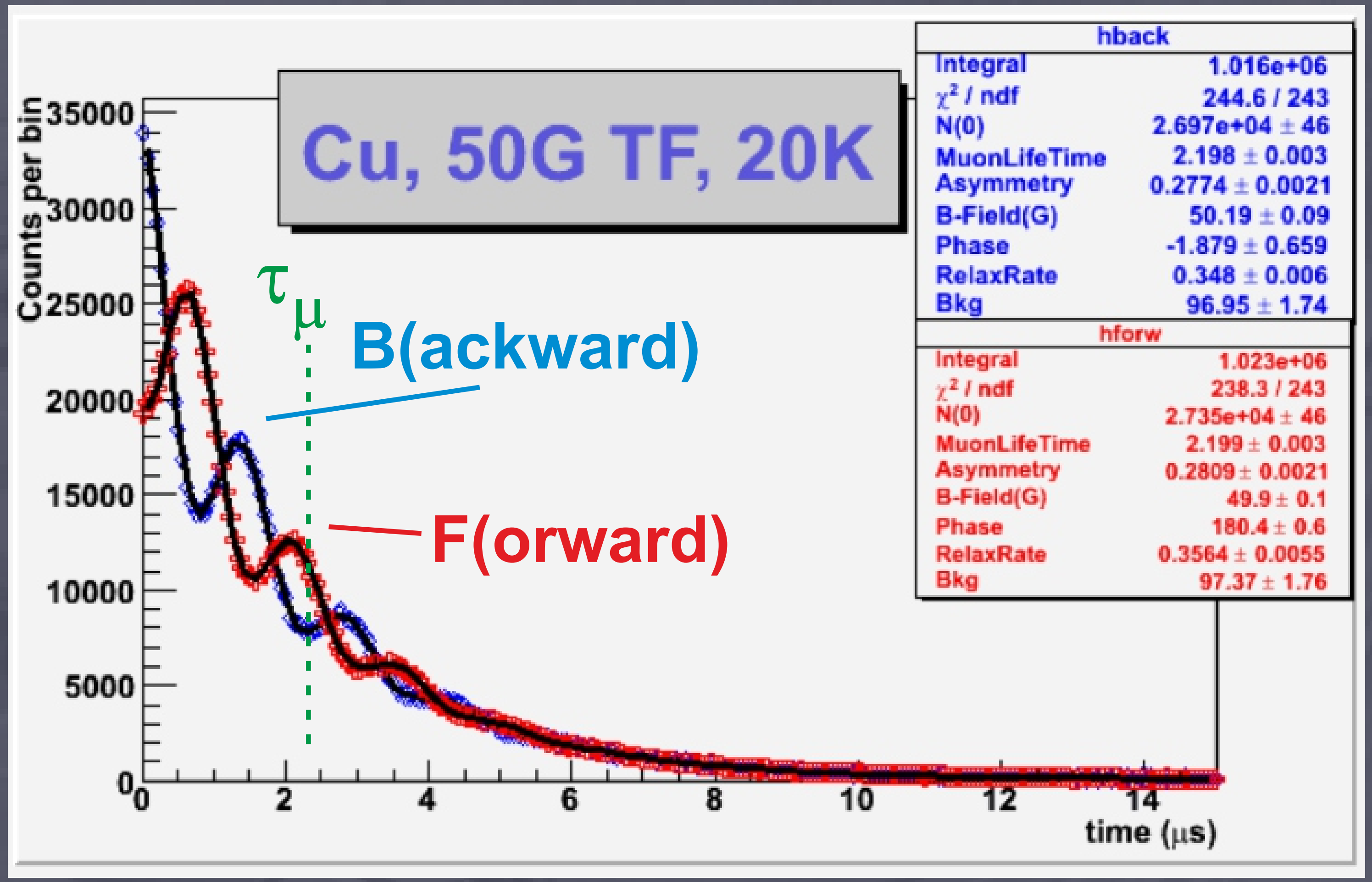

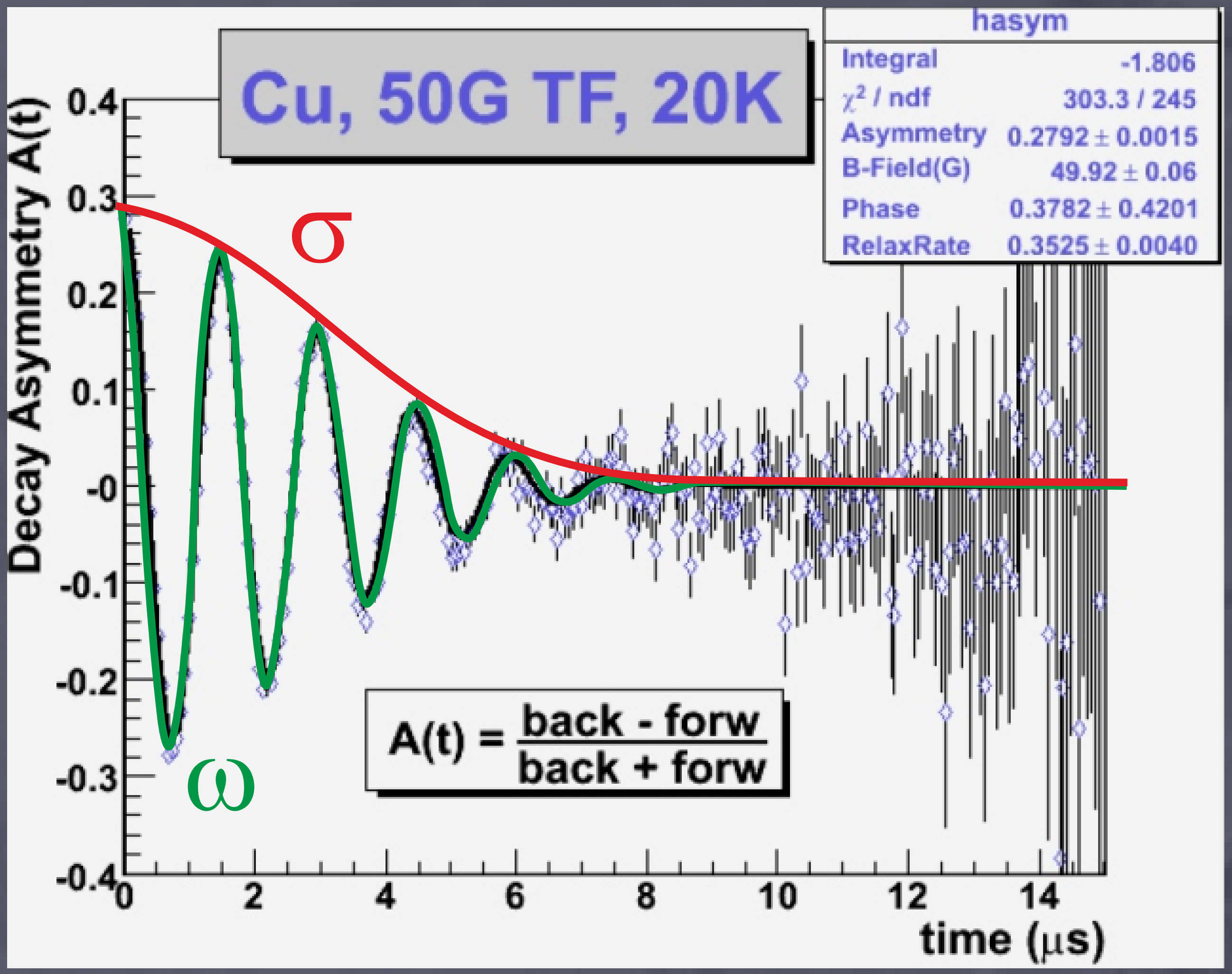

$$A(t) = A_0 \cdot \exp(\sigma^2 t^2 / 2) \cdot \cos(\omega t + \phi)$$

Frequency: $\omega = \gamma_\mu \cdot B$ gives the magnetic field (B)

Relaxation rate: $\sigma^2 = \gamma_\mu^2 \cdot \langle \Delta B^2 \rangle$ → field-distribution width (ΔB)

Gaussian: random dipoles (nuclear m.)
Lorentzian: dilute dipoles (spin glass)

Fourier / FFT

Time

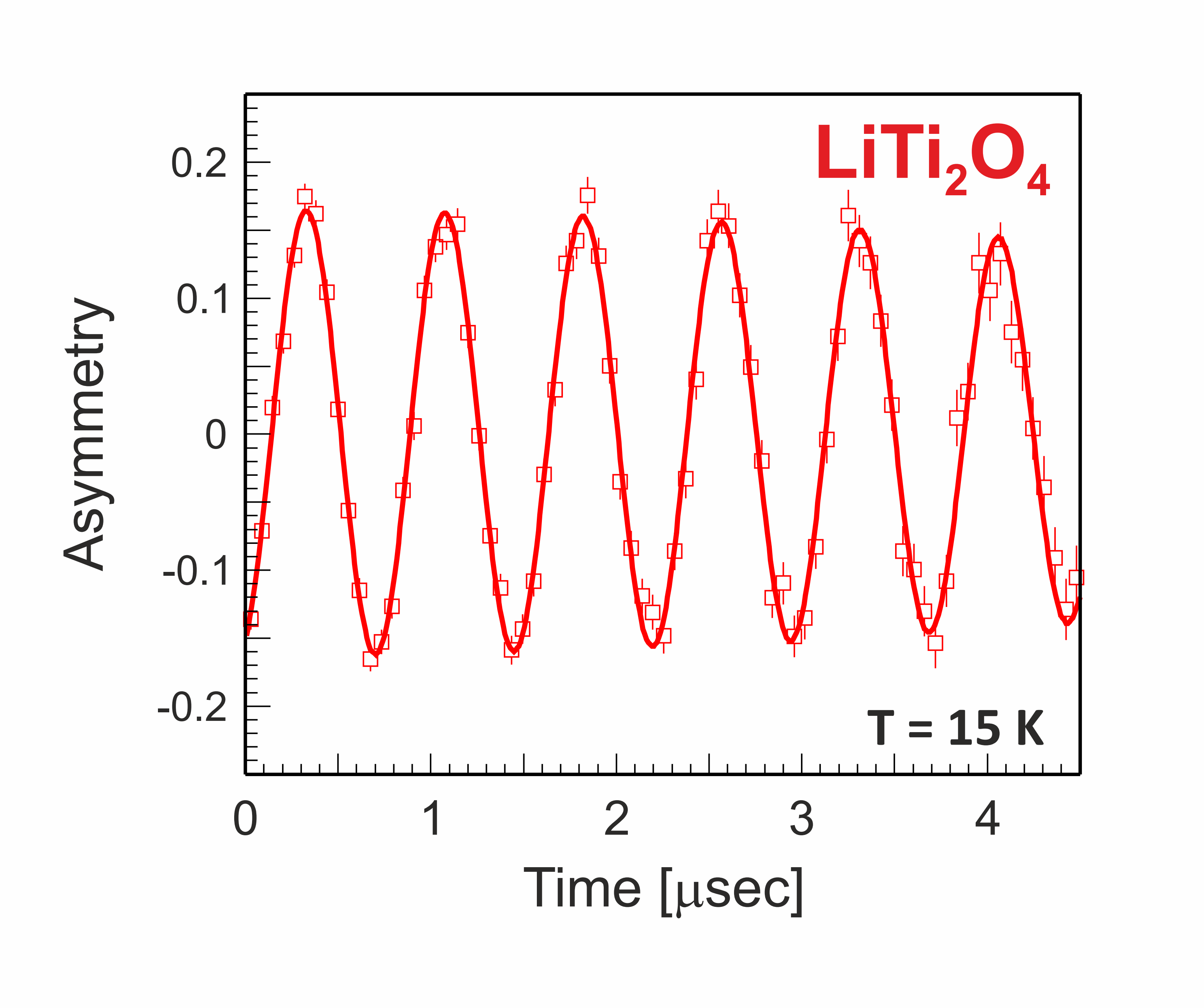

FFT

Frequency

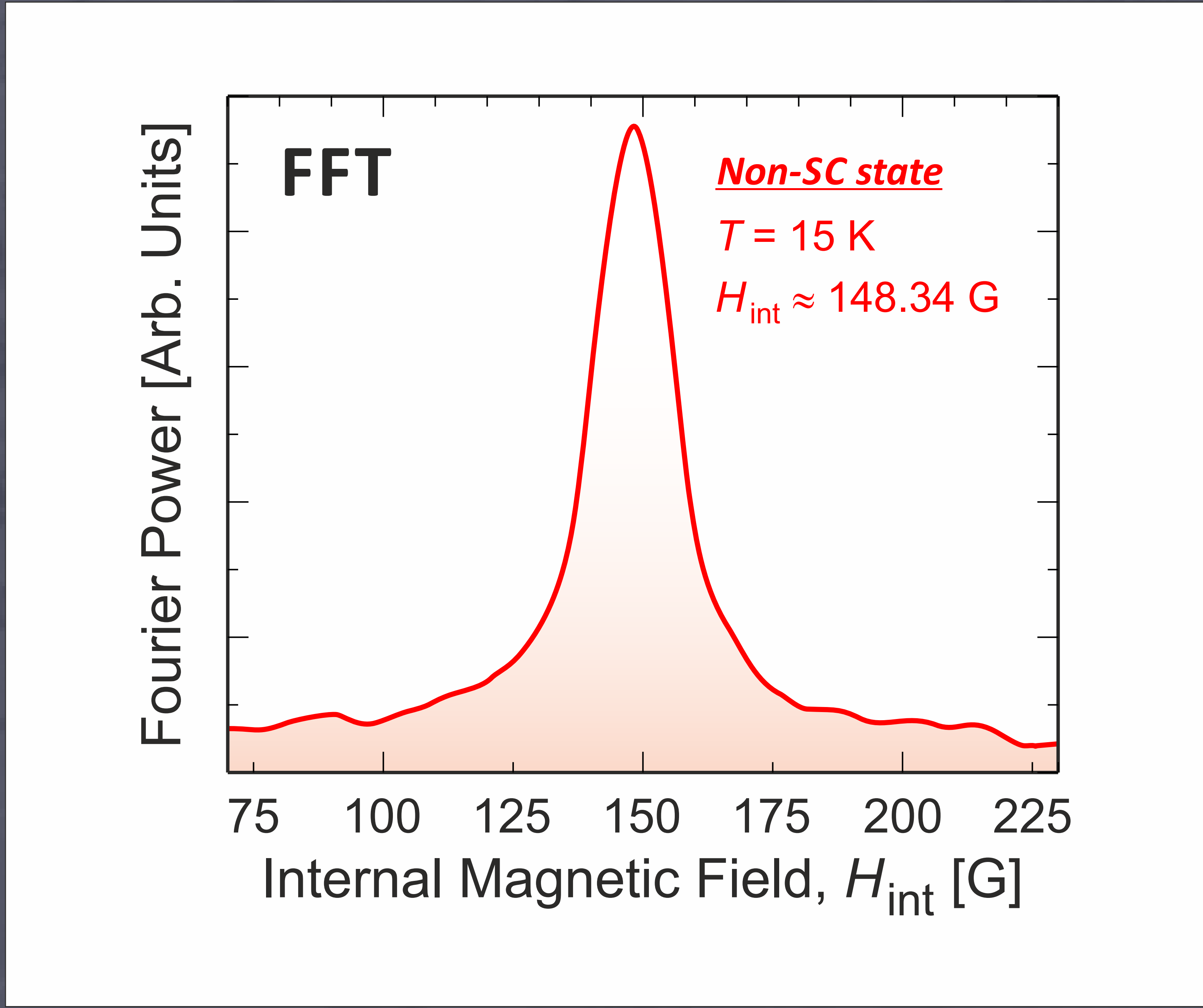

Fourier / FFT

Time

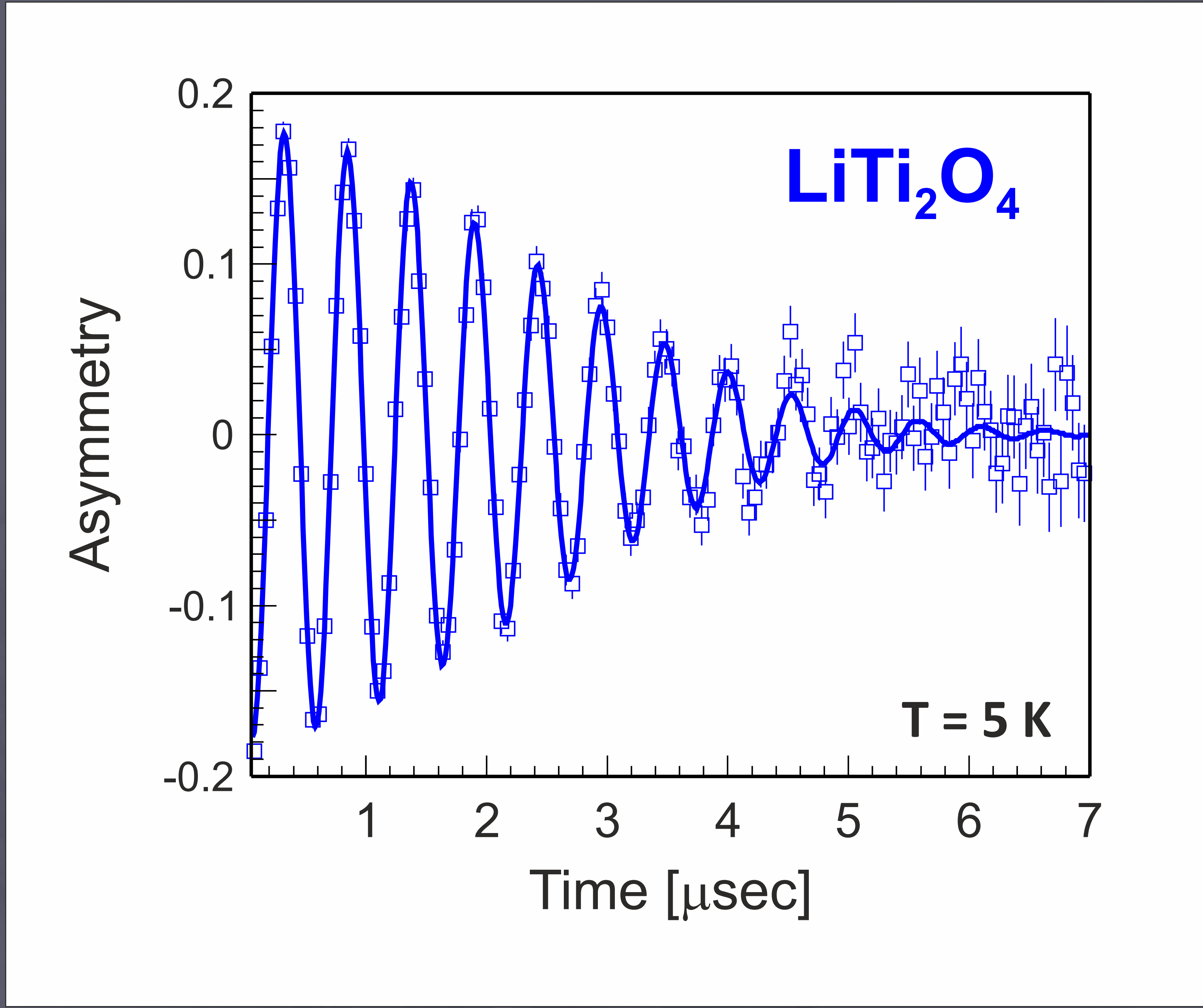

FFT

Frequency

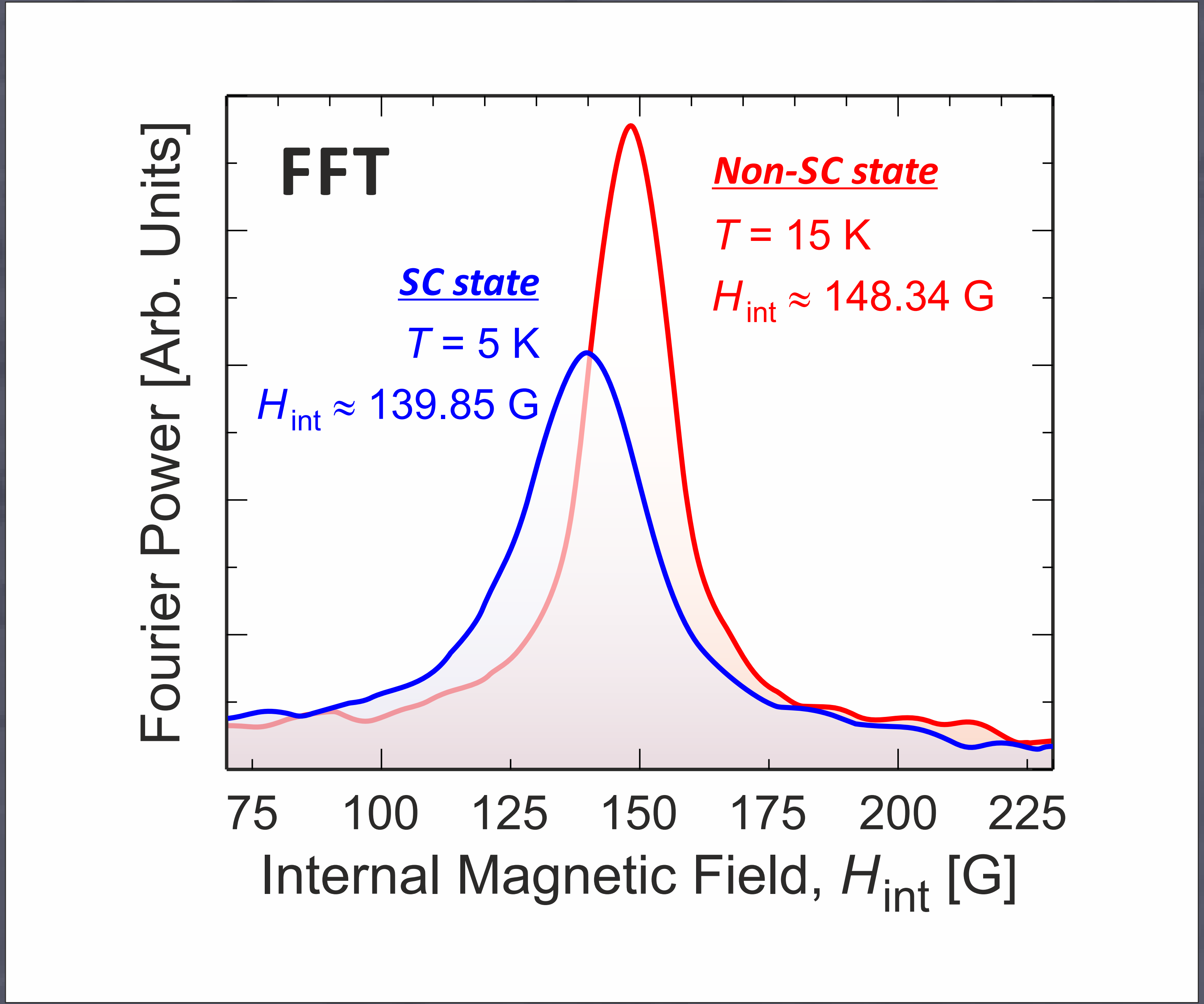

- **Width of FFT peak ∝ relaxation-rate in time-domain ∝ field-distribution width at the muon site**

Fourier / FFT

Time

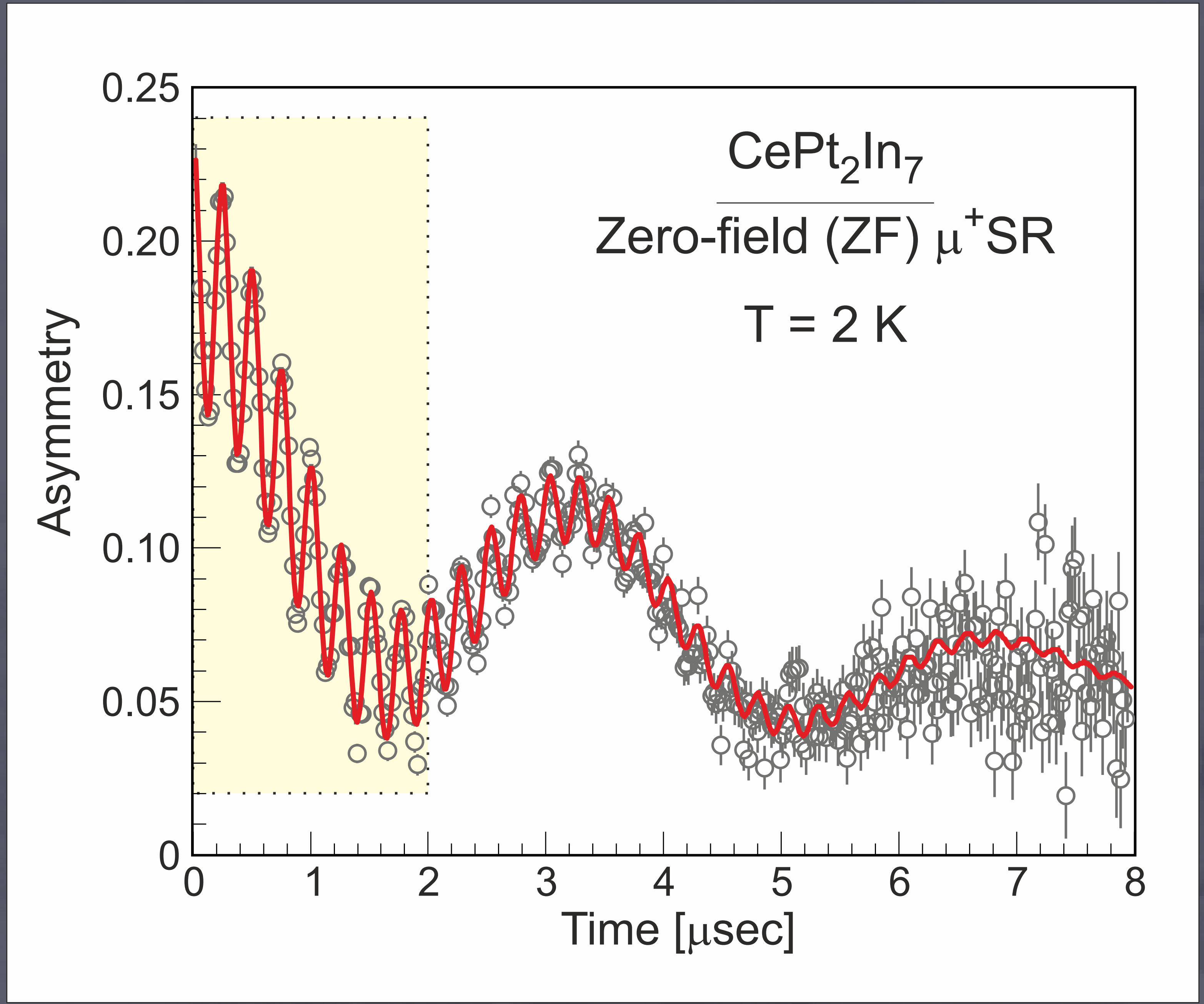

FFT →

Frequency

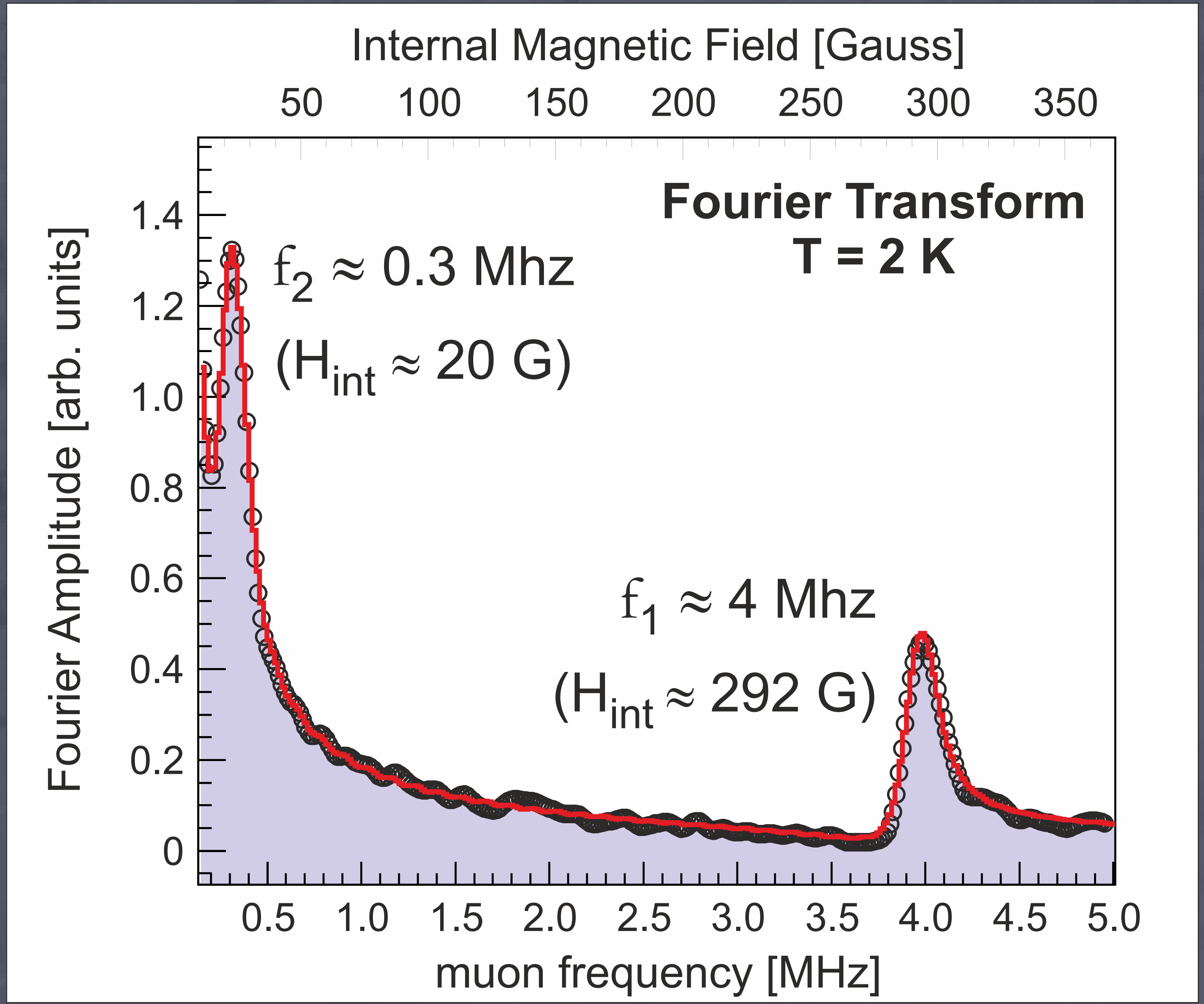

- **Different frequencies (FFT peaks) can also display different field-distributions (FFT peak widths), which can give clear indications on details in the magnetic spin order and/or dynamics.**

Fourier / FFT

Time

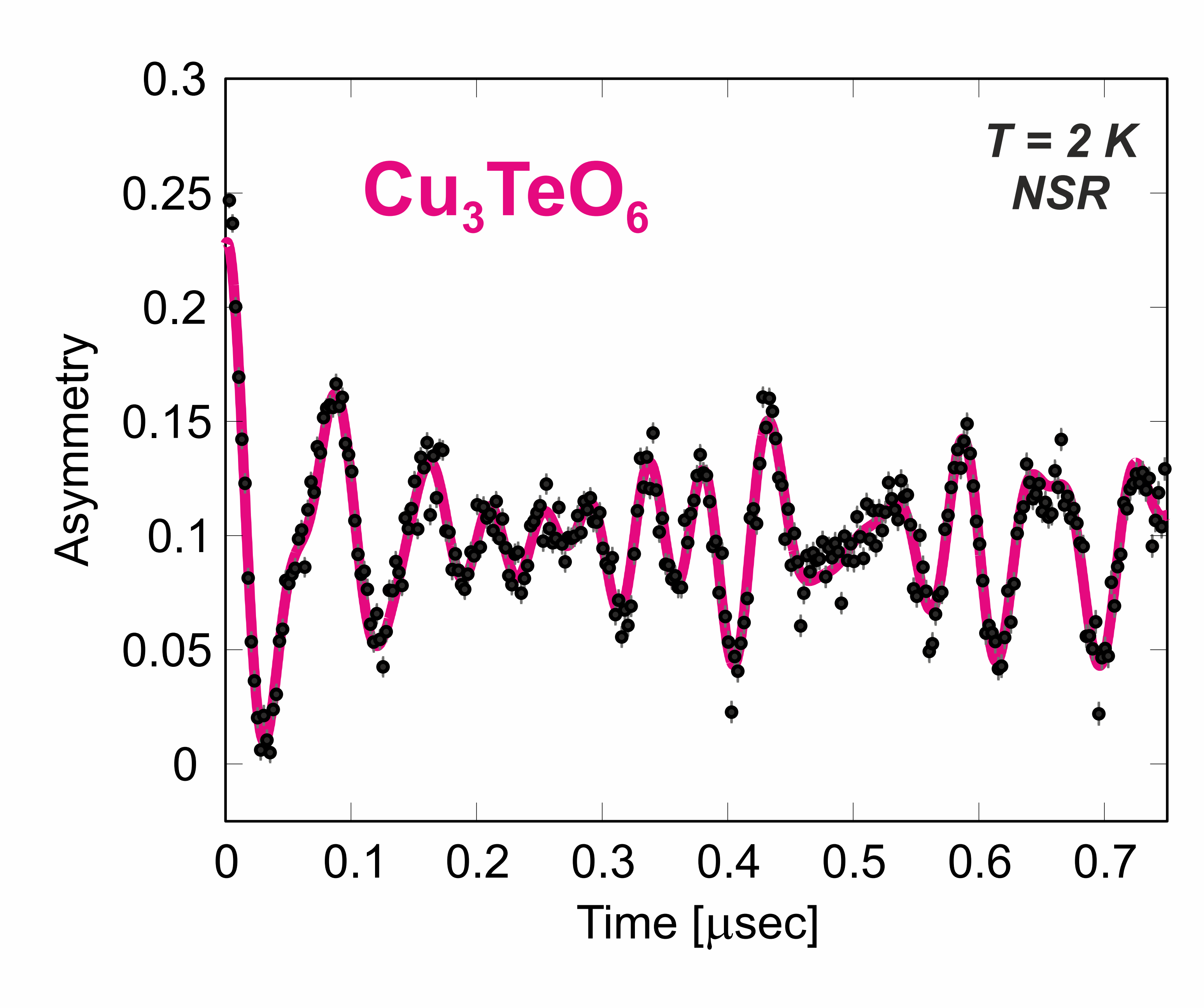

FFT

Frequency

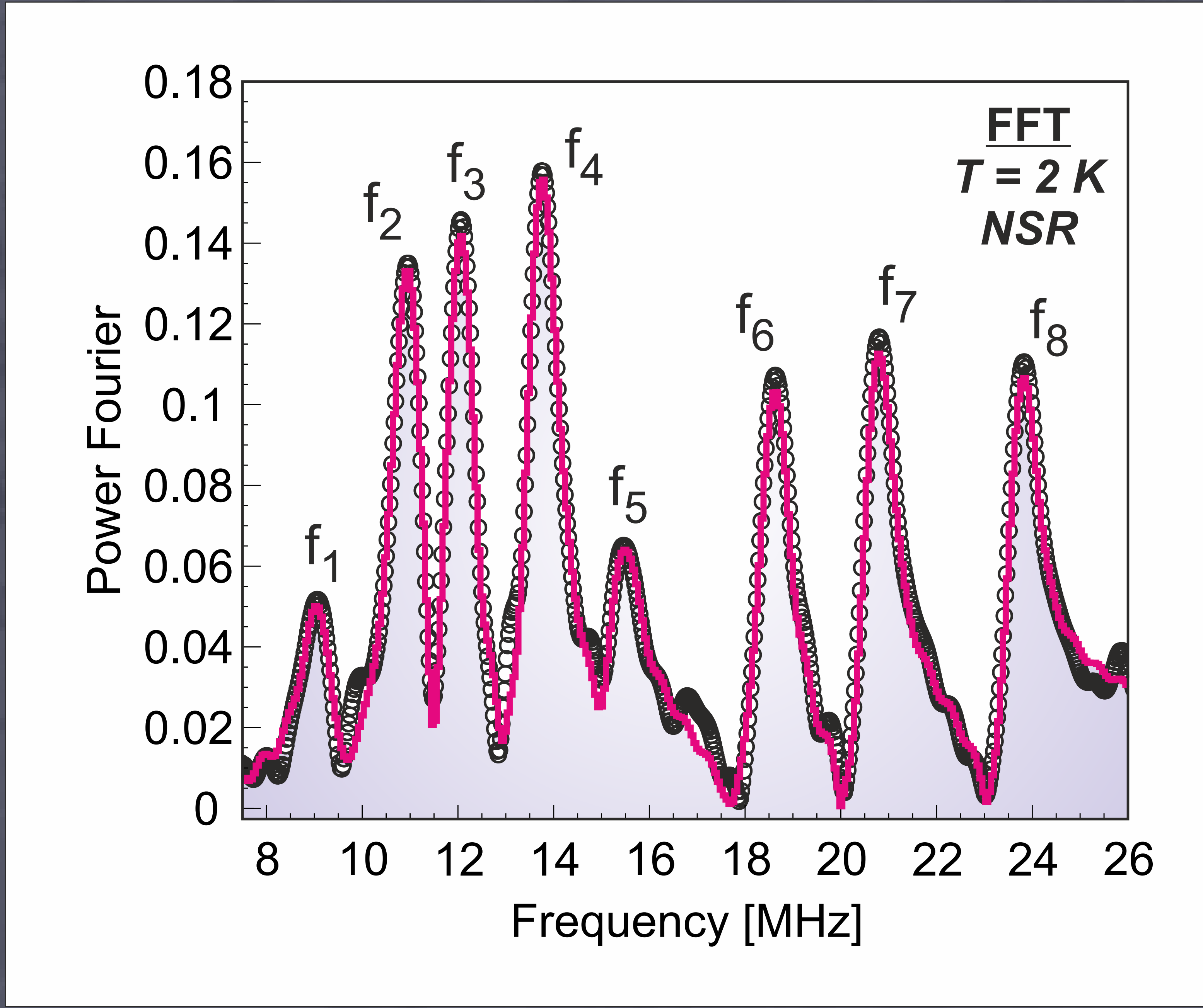

- Why do we get a set of distinct frequencies ???

Muon Stopping Mechanism

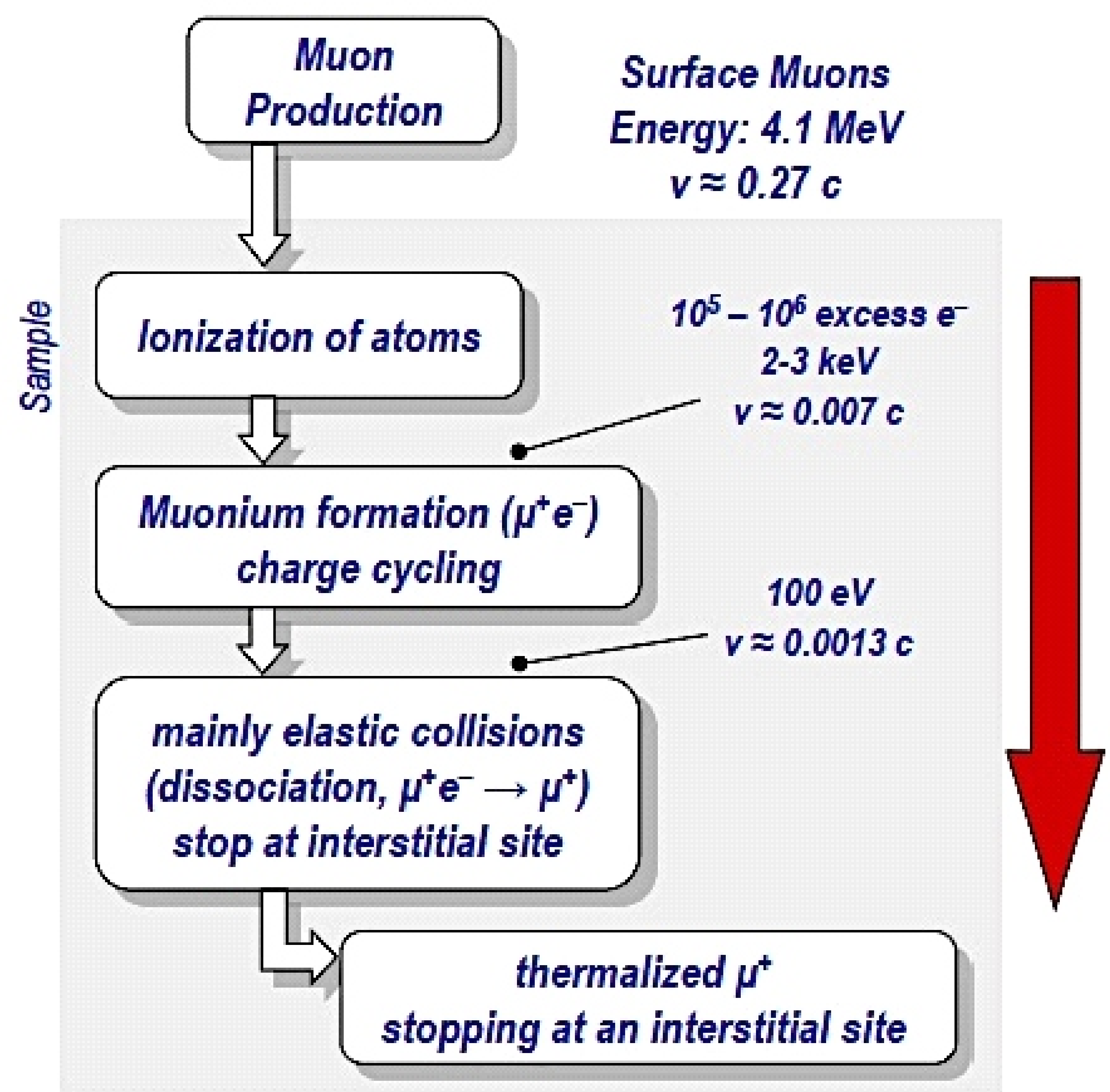

- Only electrostatic processes → no loss of polarization!
- Total stopping time in matter < 0.1 ns
- Penetration ≈ 0.1 – 1 mm

Muon Stopping Sites (in the lattice of your sample)

- Positive muons stop at potential minima in the crystallographic lattice, in oxides = close to Oxygen
- Muon sites can not be measured but calculated to certain accuracy
- Crystallographically identical sites could still be magnetically different (=multiple frequencies!)

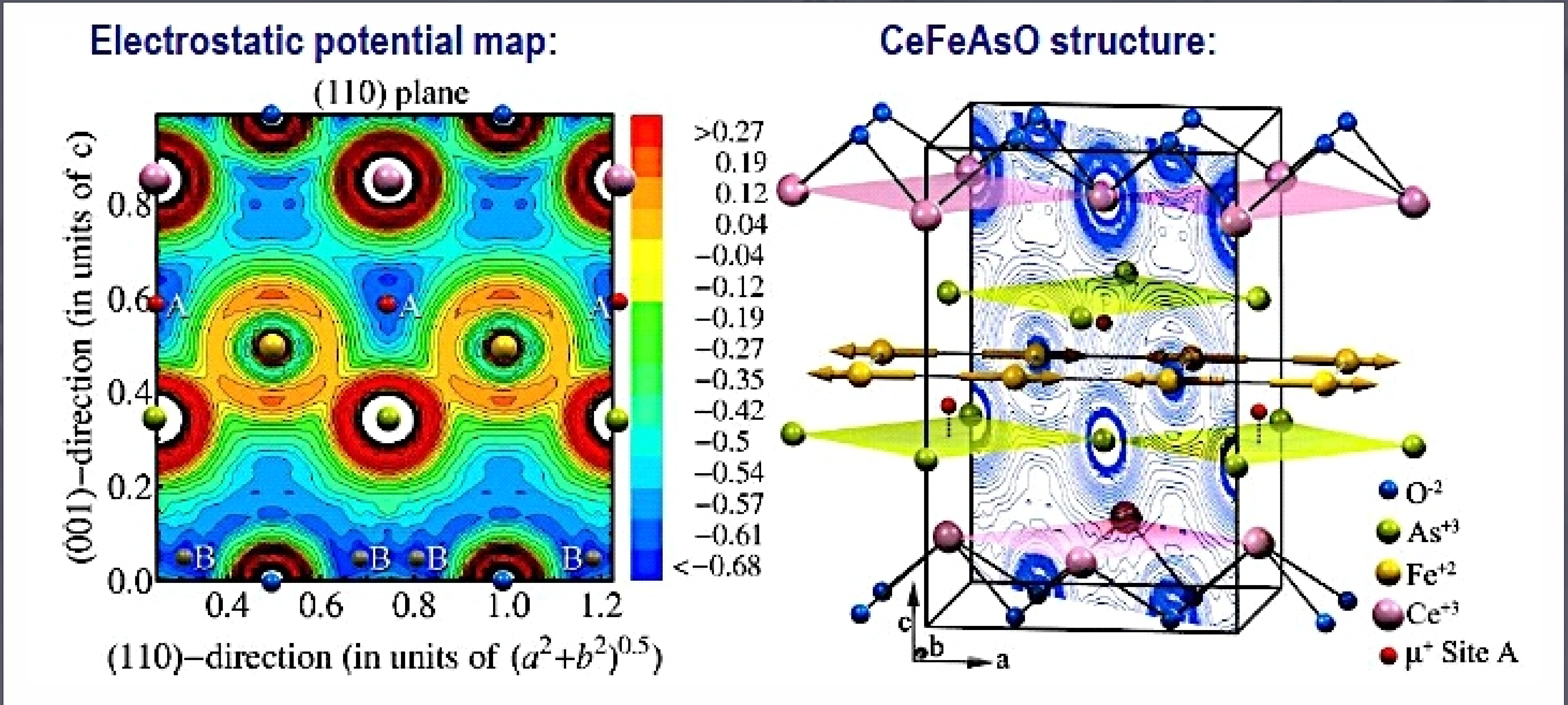

Local Magnetic Probe

Homogeneously Magnetic

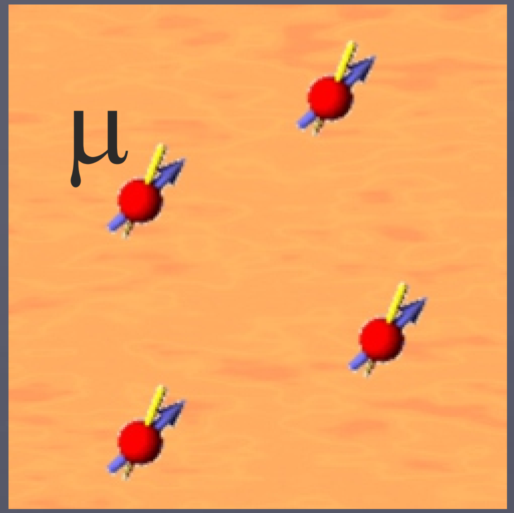

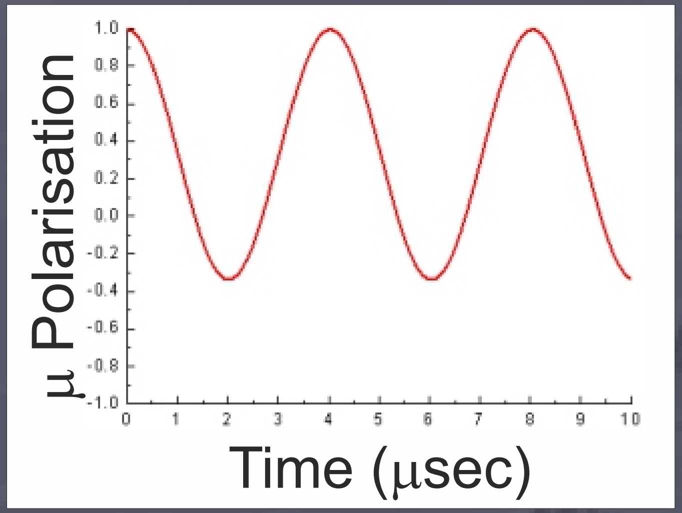

FREQUENCY =
Magnetic moment (order parameter)

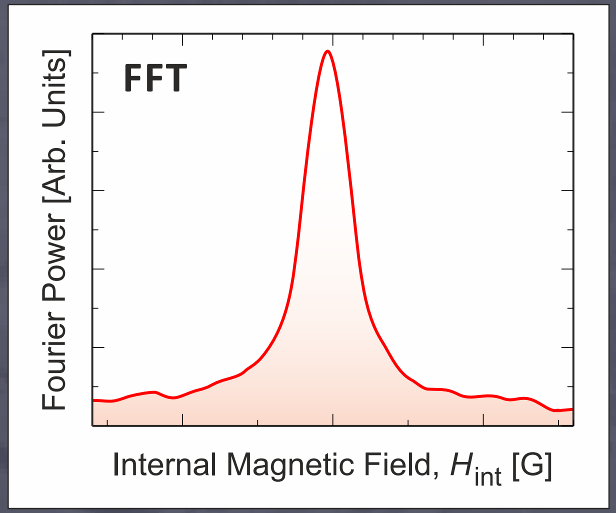

Local Magnetic Probe

Homogeneously Magnetic

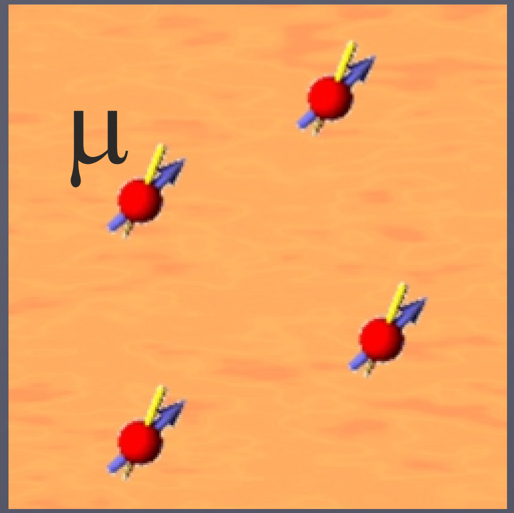

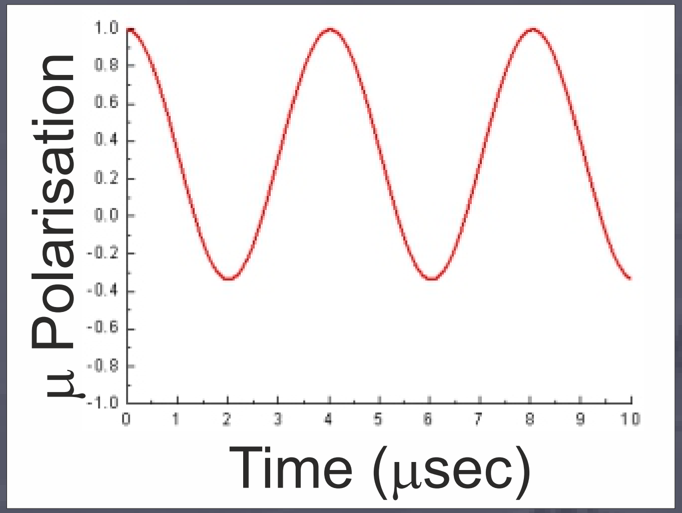

FREQUENCY =
Magnetic moment (order parameter)

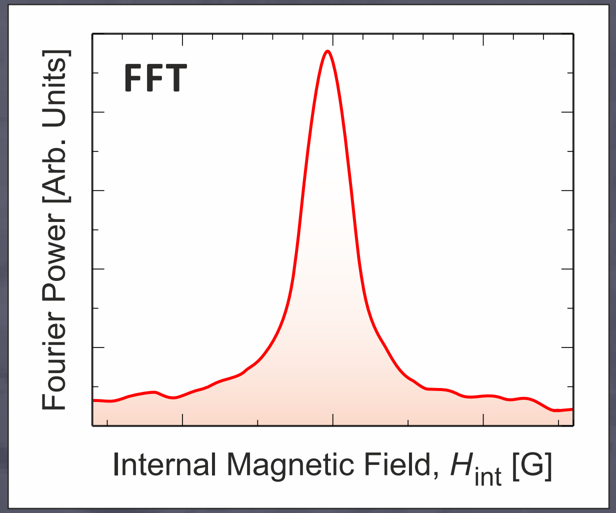

Magnetic + Non-magnetic

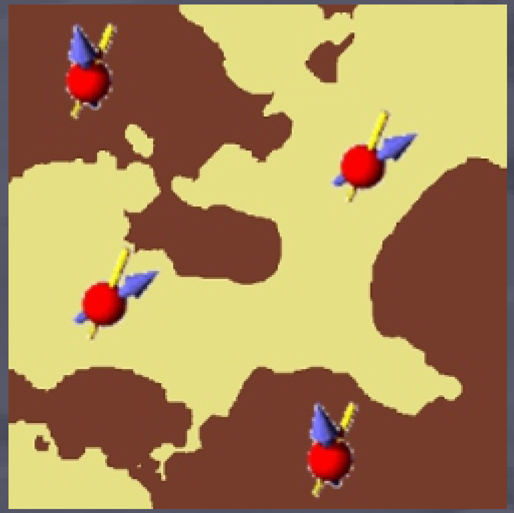

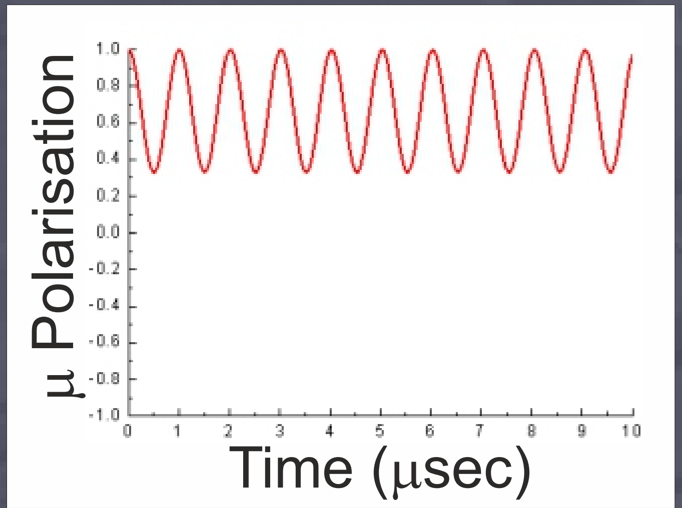

AMPLITUDE =
Magnetic volume-fraction

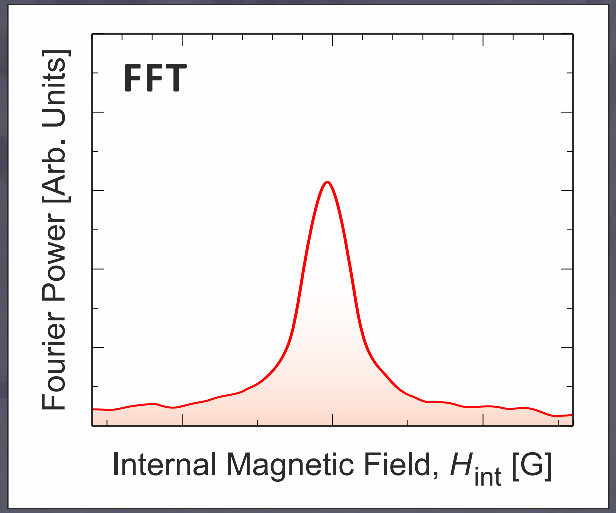

Local Magnetic Probe

Homogeneously Magnetic

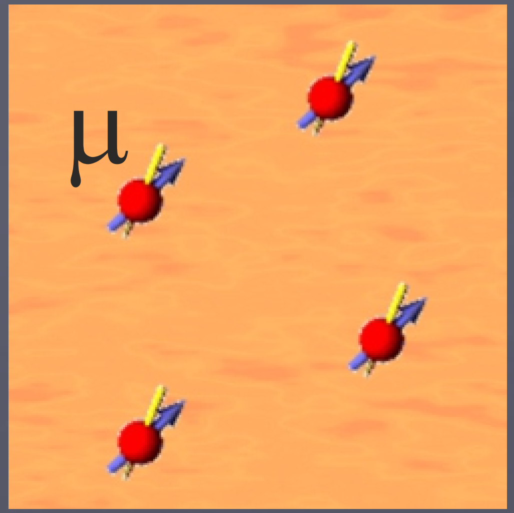

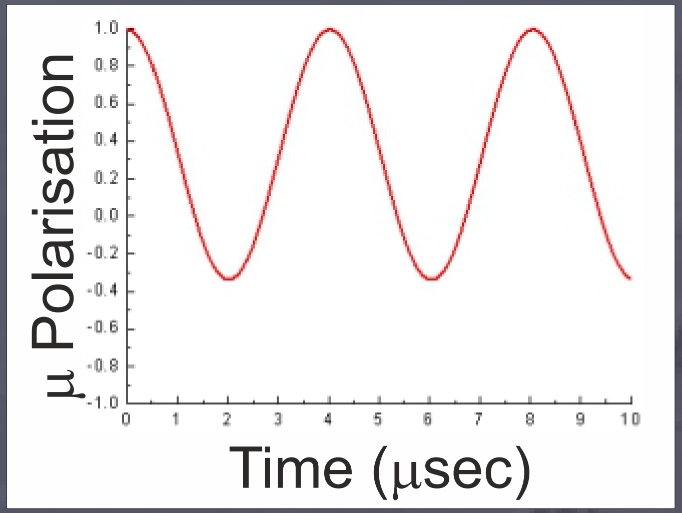

FREQUENCY =
Magnetic moment (order parameter)

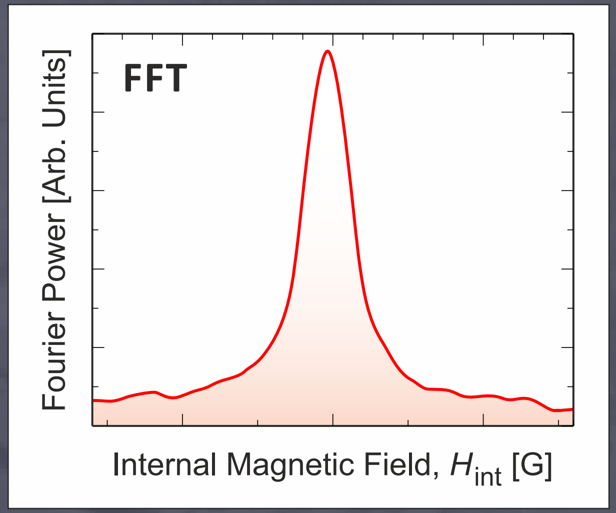

Magnetic + Non-magnetic

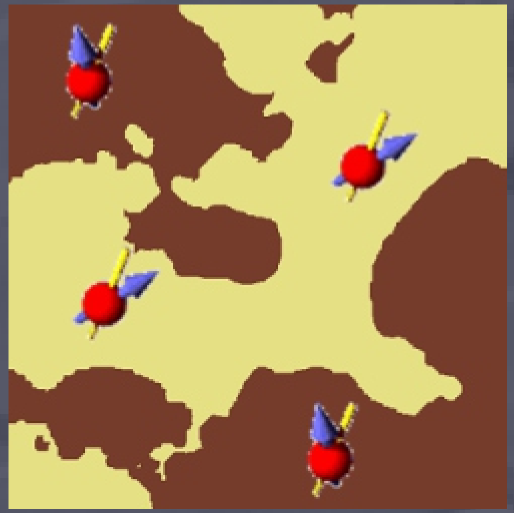

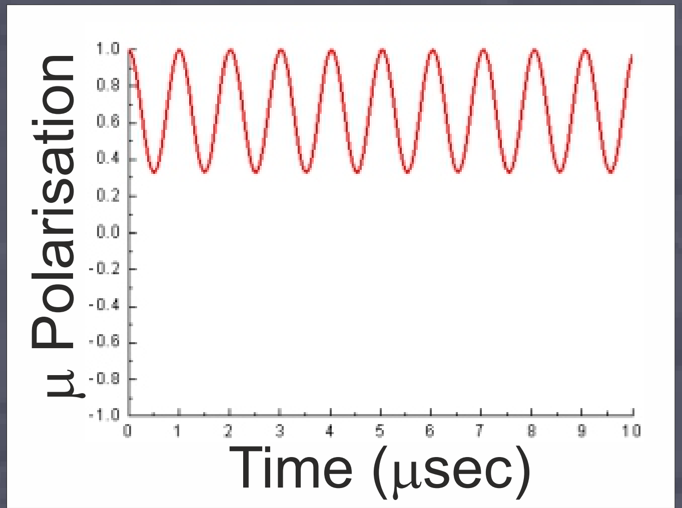

AMPLITUDE =
Magnetic volume-fraction

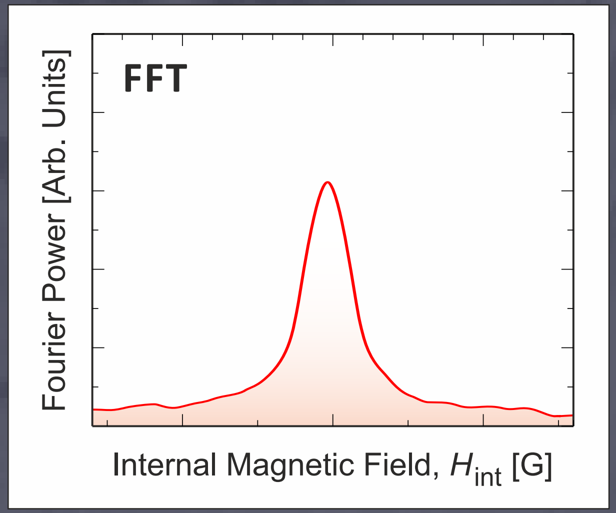

+ Field Distribution within magnetic volume

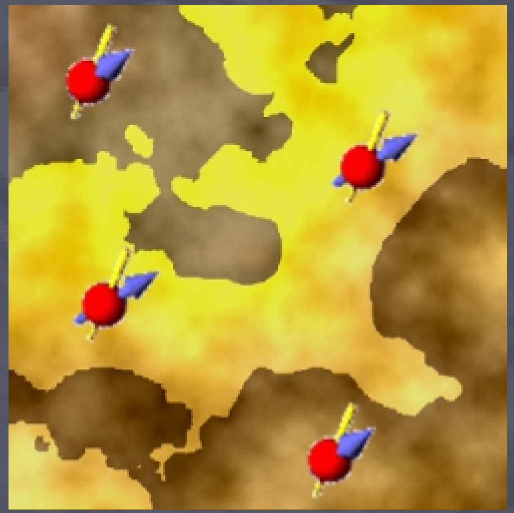

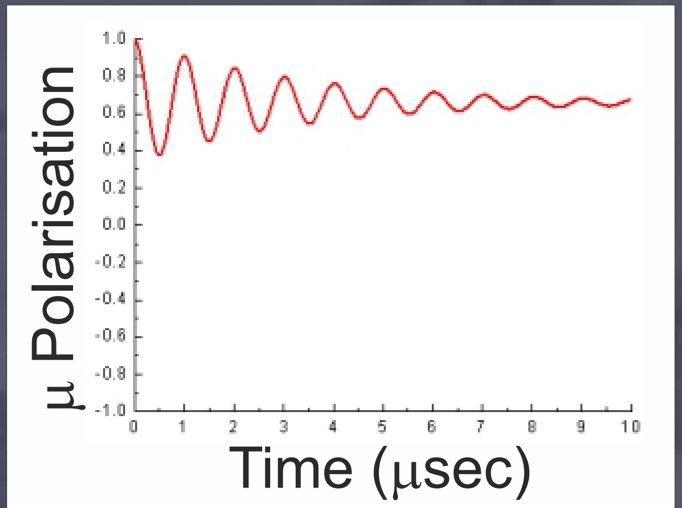

DAMPING =
Magnetic inhomogeneity

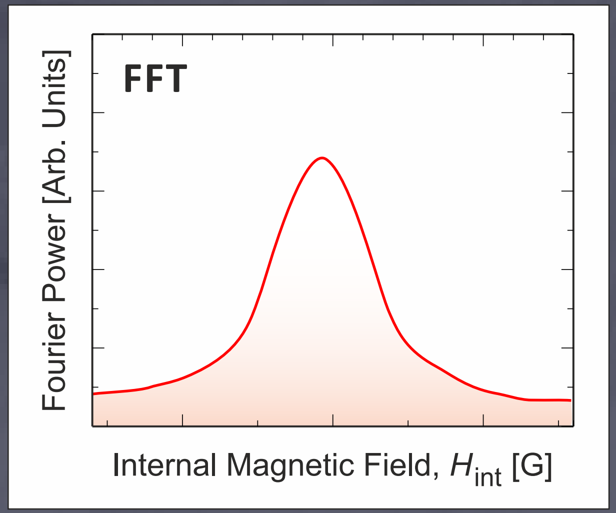

μ^+SR: Basic Idea

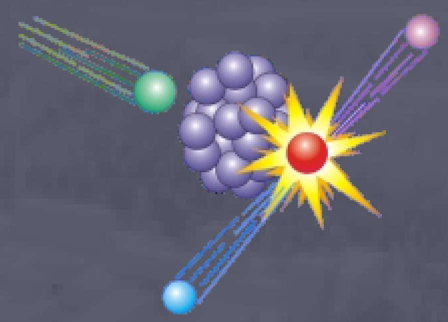

- <u>Create 100% spin-polarized</u> muons by shooting high-energy protons into a C-target

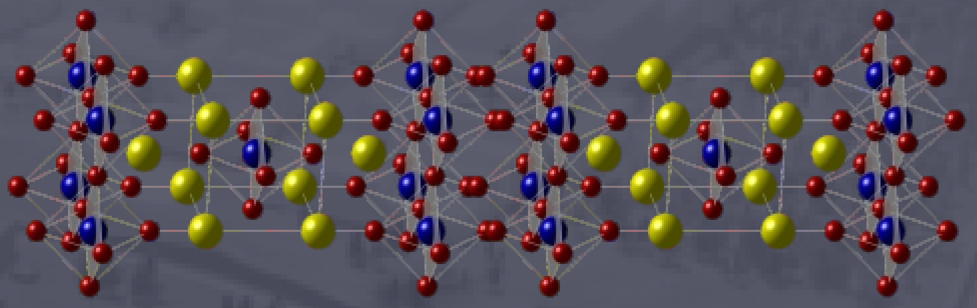

- Implant the muons into a sample of choice (bulk or thin film)

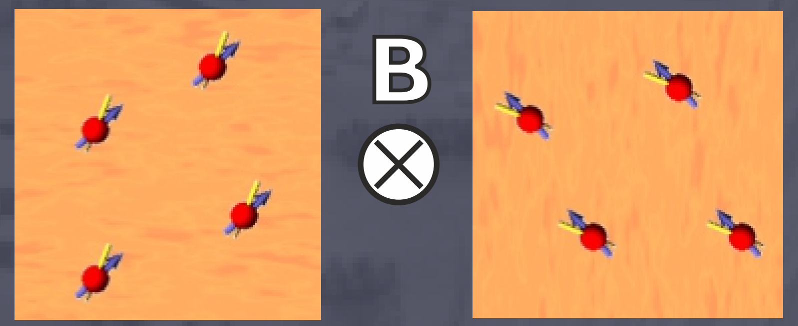

- The muons have a large gyromagnetic ratio (γ). It's spin start to Larmor-precess in very small non-parallel internal magnetic/nuclear fields.

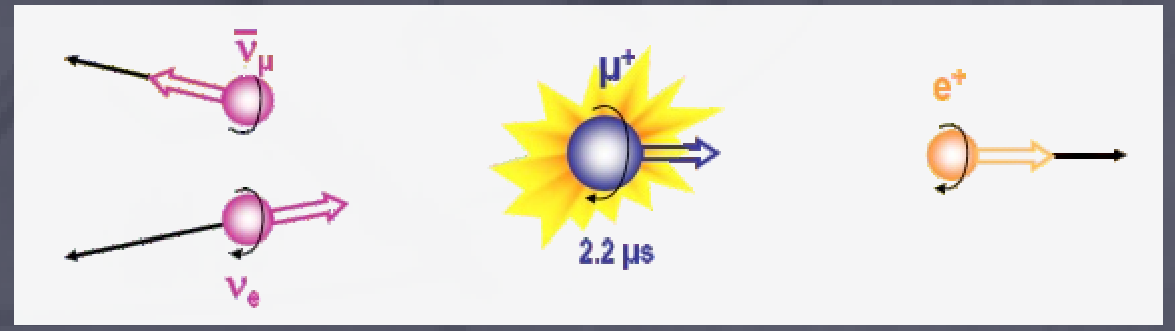

- After an average time of 2.2 μs the muon decay into a positron, preferentially emitted in the muon spin direction.

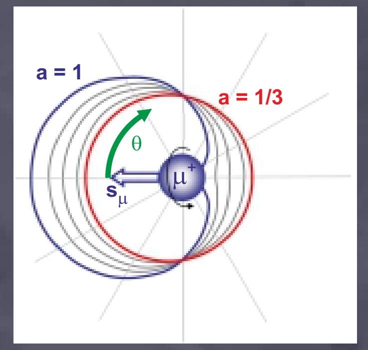

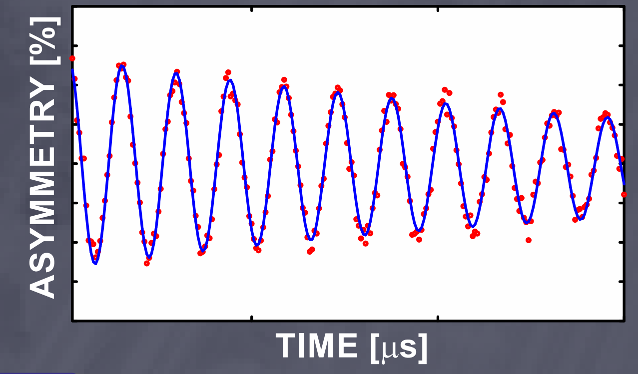

- Measure the time and spatial distribution of emitted positrons = Asymmetry (t) = muon spectra.

Reveals how the spin-direction of the implanted muons is affected by the sample i.e. muons are <u>very sensitive local probes</u> of static and/or dynamic internal fields !

Zero-Field (ZF) μ^+SR

- No externally applied magnetic field

- **Study the evolution/relaxation of the muon polarization due to <u>internal</u> static or dynamic magnetic fields / field-distribution**

- Extract temperature dependent data:

  $\nu(T)$: magnetic order parameter
  $\lambda(T)$: ~dynamics (relaxation)

- Very sensitive magnetic probe, ordered moments down to 0.001 μ_B can be detected

- Above T_N if only random nuclear fields are present
  → **Kubo-Toyabe function**

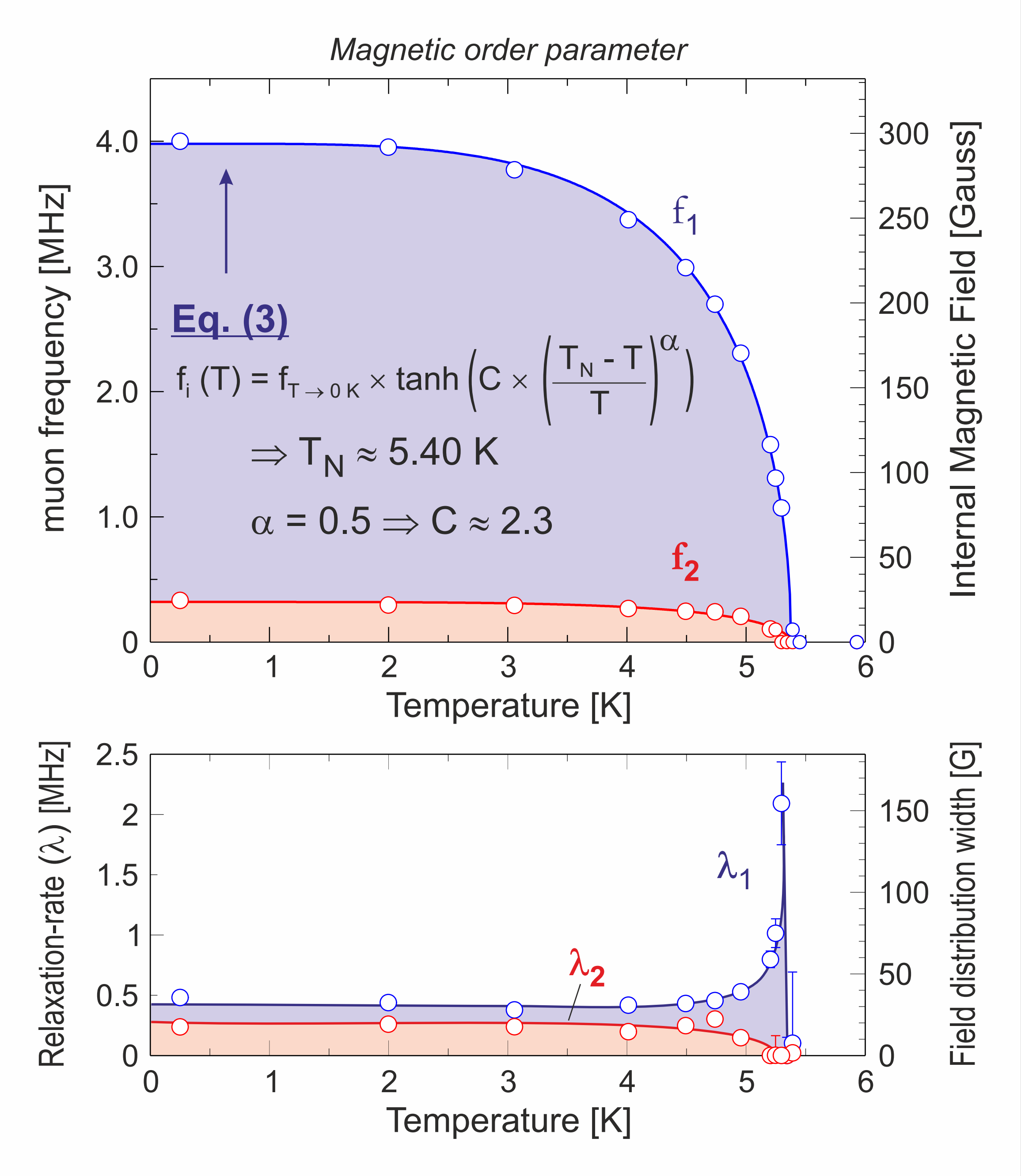

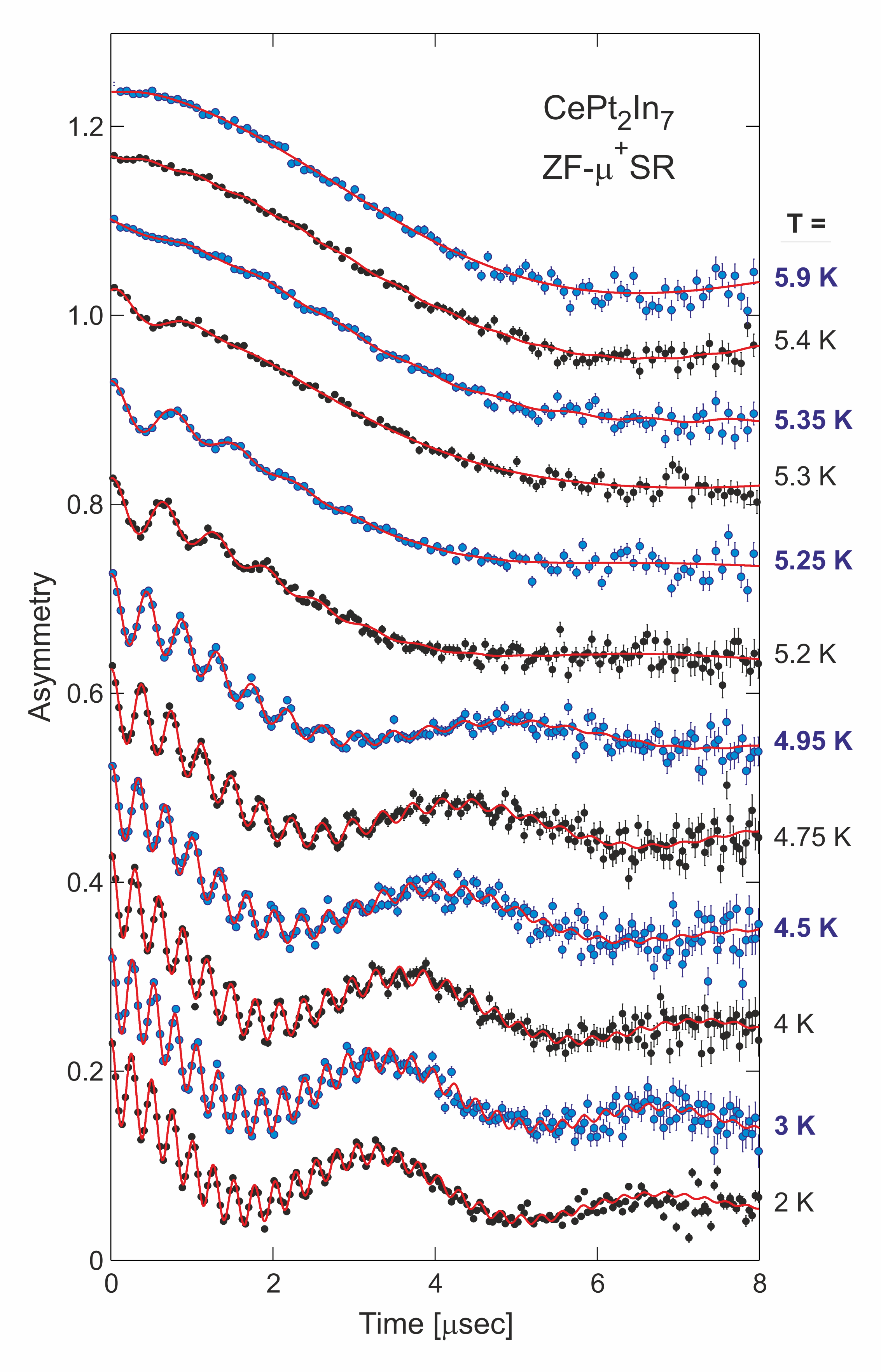

Weak-Transverse Field (wTF) μ^+SR

- **Externally applied magnetic field <u>perpendicular</u> to the original muon spin direction**
- **Muon precesses at a frequency that is proportional to the resulting field size at the muon stopping site in the material**
- **Commonly used to achieve a transition temperature (fast) and to calibrate "zero-level" (α) for the data**
- **Study magnetic field distribution of vortex lattices in HTSC**
- **Study magnetic Knight Shifts (fractional difference in local/external field)**

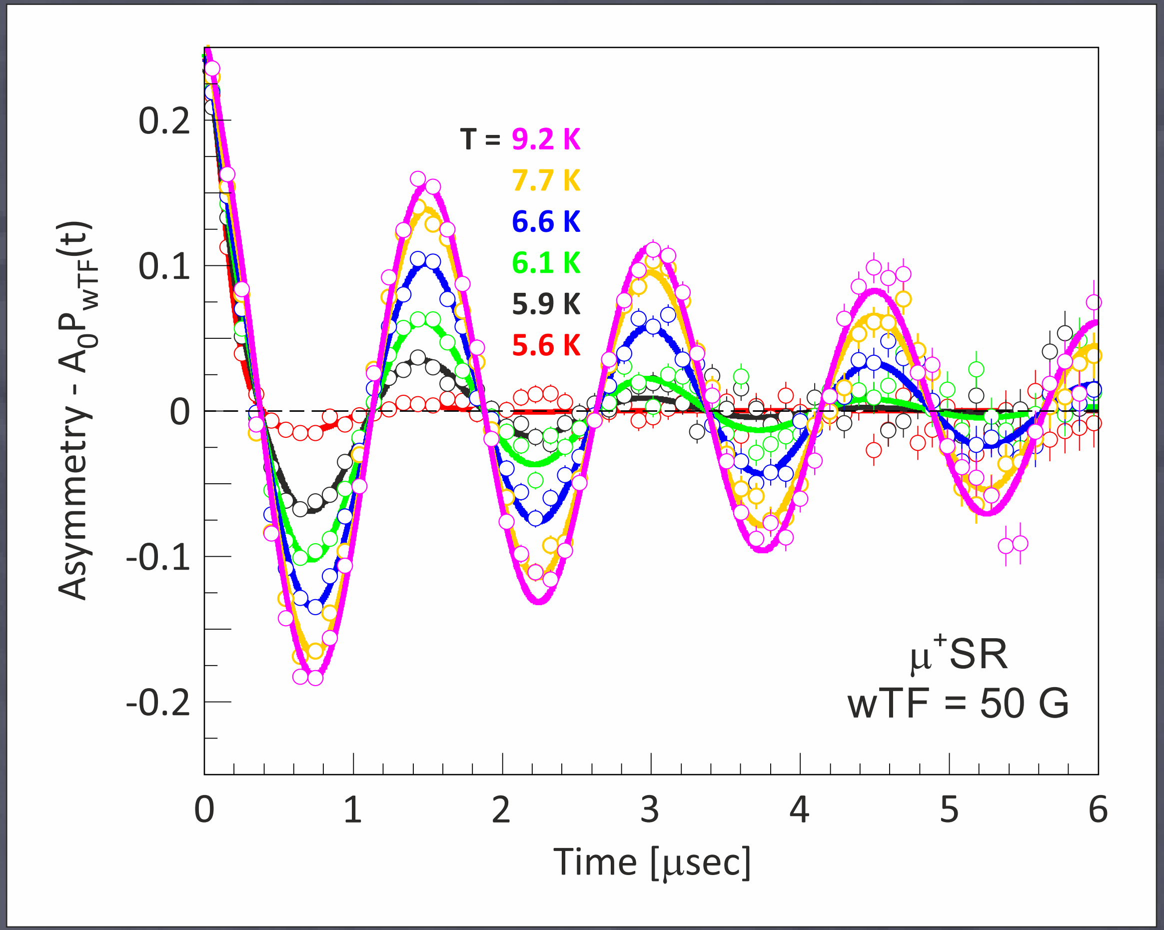

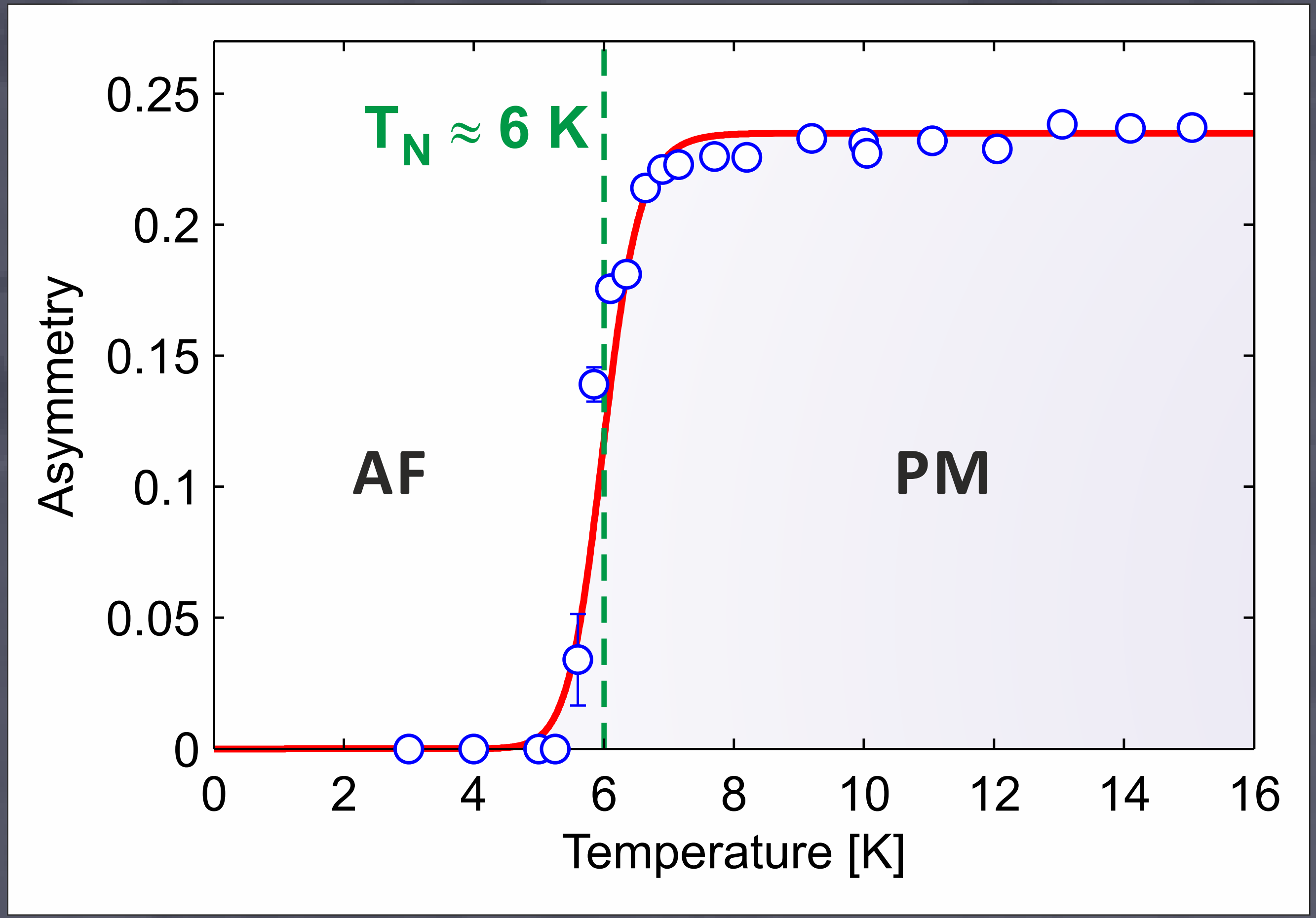

Longitudinal-Field (LF) μ^{+}SR

- **Externally applied magnetic field parallel to original muon spin direction**
- **Decouple the magnetic order by "locking" the initial muon spin**
- **Distinguish between static and dynamic contributions via decoupling of static internal field**

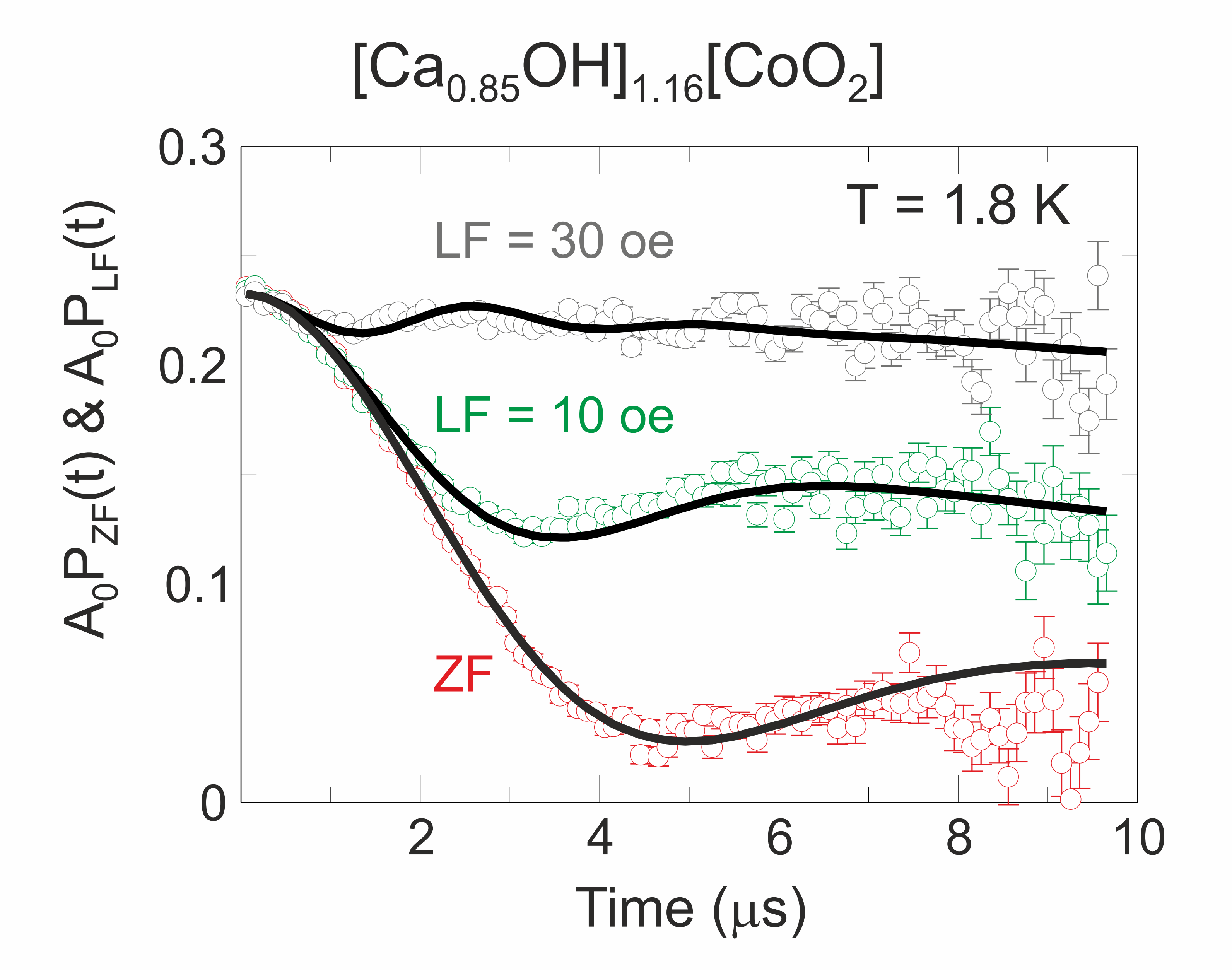

Muon Sources

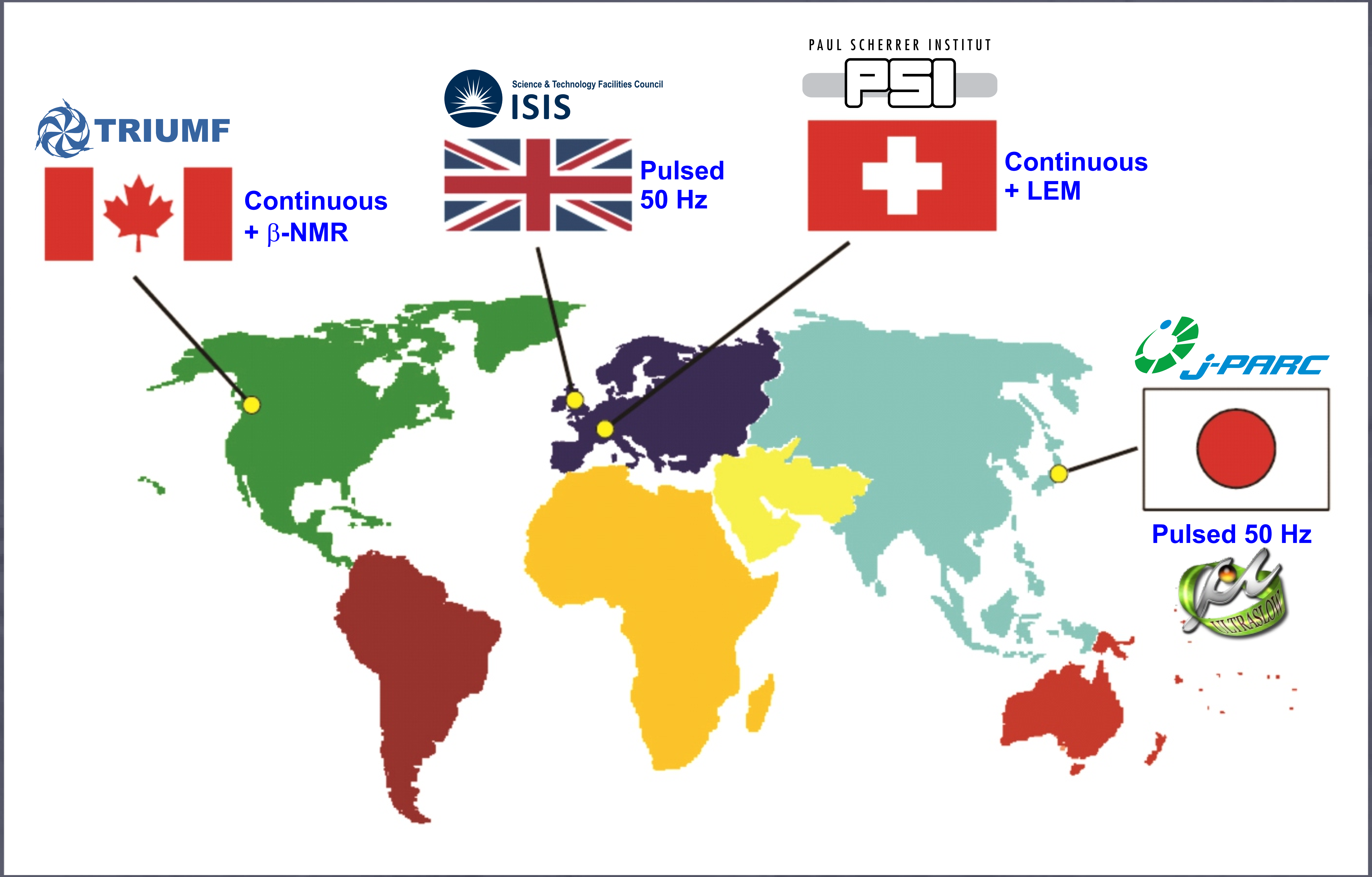

Pulsed vs. Continuous Muon Source

TRIUMF

PAUL SCHERRER INSTITUT PSI

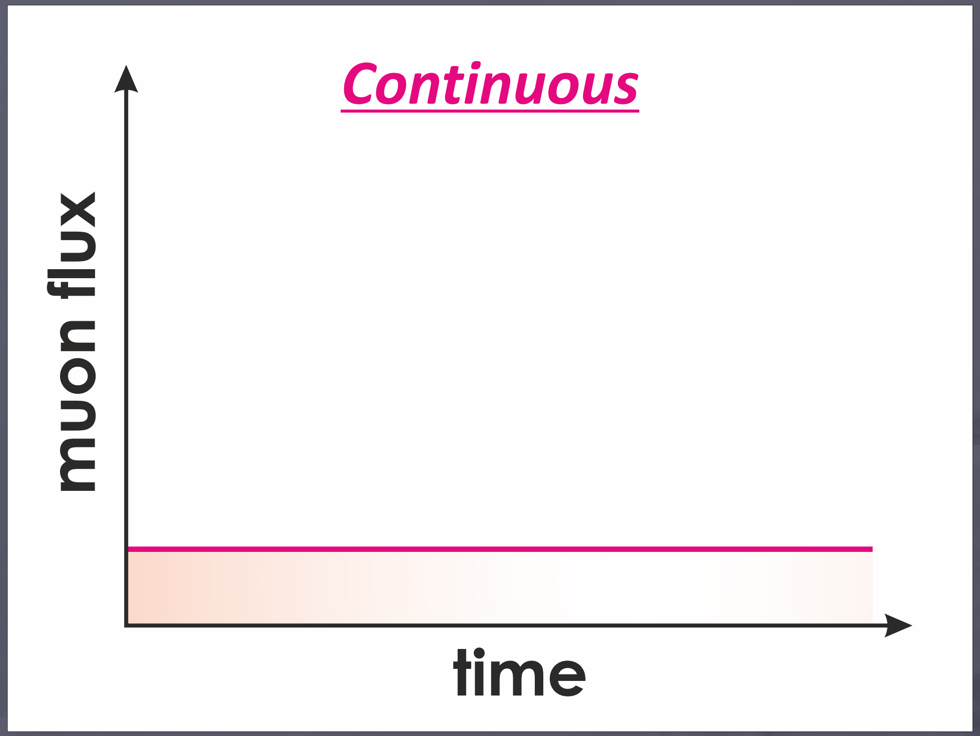

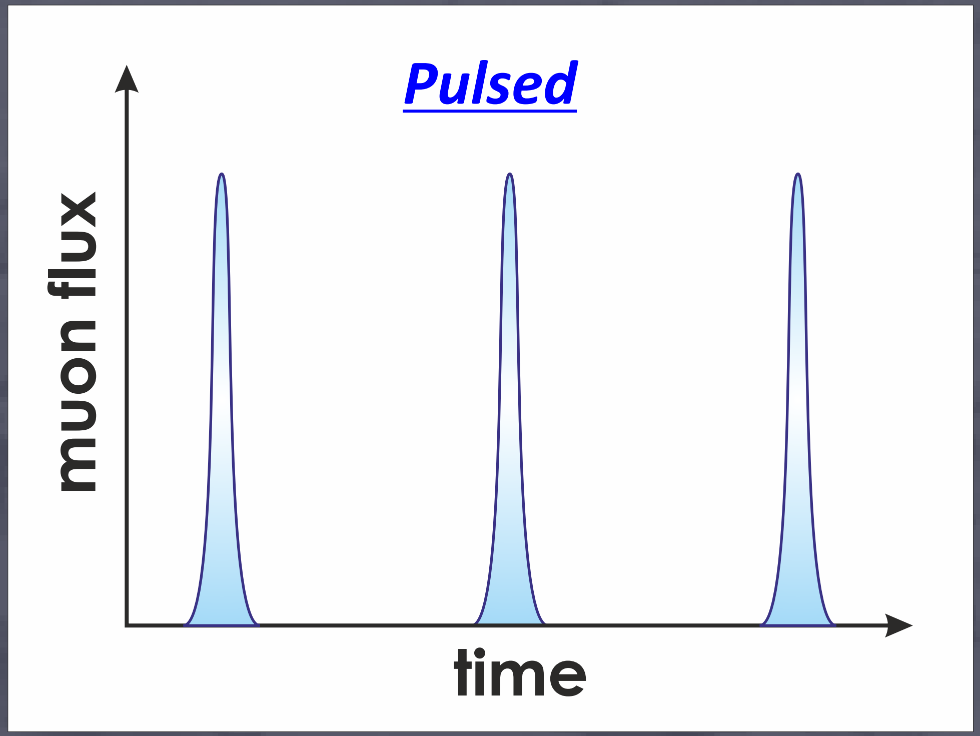

Science & Technology Facilities Council ISIS

J-PARC

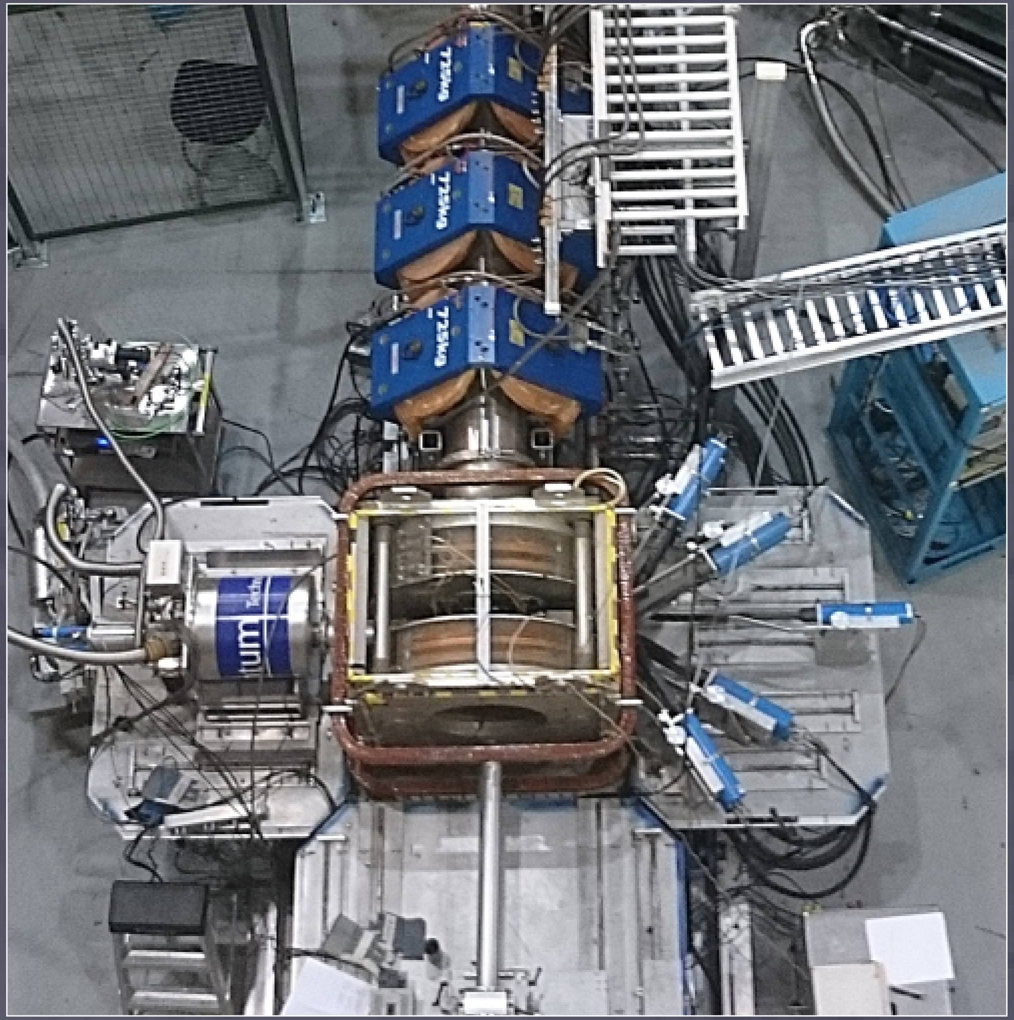

2-6 Detectors

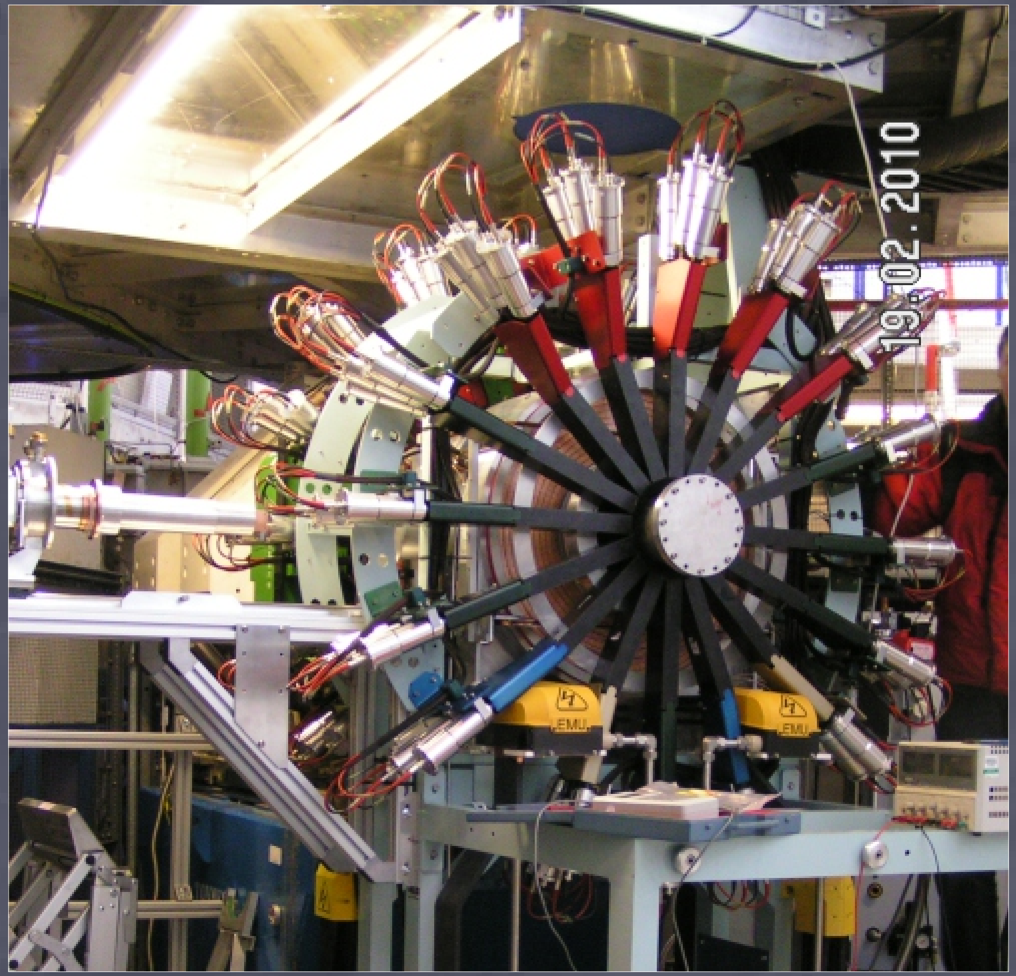

100's Detectors

Pulsed vs. Continuous Muon Source

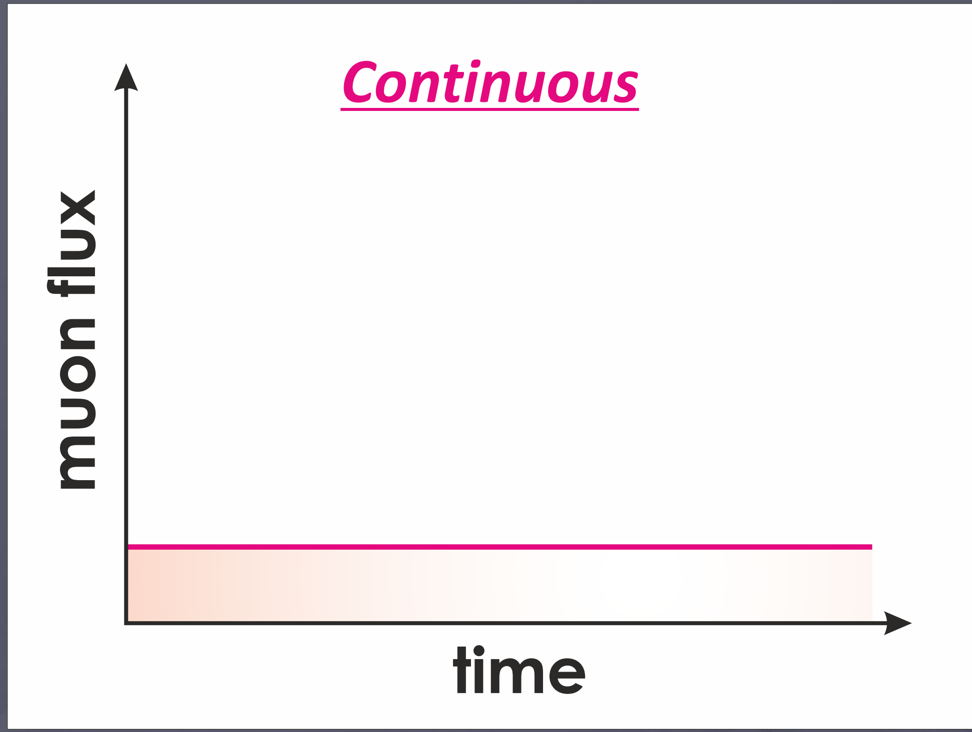

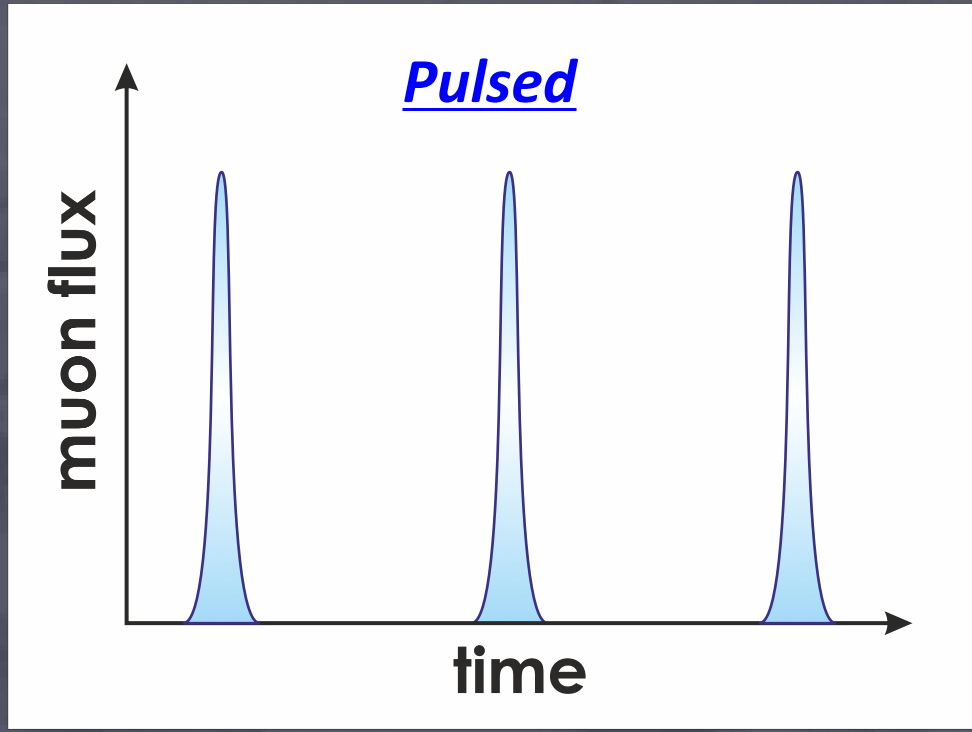

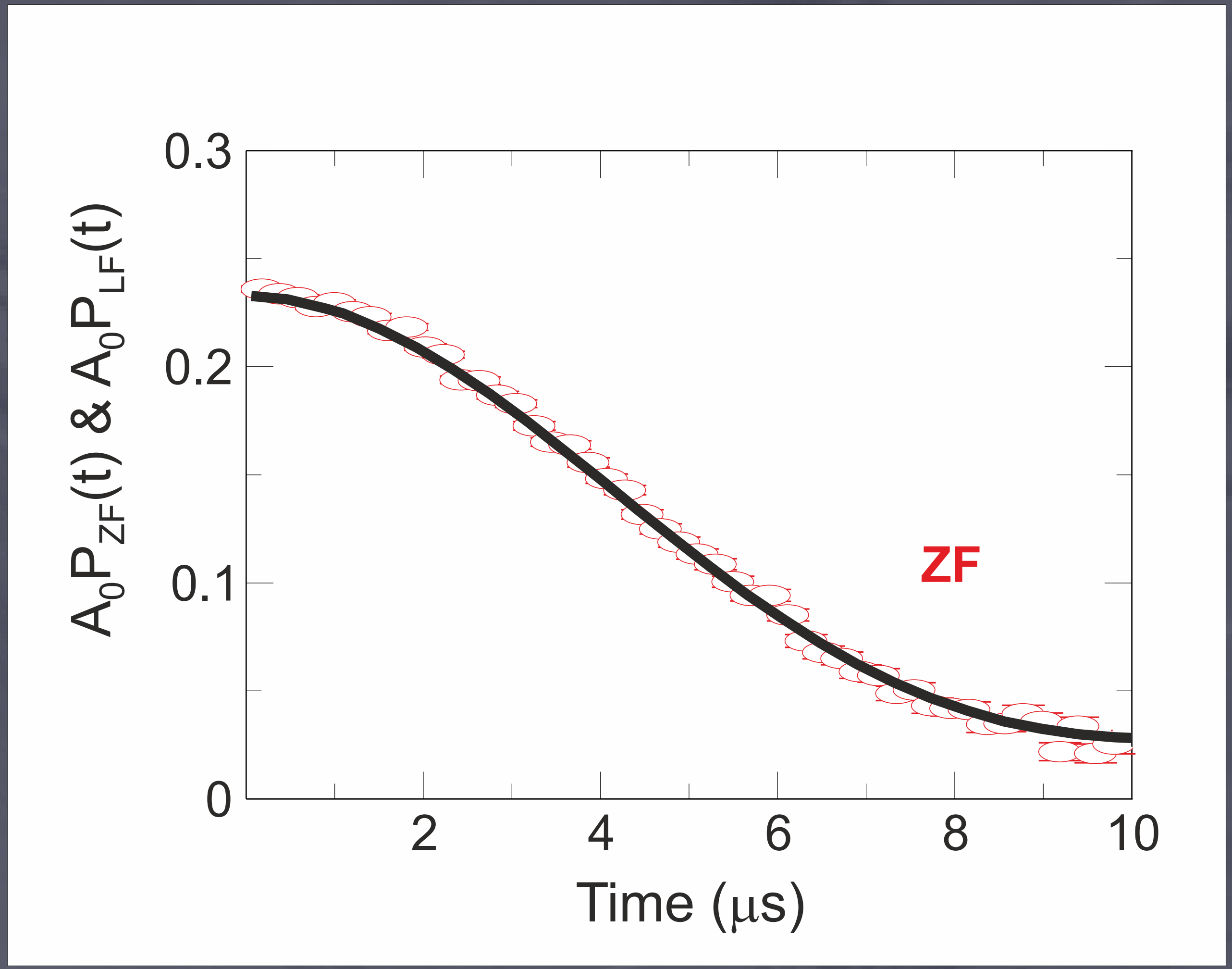

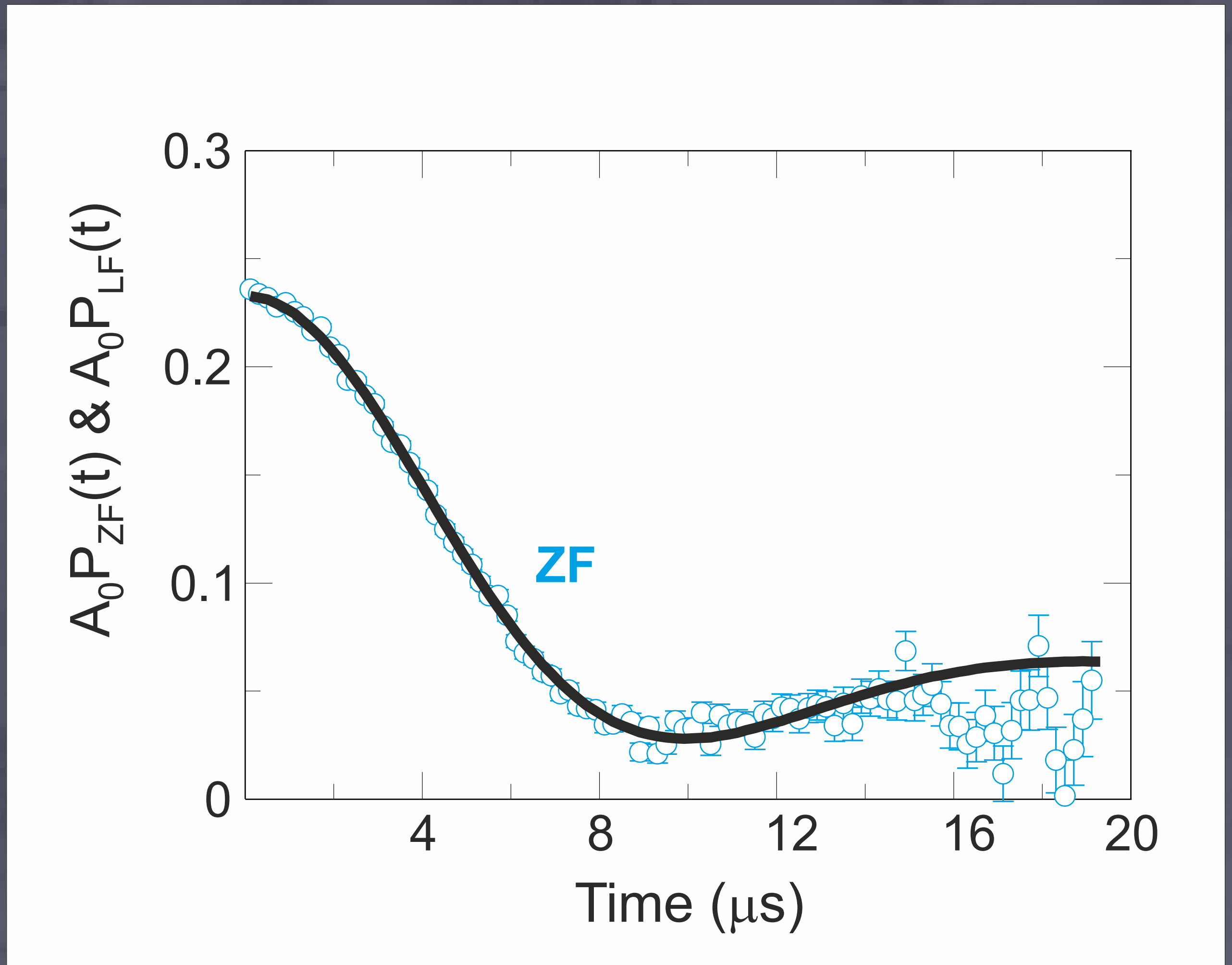

Pulsed vs. Continuous Muon Source

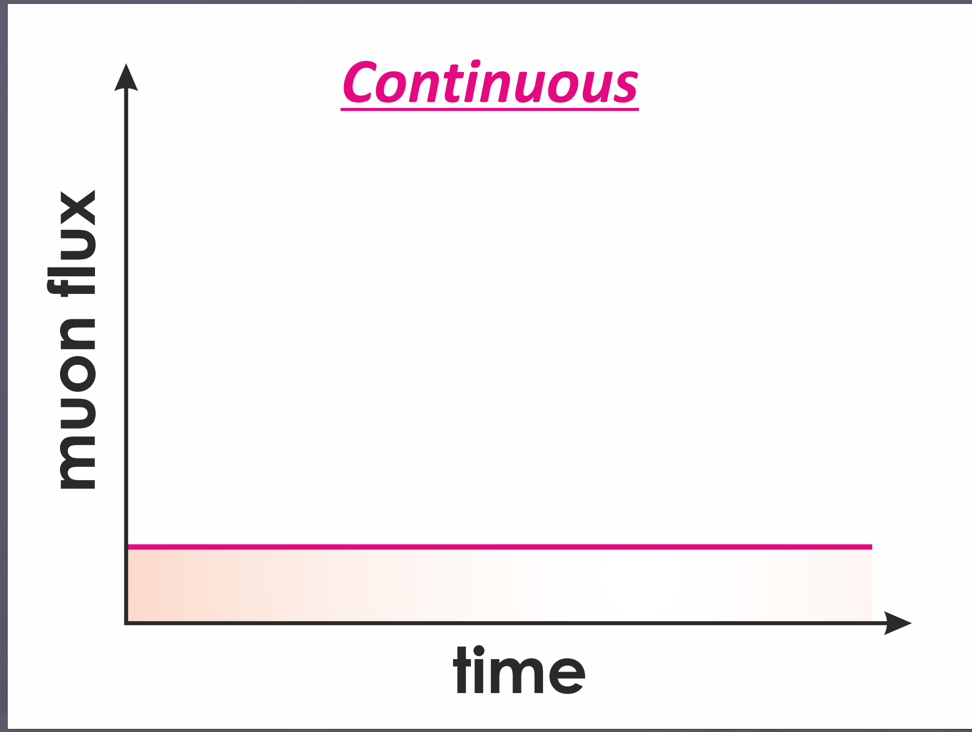

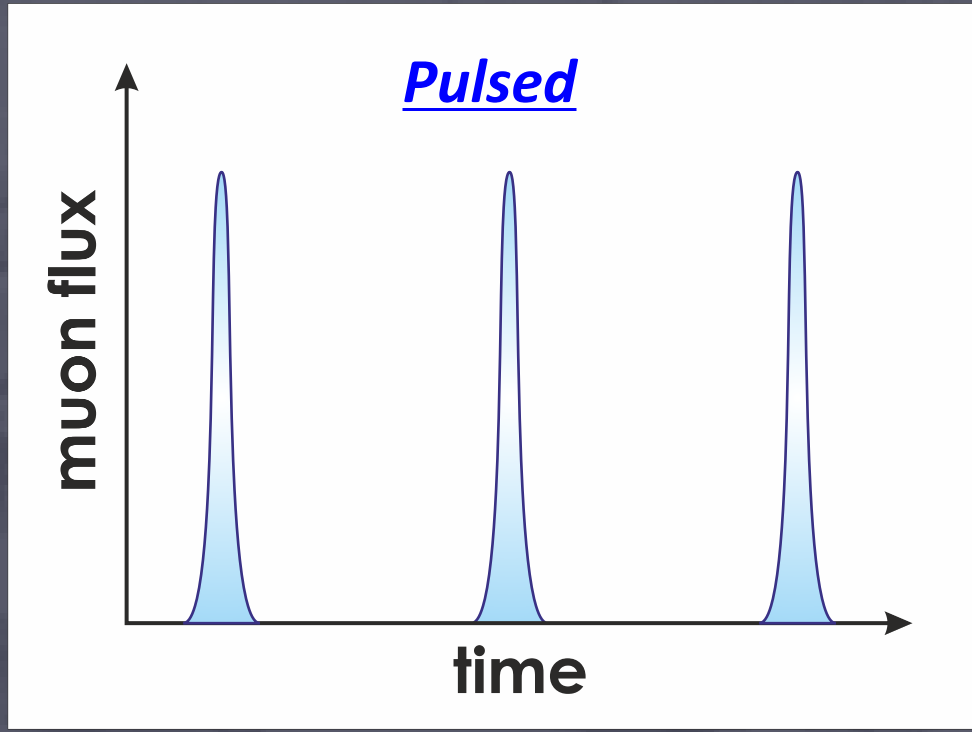

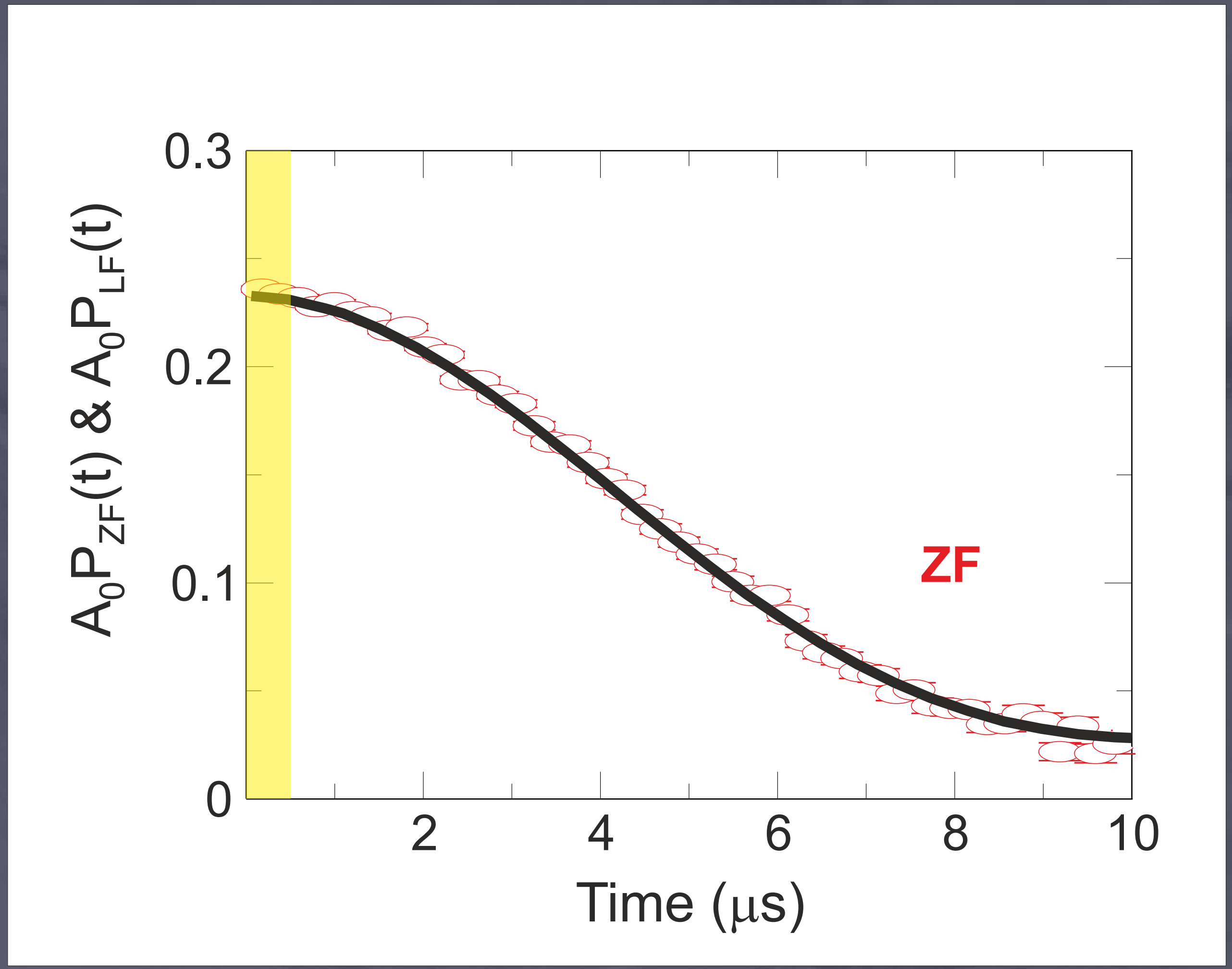

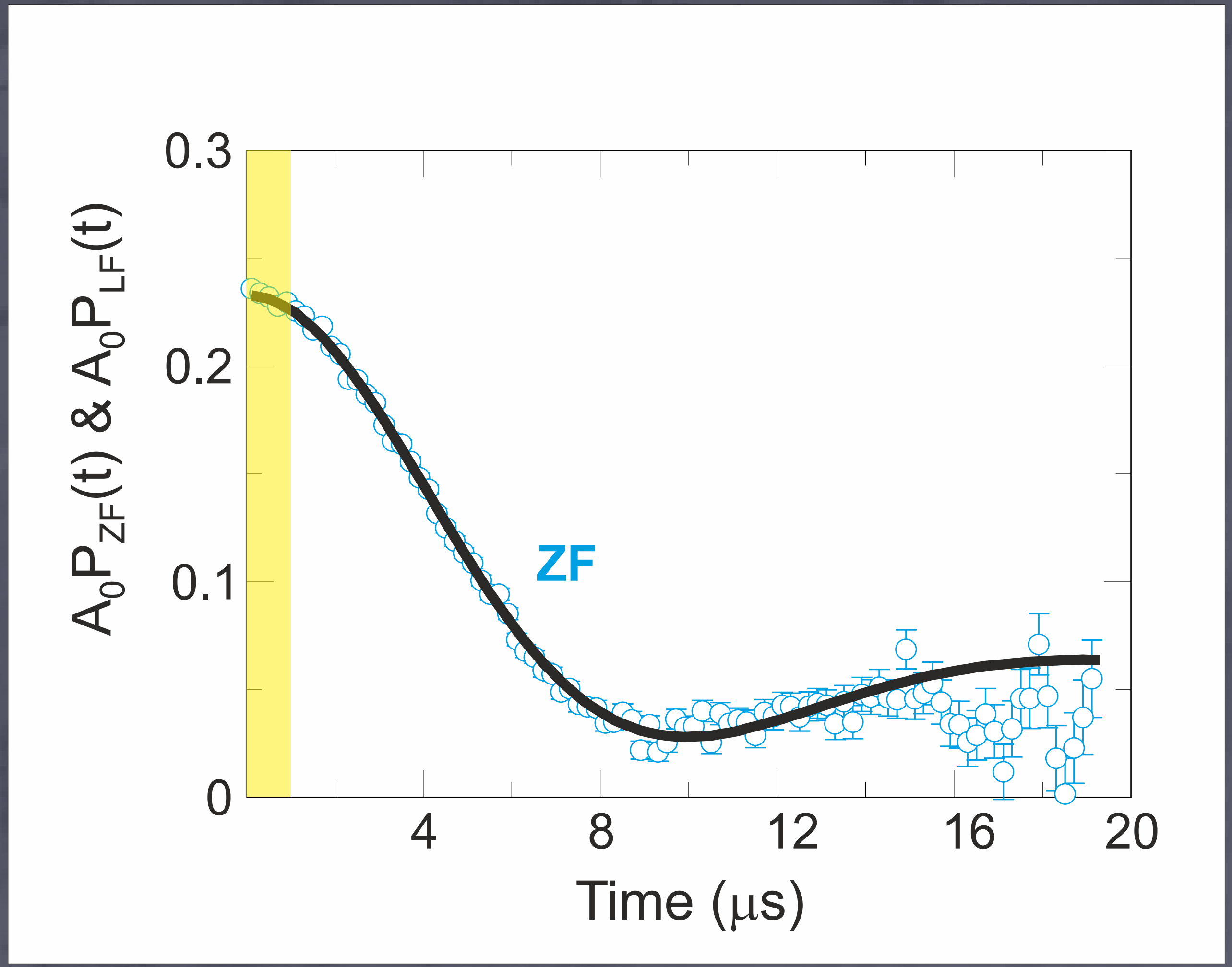

Pulsed vs. Continuous Muon Source

TRIUMF
PAUL SCHERRER INSTITUT
PSI

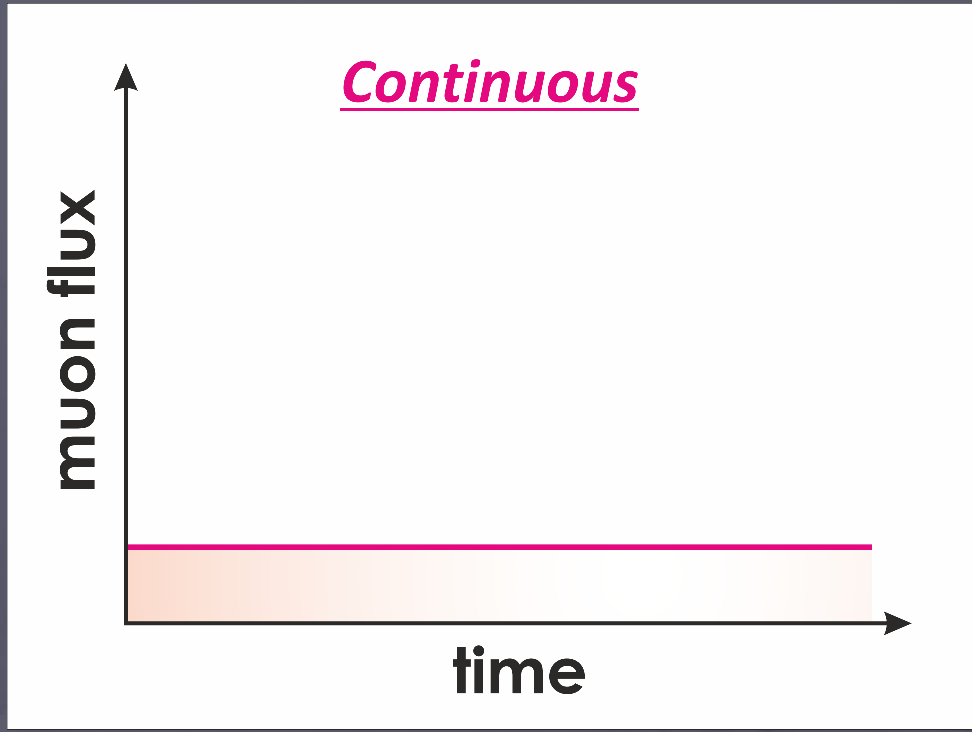

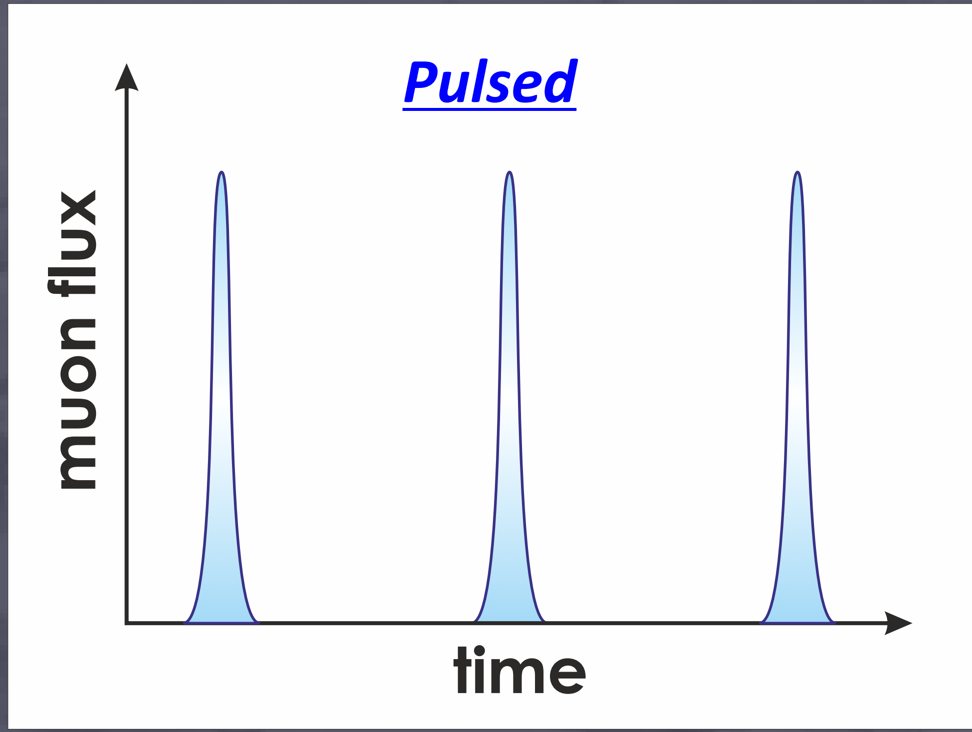

Science & Technology Facilities Council
ISIS
J-PARC

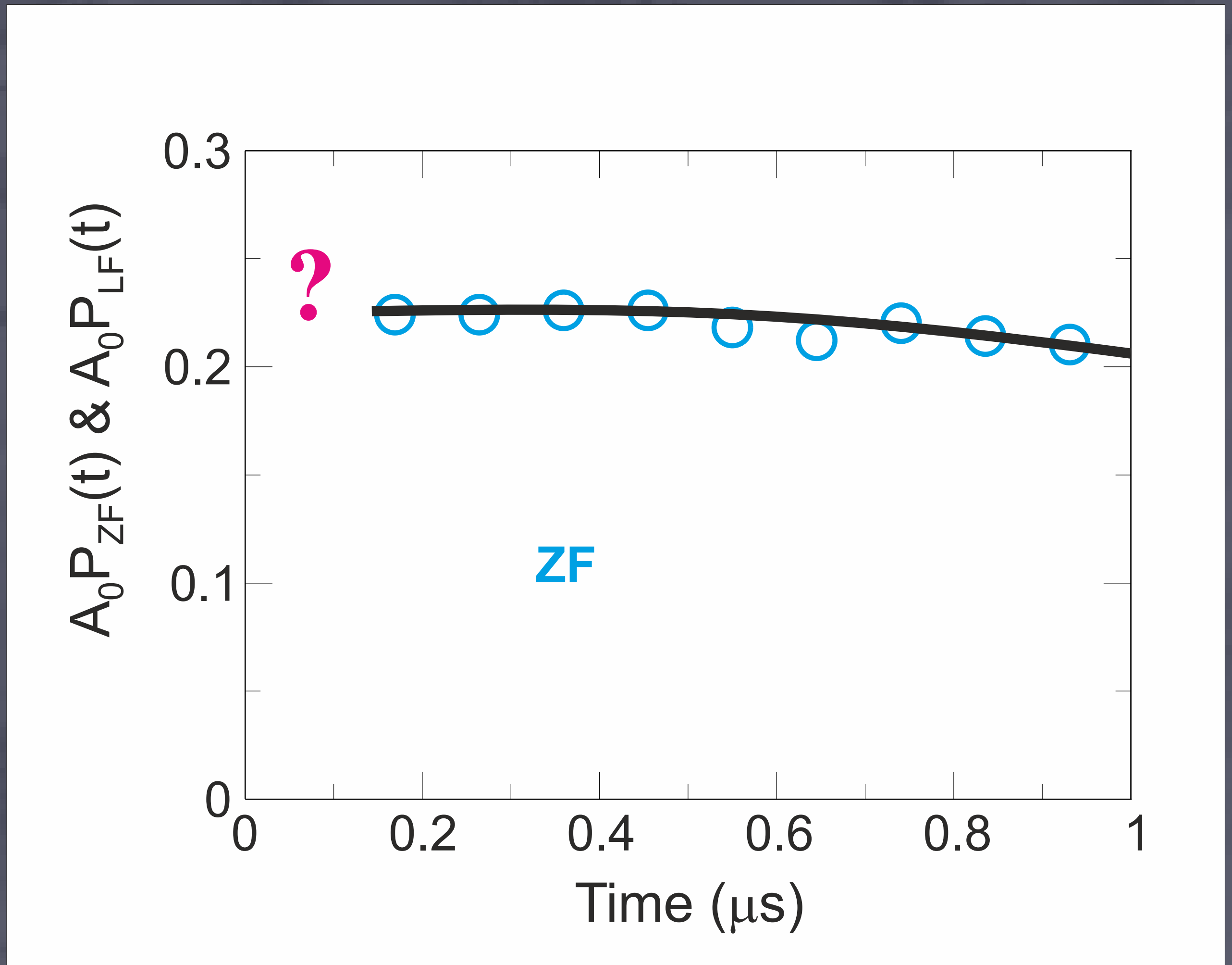

Pulsed vs. Continuous Muon Source

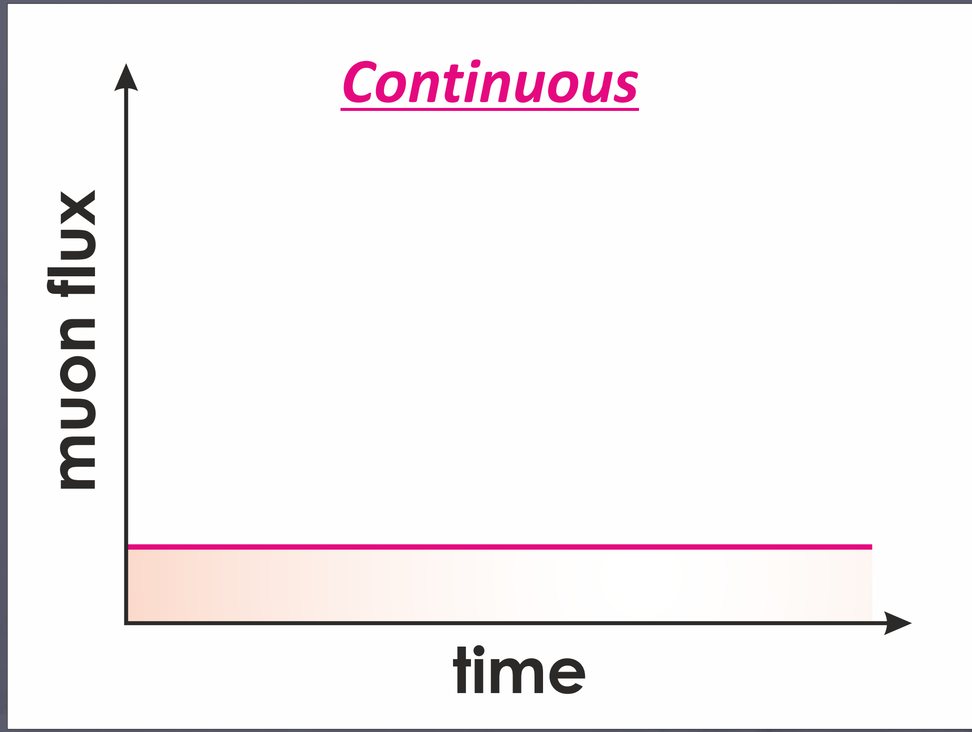

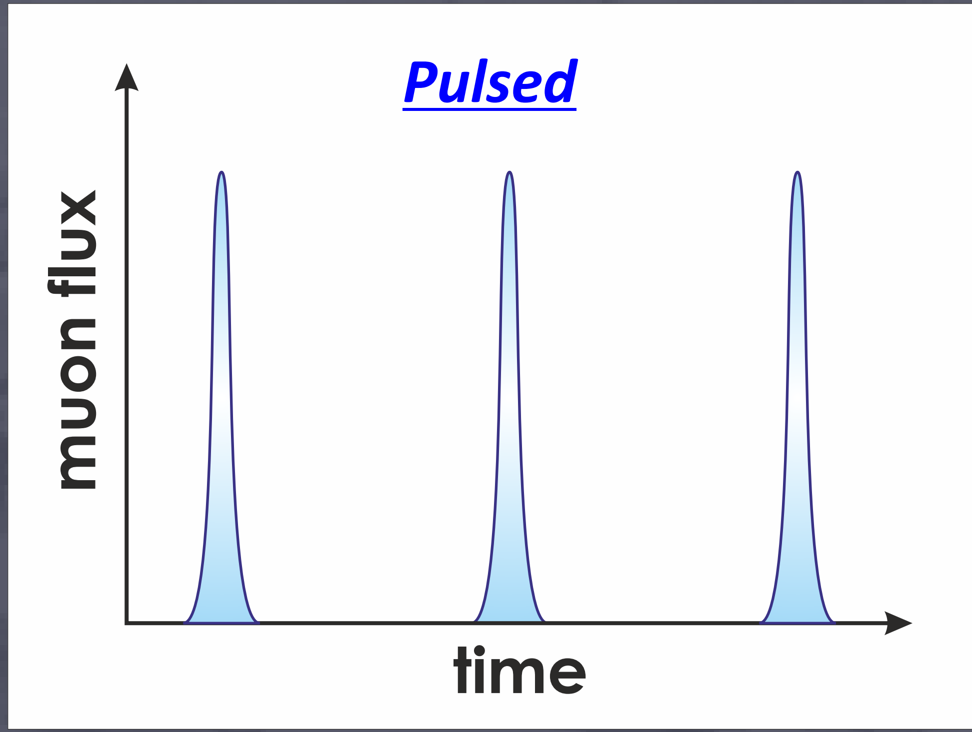

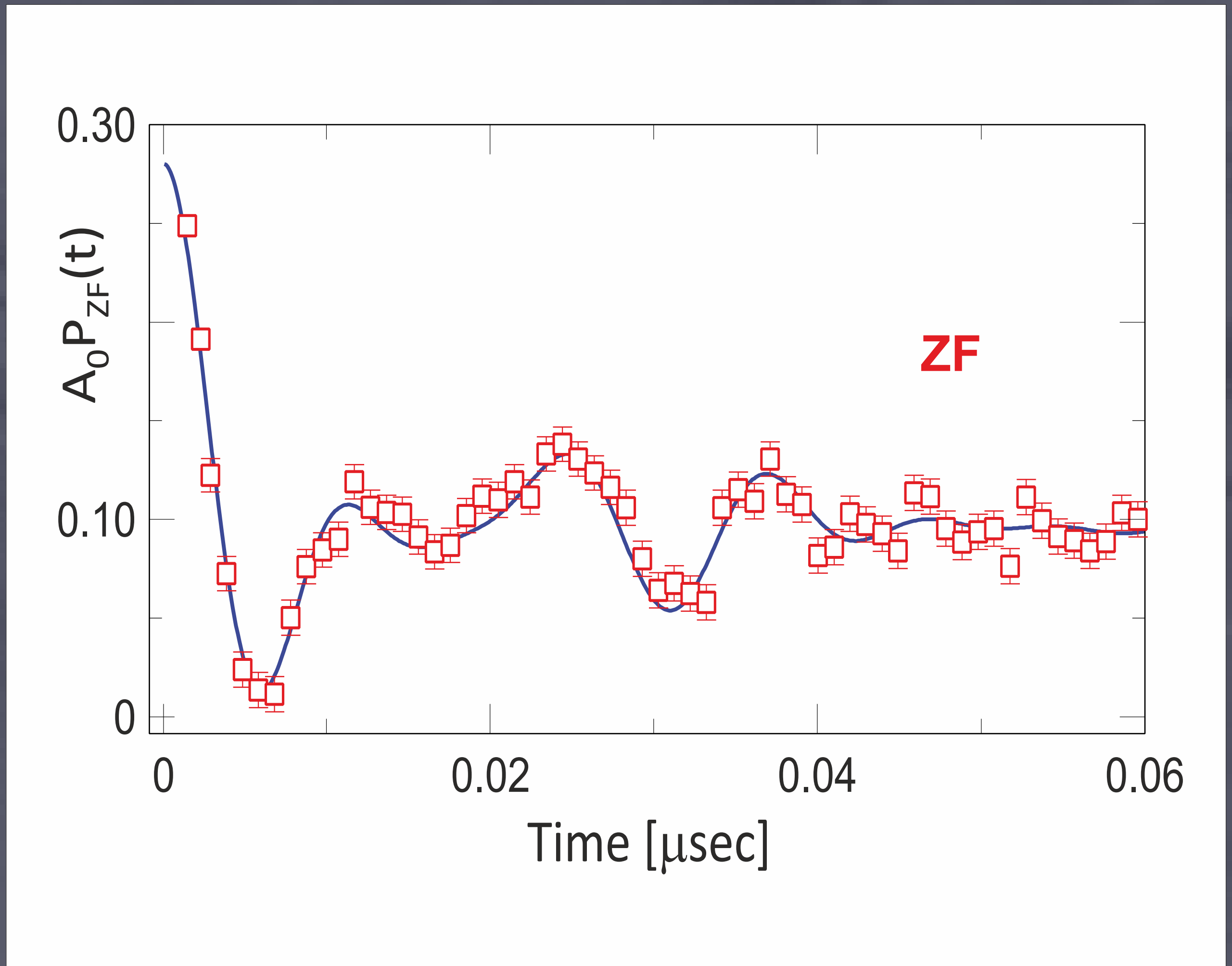

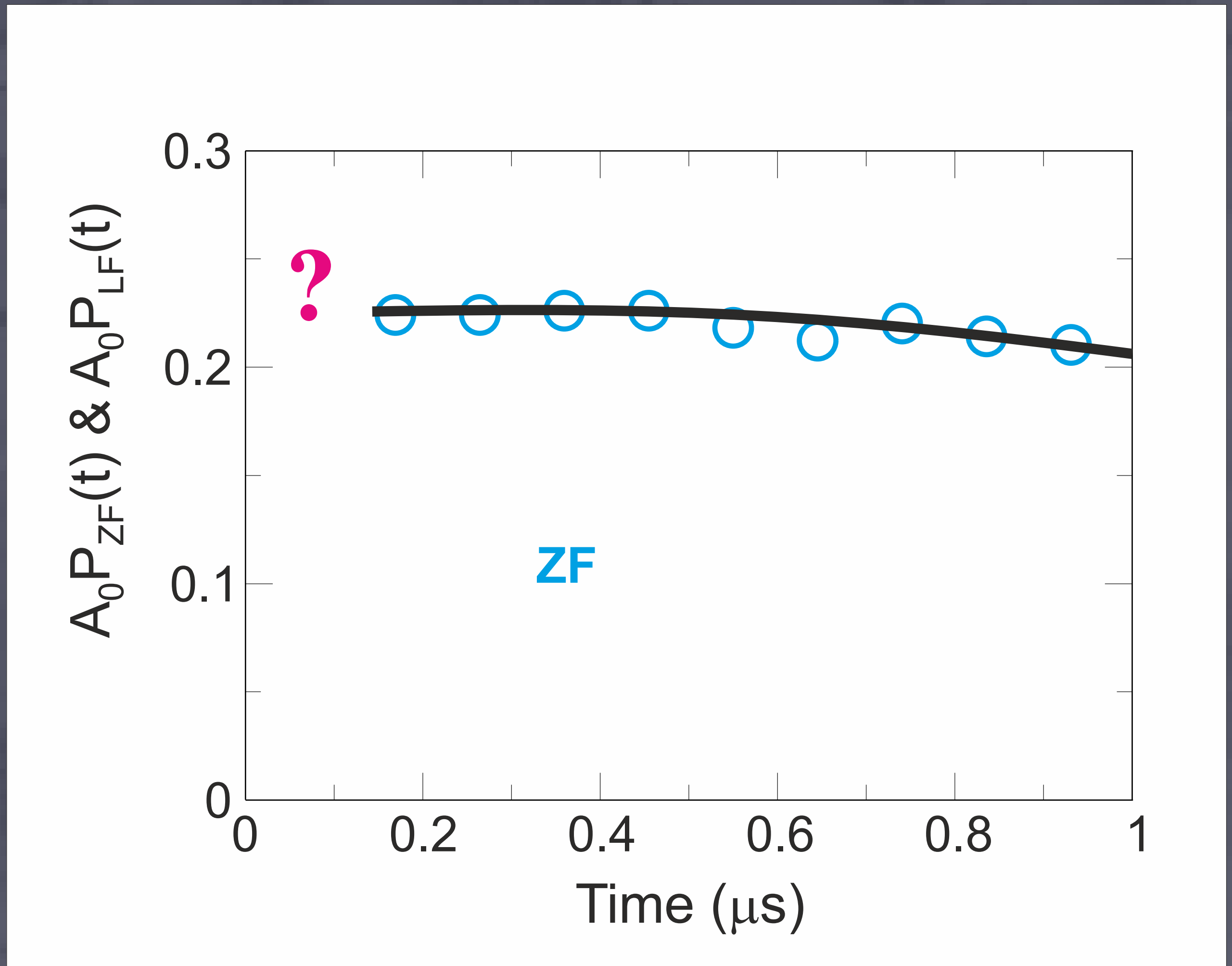

Pulsed vs. Continuous Muon Source

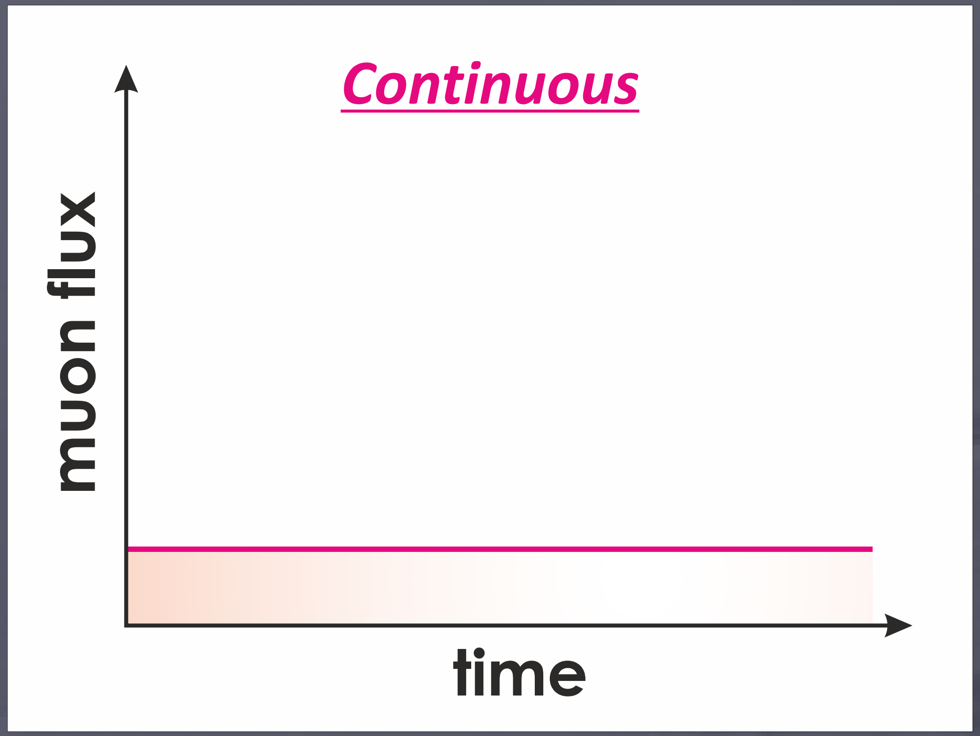

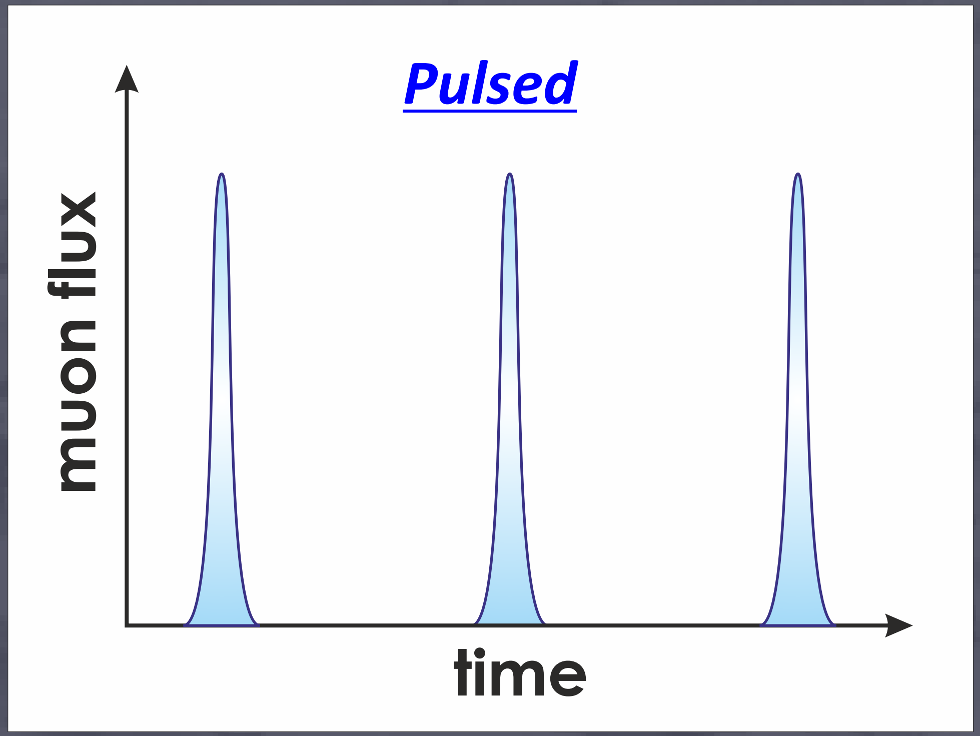

- Low flux = ‘One muon at the time’
- Few positron detectors
- Shorter total time window
- Better time-resolution (high frequencies)
- Study static magnetic order + fast dynamics
- Sample size 0.05 - 1 gram

- High flux = “many muons at the time”
- 100 positron detectors
- Longer total time window
- Low time-resolution (low frequencies)
- Study magnetic dynamics, nuclear spins, etc.
- Sample size 0.3 - 2 gram

Sample Conditions

- General Purpose (1.5 - 300 K, 0 - 4000 G)

- Low-temperature (10 mK)

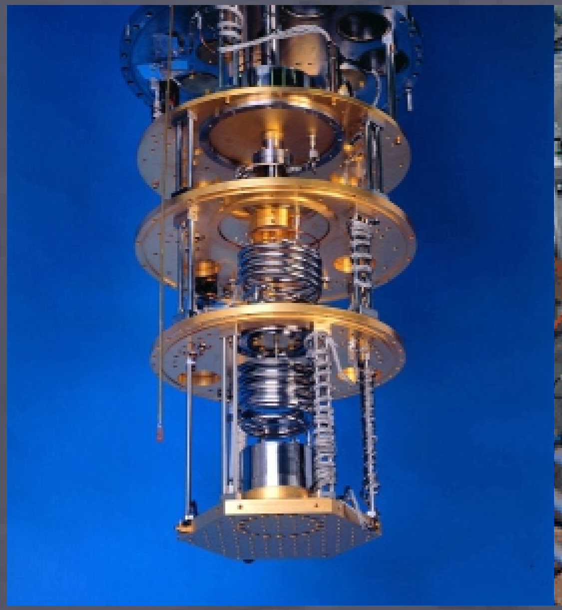

- High-field (0 - 9.5 T)

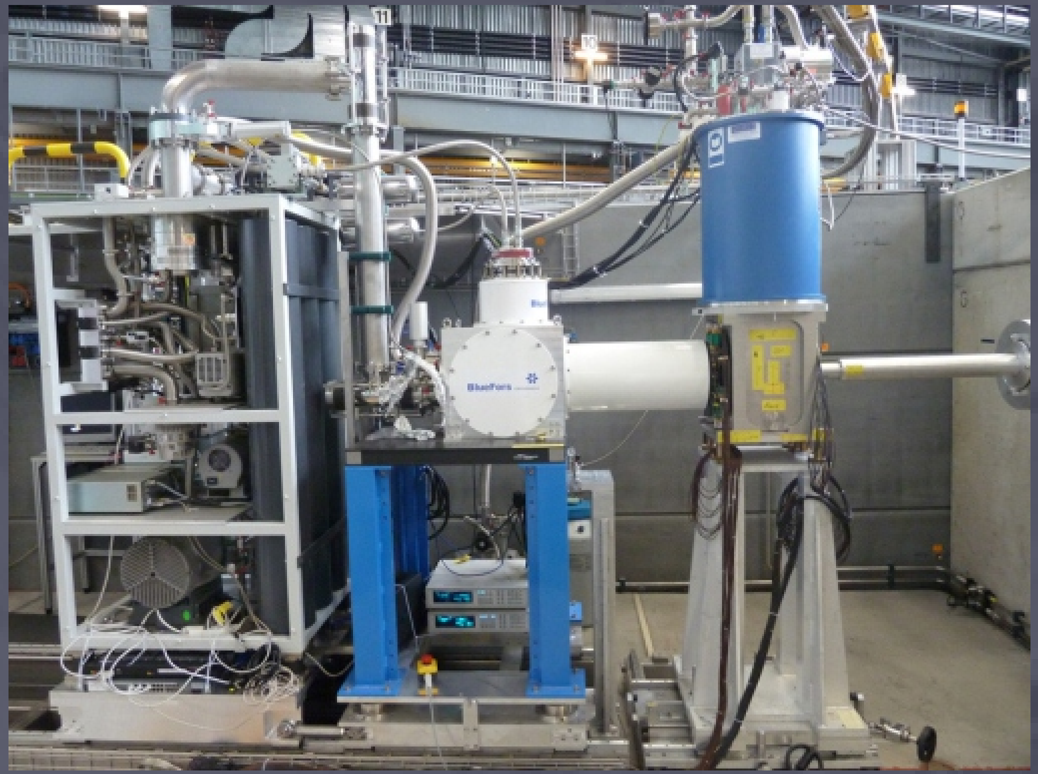

- High-pressure (0 - 35 kbar)

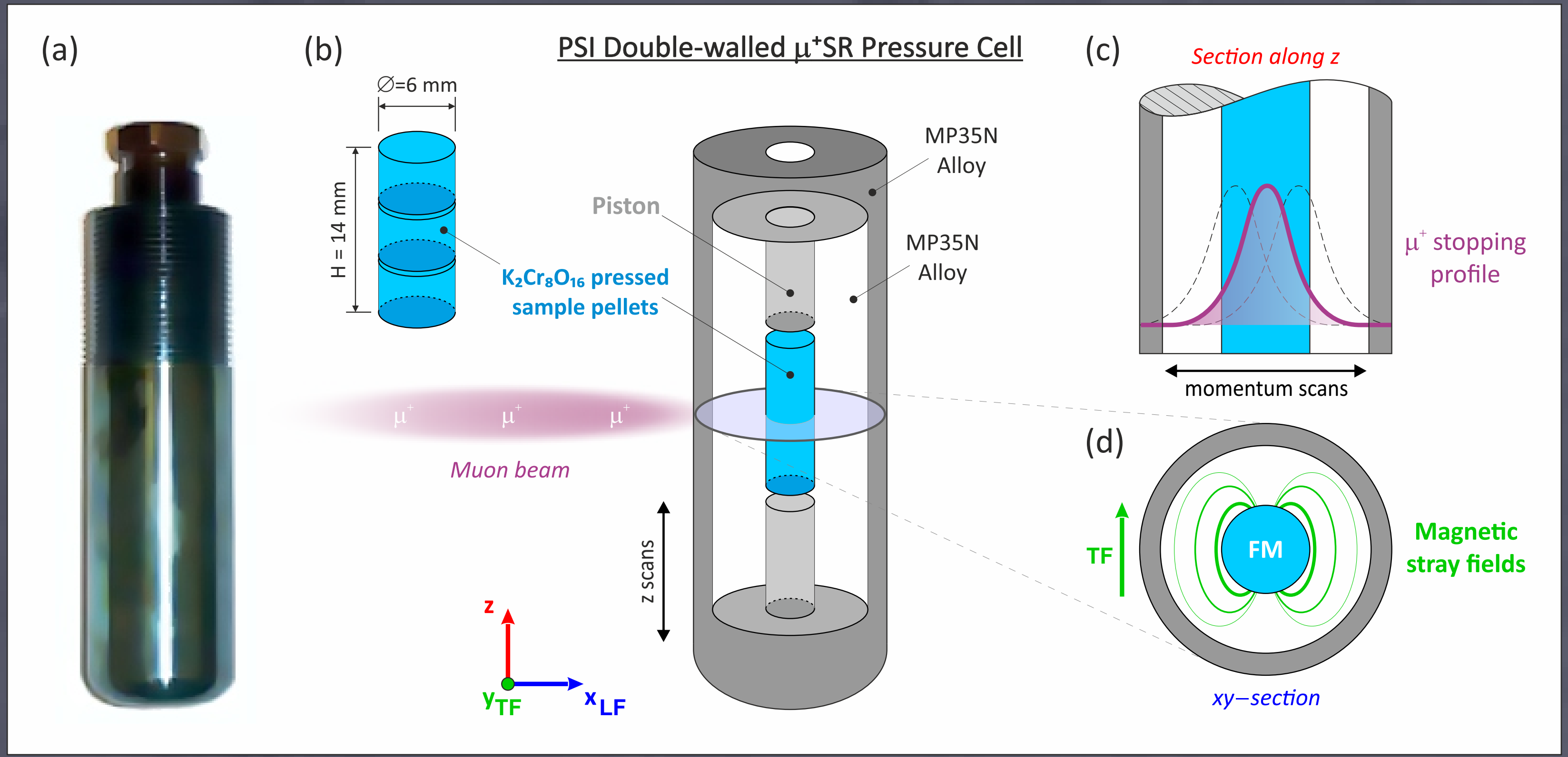

Low-Energy μ^+SR (LEM)

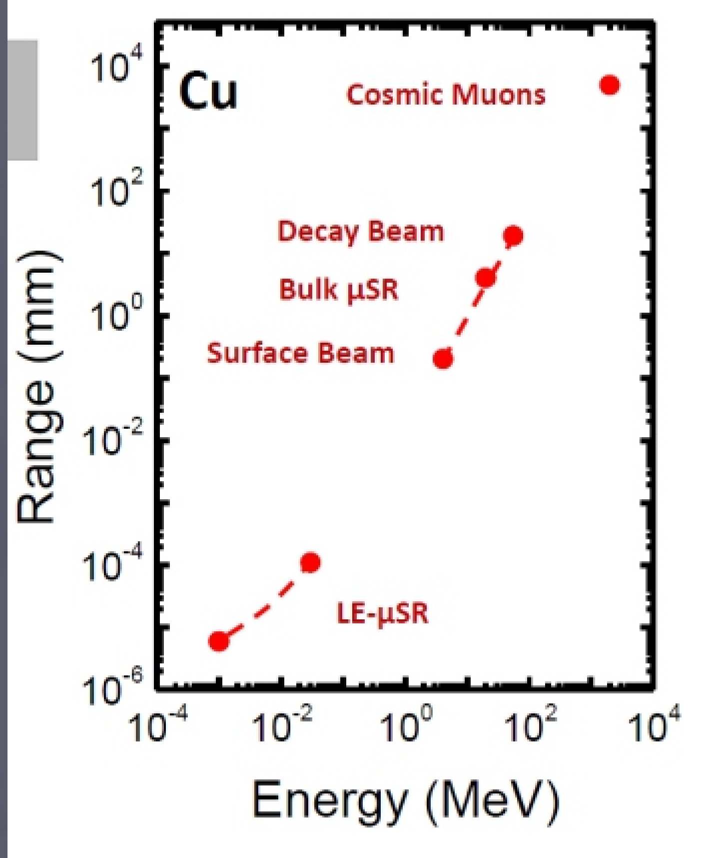

- Muons have very different energy depending how they were created
- A special sub-section of μ^+SR is the LEM technique where slow muons are utilized, which is only available at PSI (soon also J-PARC)
- Open the door to studies of thin films (> 'few' nm) and multi-layers (< 500 nm)
- By tuning the muon implantation depth one can study *e.g.* spin order in all the individual layers including their interfaces !!!

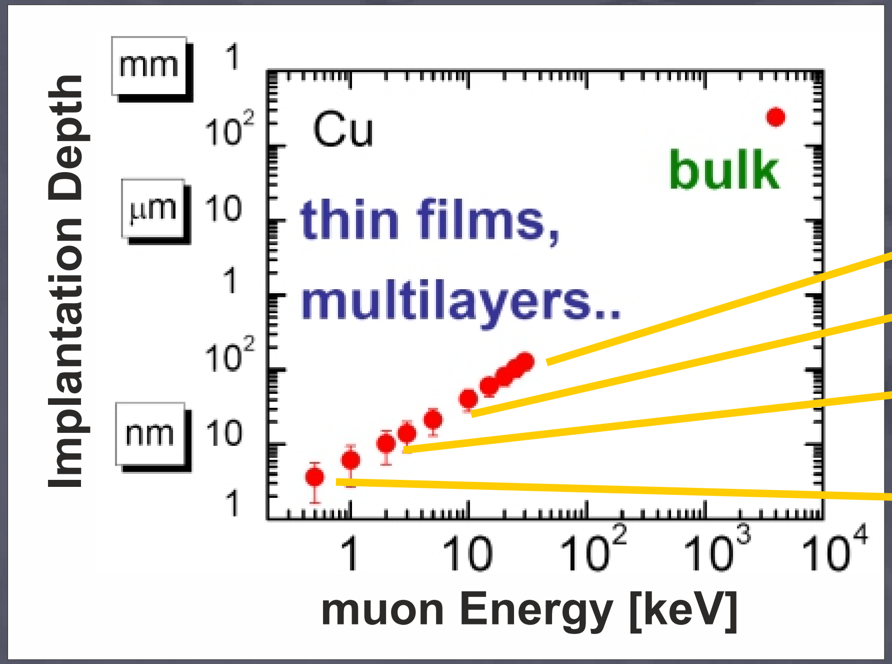

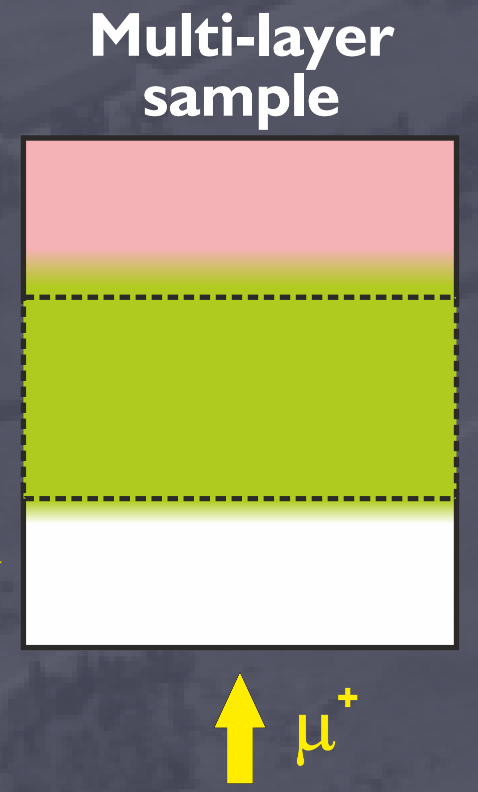

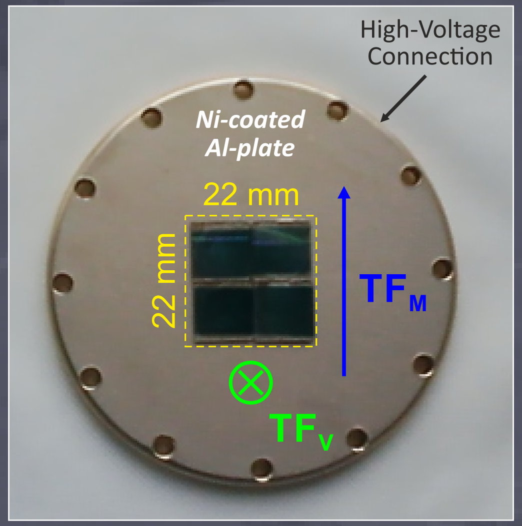

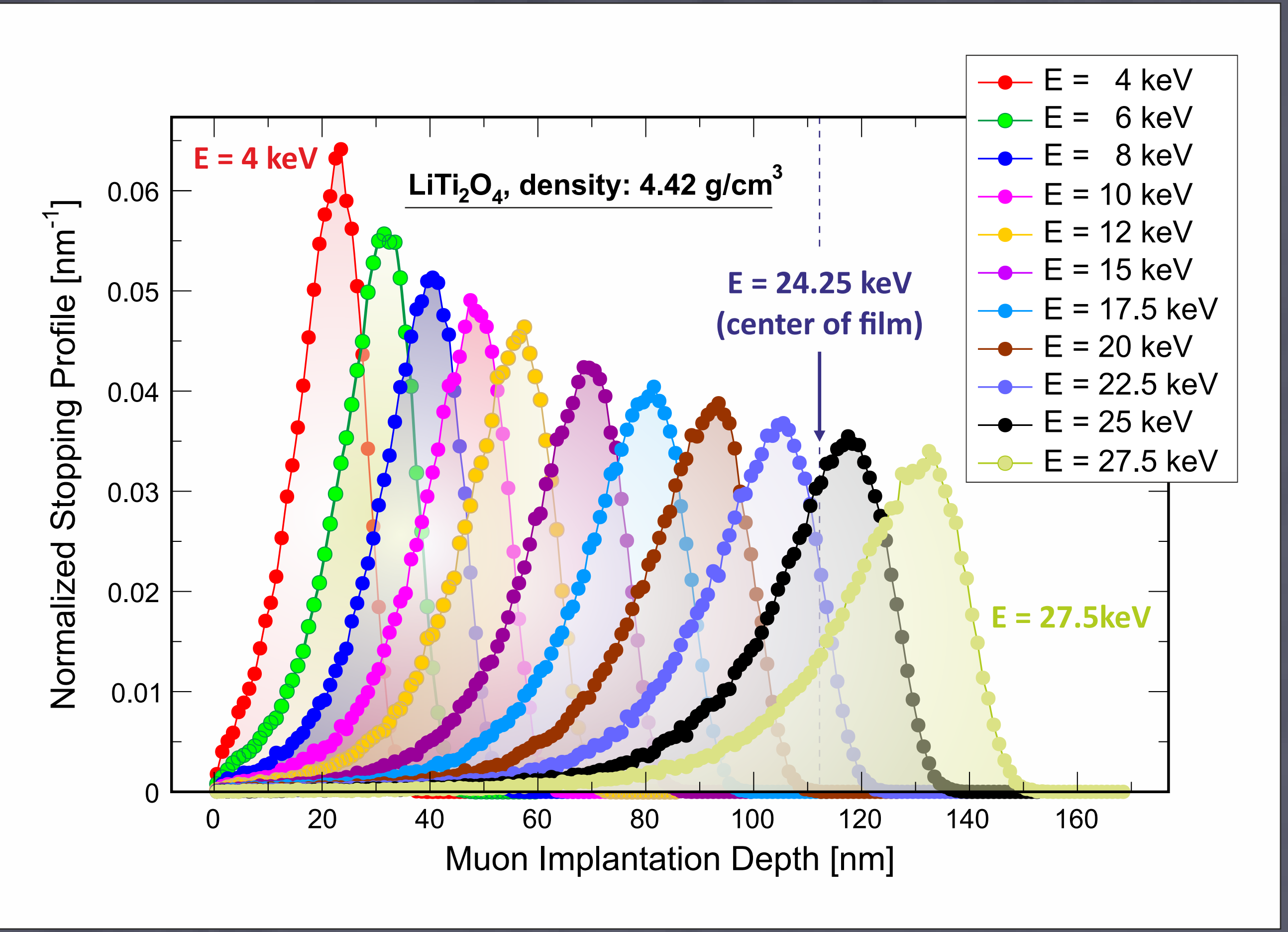

Some Science Examples Covered by μ^+SR

- Magnetic order + spin dynamics

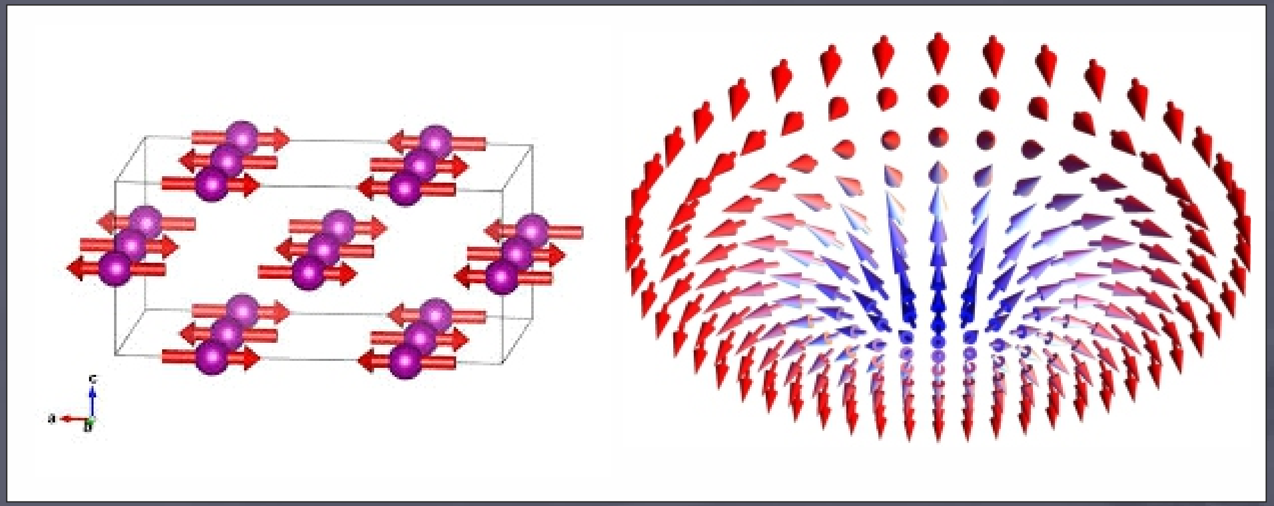

- Charge Carrier Dynamics

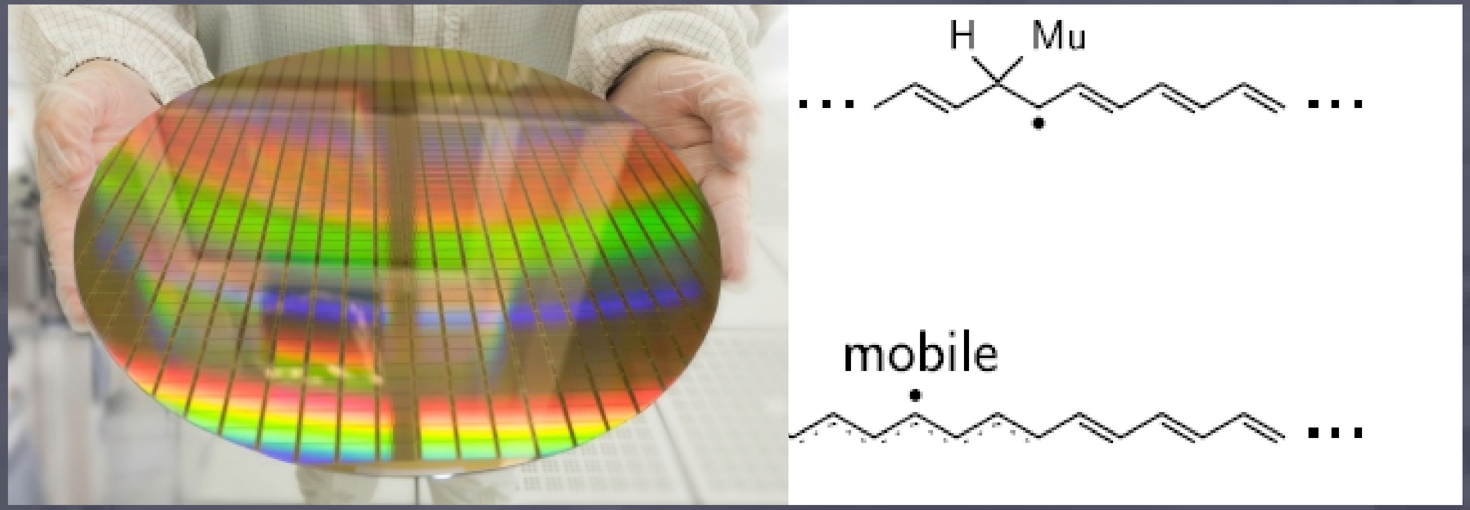

- Superconductors

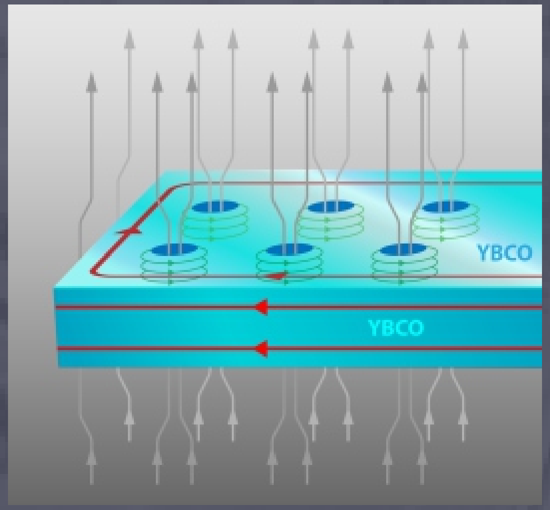

- Ion-dynamics in energy materials

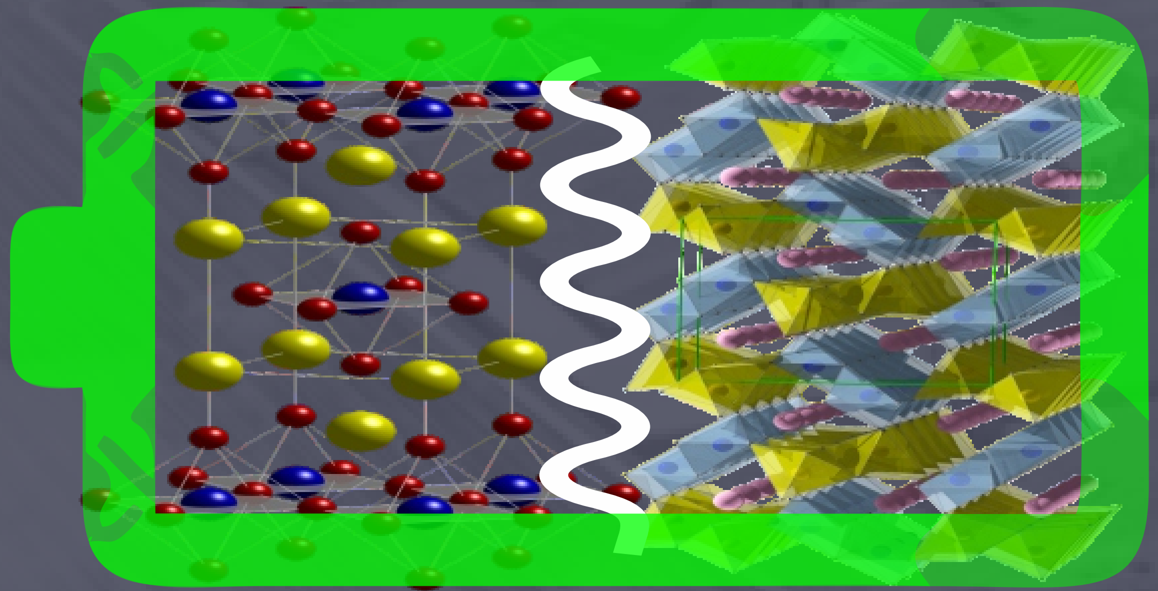

- Quantum Phase Transitions

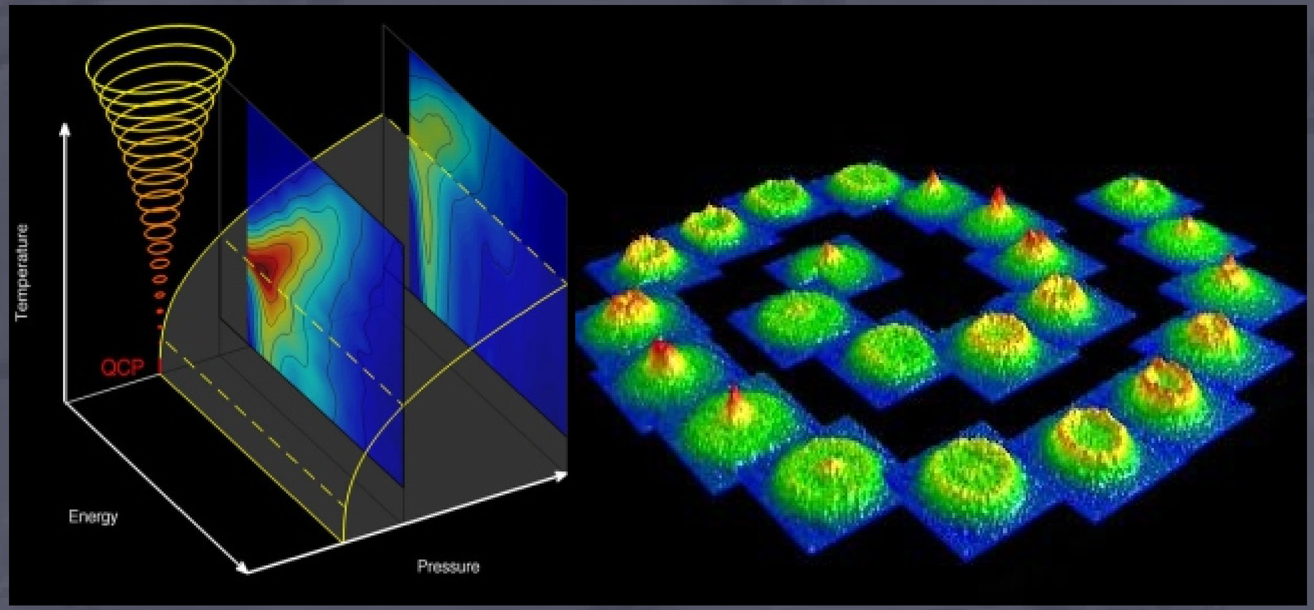

- Polymer Dynamics

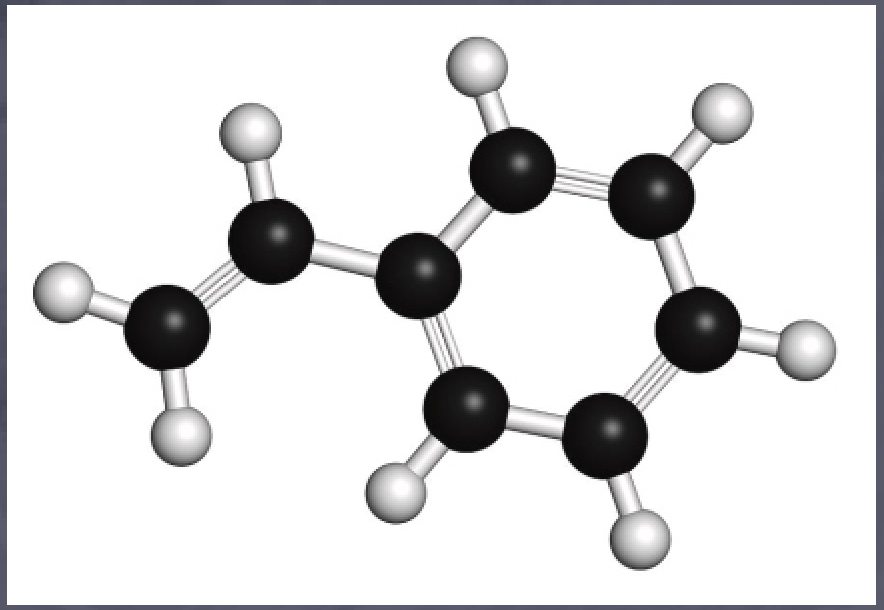

Example #1
Quantum Phase Transition in PHCC
High-pressure Muon Spin Rotation/Relaxation

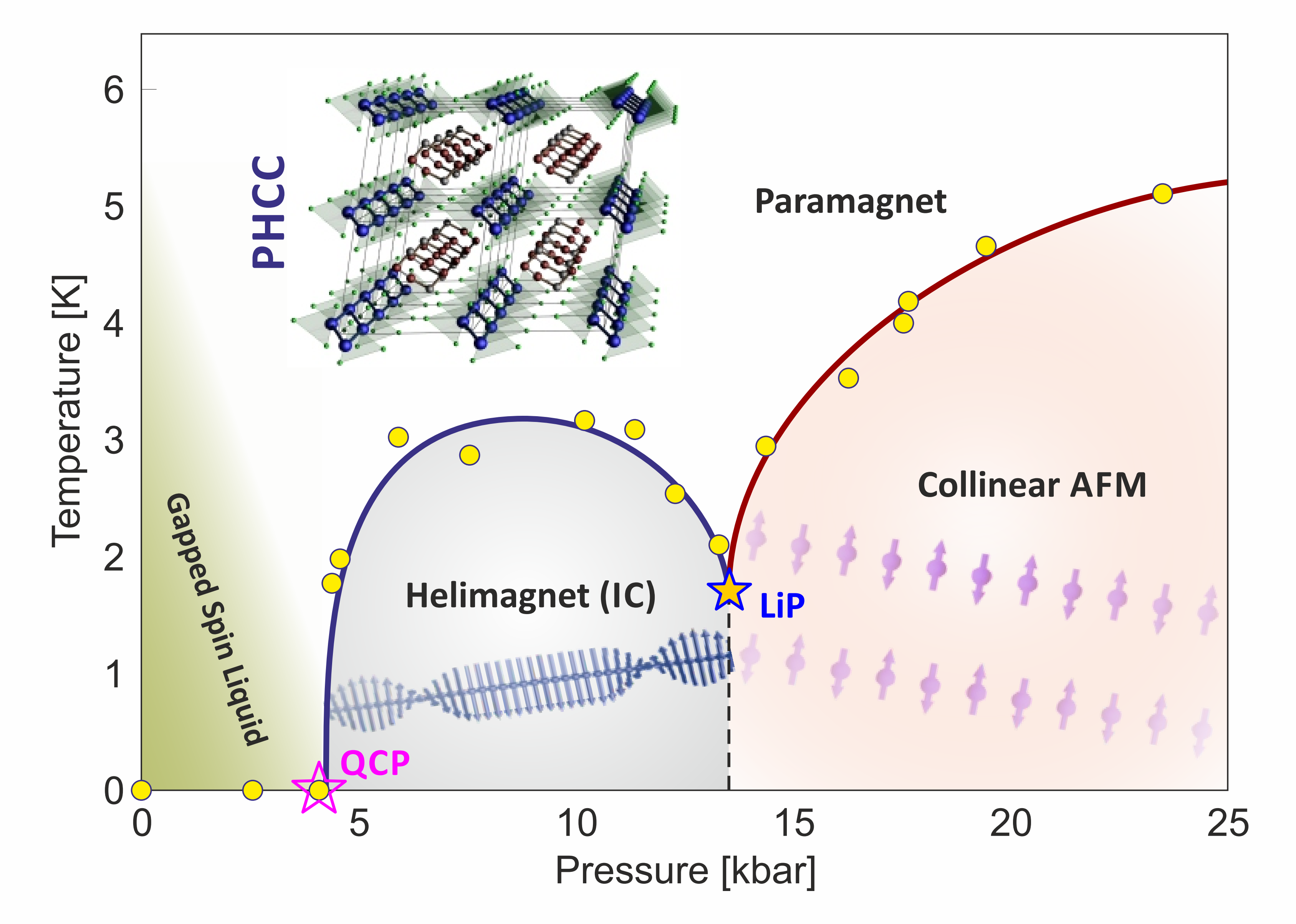

M. Thede, M. Mansson *et al.* Phys. Rev. Lett. 112, 087204 (2014)

PHCC

- 'Our' organometallic model compound of choice is *Piperazinium hexachloro-dicuprate* or PHCC = $[C_4H_{12}N_2][Cu_2Cl_6]$
- PHCC crystallizes in a triclinic P-1 space group.
- Large single crystals (10×10×25 mm), m ≈ 2 grams, fully deuterated.

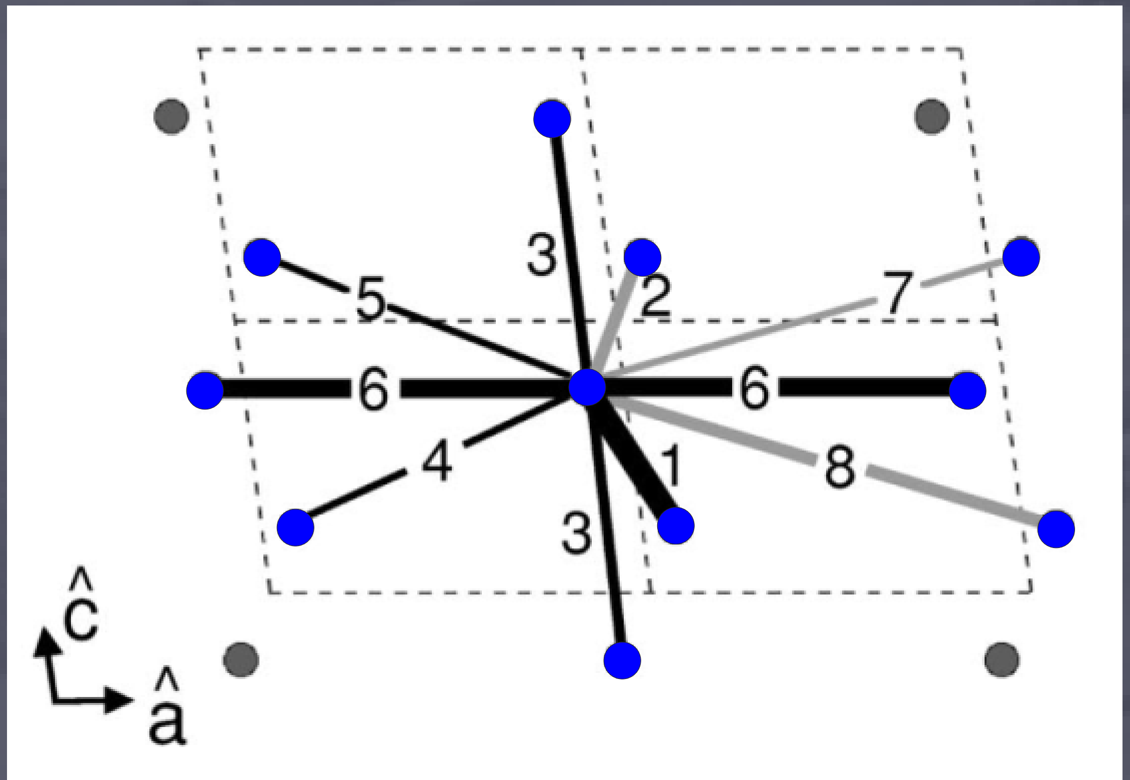

- Display a Cu-Cl sheets spanning the ac-plane
- Features a complex spin network of $S = ½$, Cu^{2+} ions bridged by 8 possible (3 frustrated) Cu–Cl–Cl–Cu superexchange pathways.

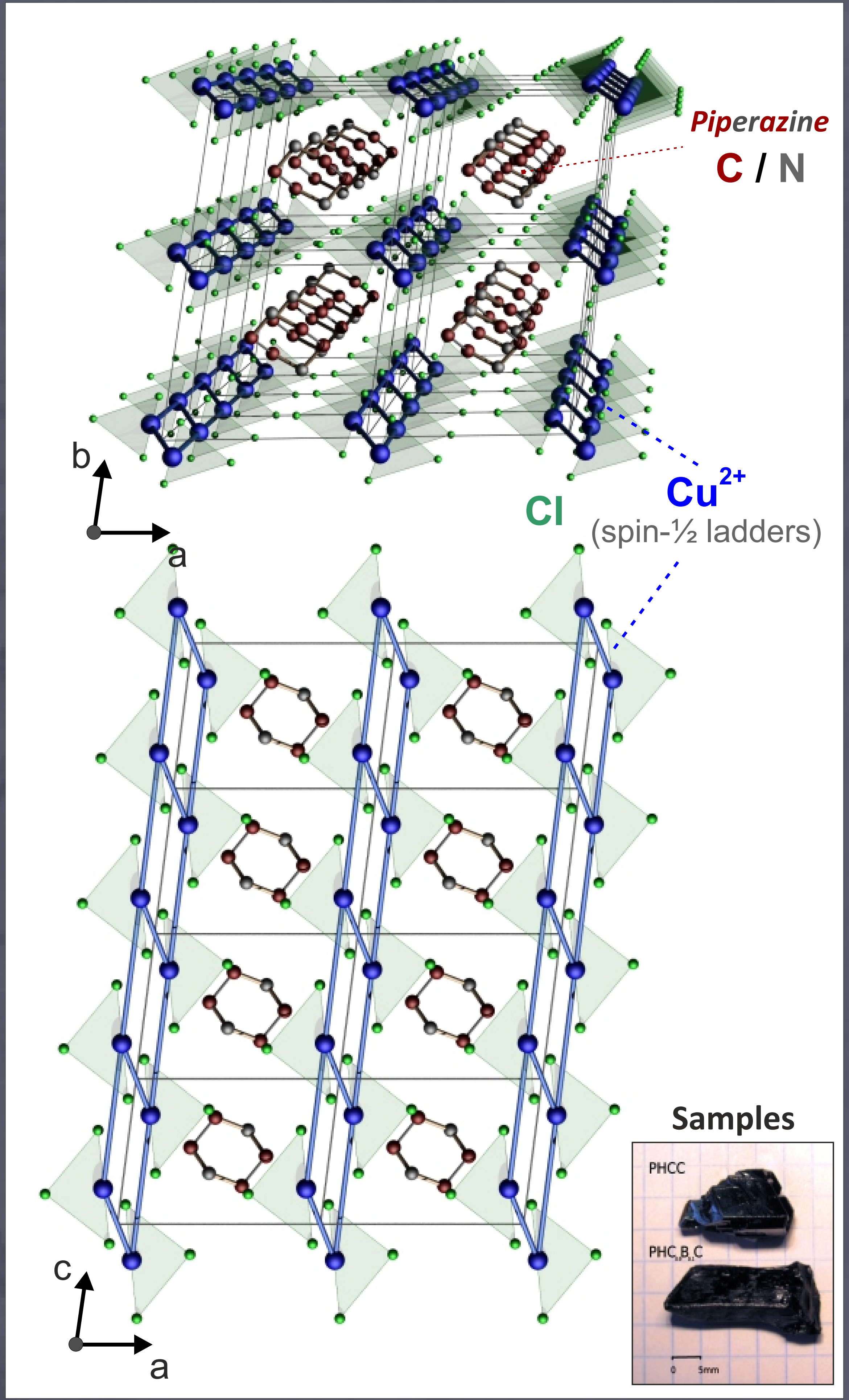

- Within the planes the Cu-ions seem to form slightly skewed spin-ladders along the c-axis.

PHCC: Spin Liquid

- PHCC does not order even at lowest temperature (*e.g.* no magnetic Bragg peaks)

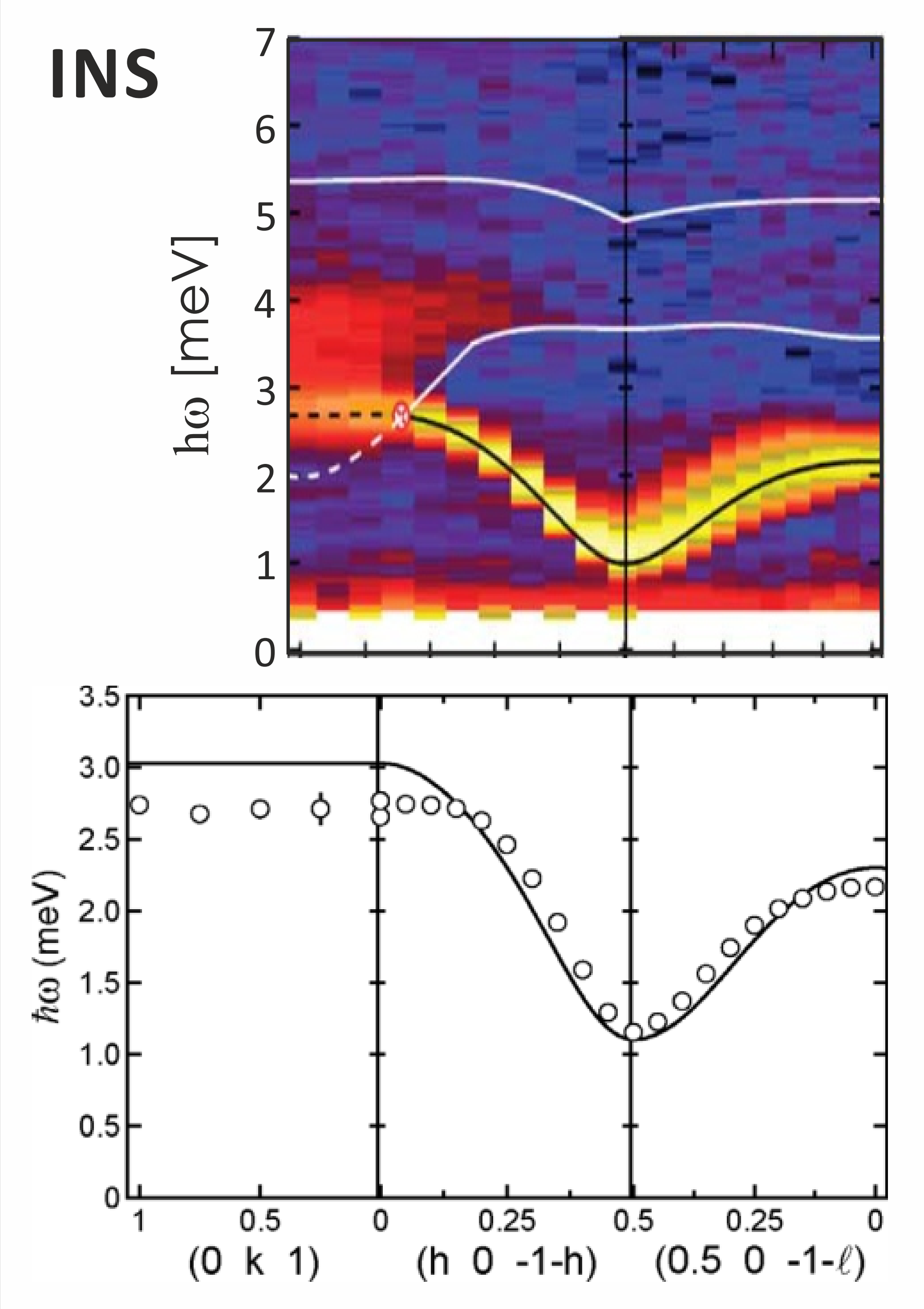

M.B. Stone et al. Nature 440, 187 (2006)

- Susceptibility data $\chi(T)$ show an exponentially activated dependence characteristic of a gapped Heisenberg antiferromagnet (+ PM background).
- The magnetic excitation spectrum (INS) is dominated by a single propagating mode with a clear singlet/triplet gap Δ = 1 meV and magnon band-width of 1.8 meV in the $(\mathrm{h}\ 0\ \mathrm{l})$ plane.
- Some information on exchange constants could be given but there are up to 6 or even 8 possible exchange pathways so exact Hamiltonian is unknown.
- However, it's clear that the mode has no dispersion along b* indicating that neighboring a-c planes are magnetically decoupled.

Ground state of PHCC is a quantum spin liquid

Field-Induced Magnetic Order in PHCC

- Susceptibility & specific heat show field-induced magnetic order in PHCC: $H_c \approx 7.5$ T / T = 100 mK.
- For low H, specific heat increases at lower T = spin gap is decreasing.
- Neutron diffraction experiments show that a long-range commensurate AFM order is present ⊥ H. ***No signs of an incommensurate order !!!***
- At H = 14 T, order parameter typical for 2nd order phase transition $T_N = 3.7$ K.

M.B. Stone *et al.* New J. Phys. 9, 31 (2006)

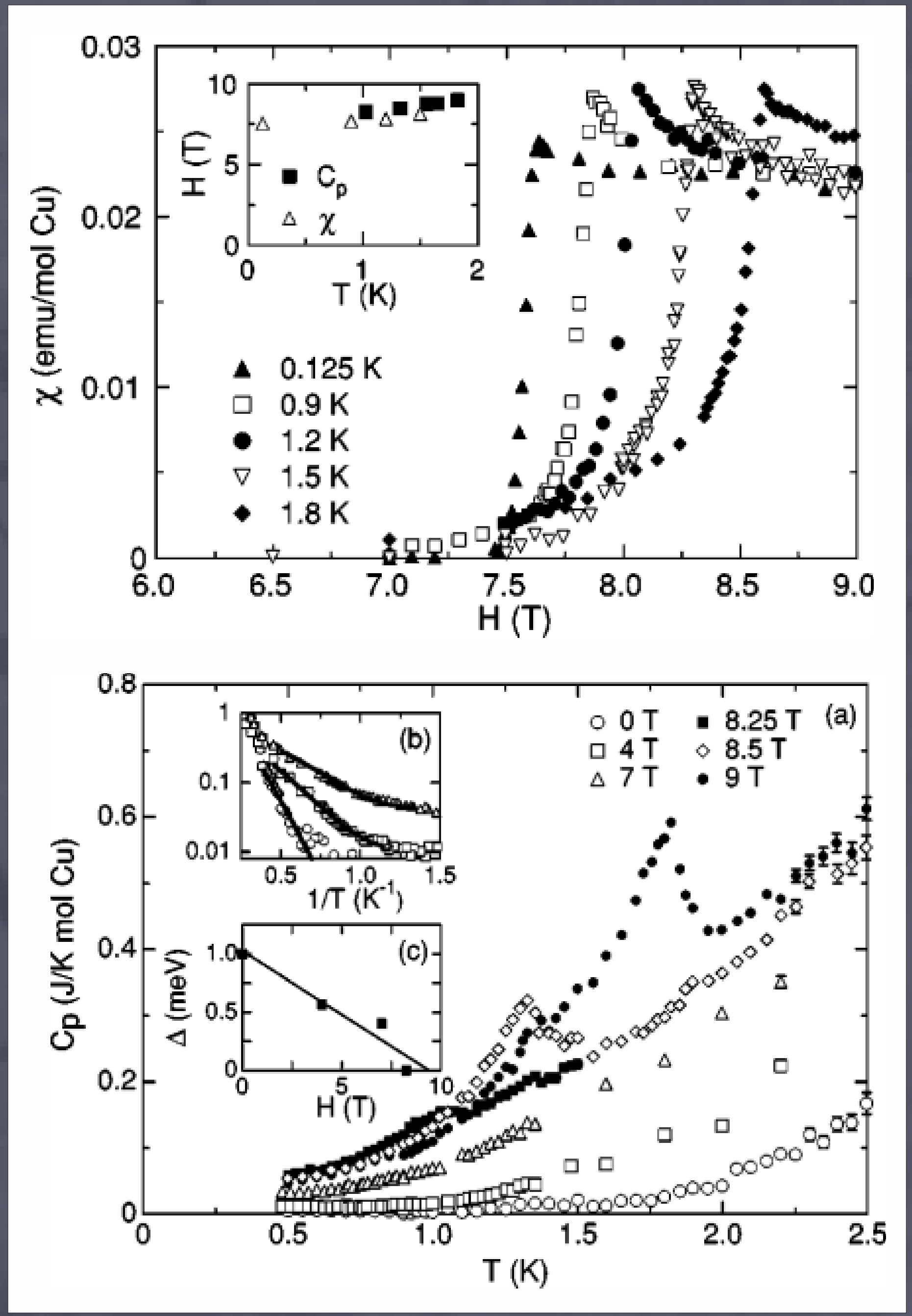

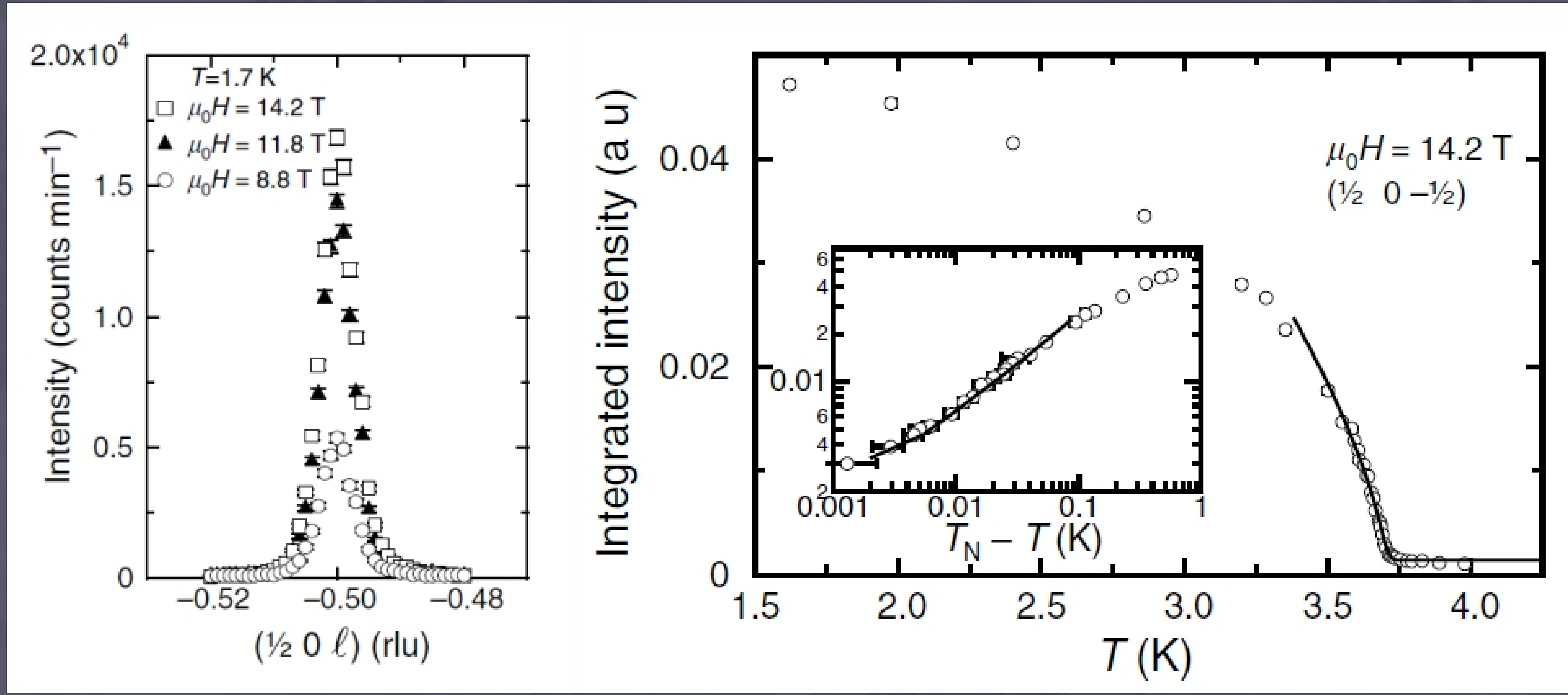

Field-induced Bose-Einstein Condensation in PHCC

PHCC: INS under Hydrostatic Pressure

- BEC can not only be induced by an external field but also other exchange tuning *e.g.* pressure.
- Tao Hong *et al.* performed INS under hydrostatic pressure of PHCC single crystals.
- Show decreasing spin gap with P but signal weakens a lot.
- Indicates a BEC for pure PHCC occuring at $P_c \approx 20$ kbar.

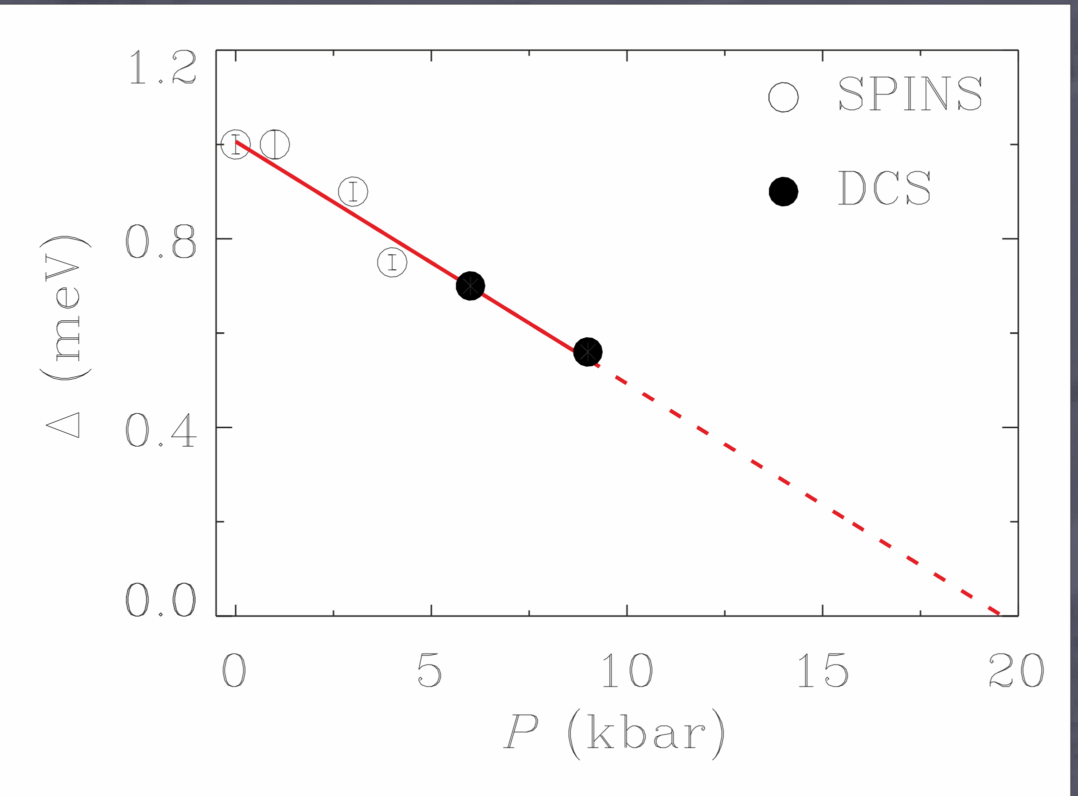

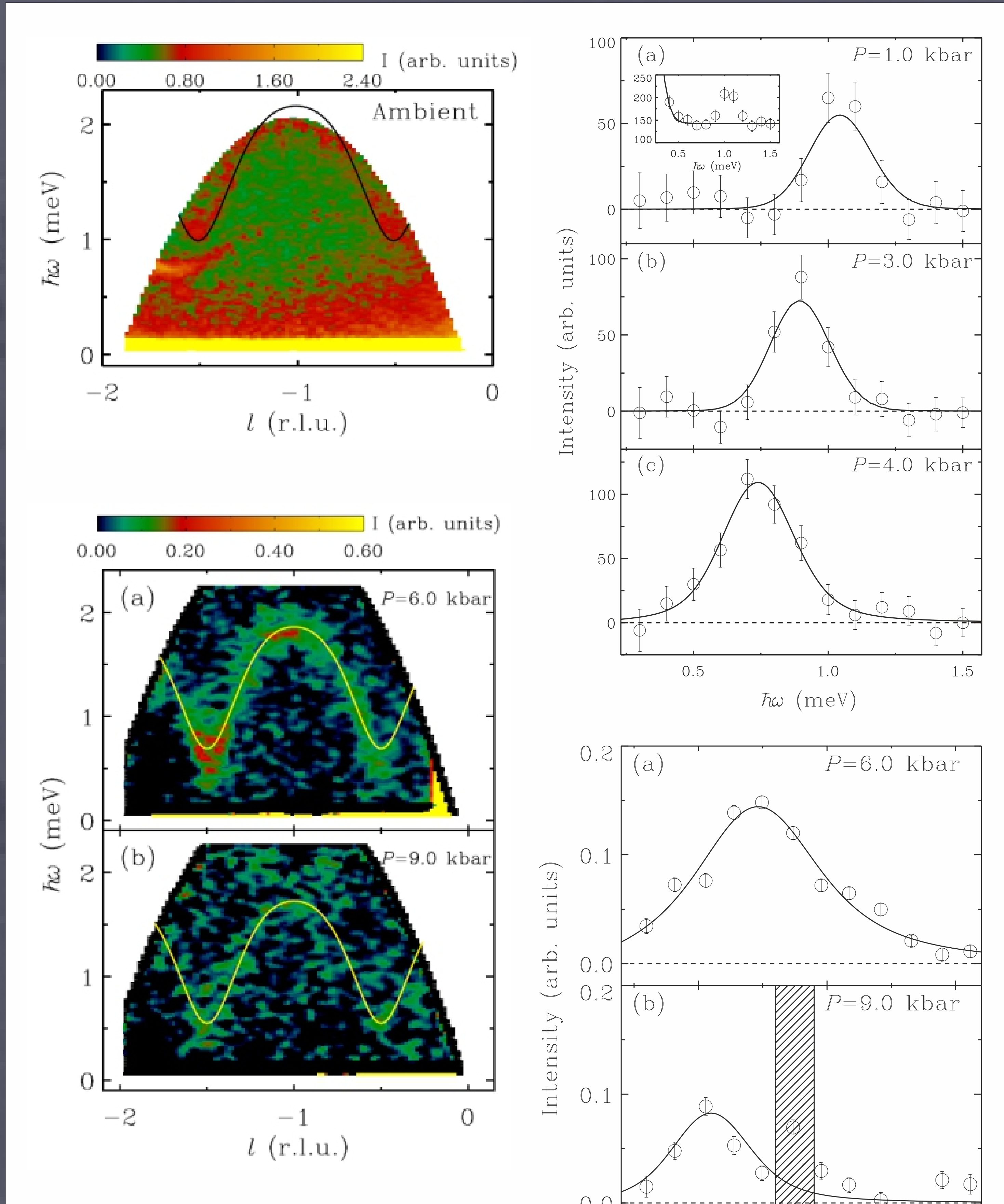

T. Hong *et al.*
Phys. Rev. B 82, 184424 (2010)

Ambient Pressure μ^+SR

- To verify the ambient pressure properties using μ^+SR we have conducted ZF and LF measurements of PHCC/X using the GPS and LTF spectrometers at PSI.

- ZF at T = 10 mK show clear absence of static LRO and only an exponential decay i.e. indication of either static SRO <u>or</u> spin dynamics.

- LF decoupling data clearly rules out SRO and as expected PHCC/X show strongly dynamical spins due to low-temperature quantum fluctuations.

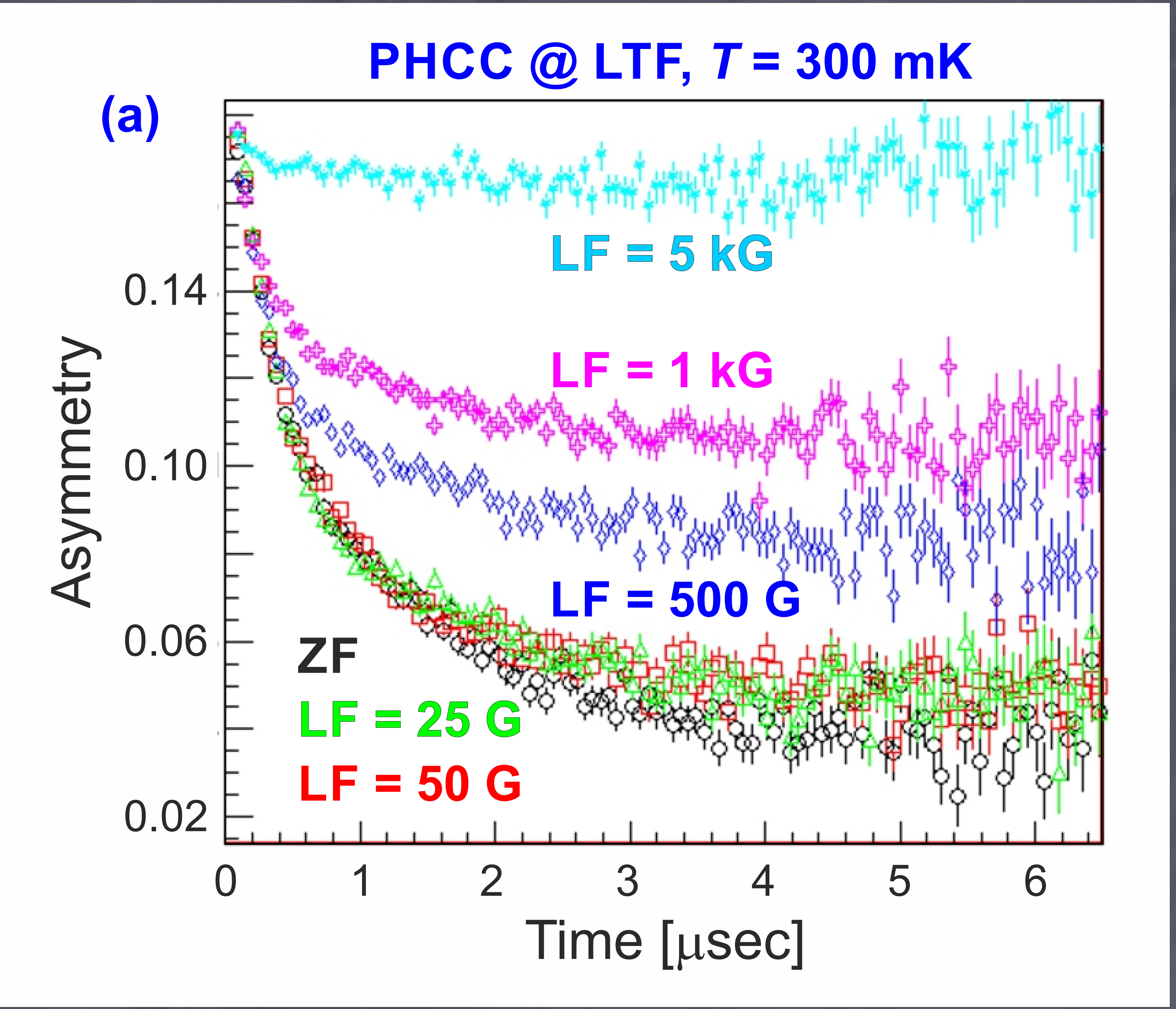

PHCC @ p = 24 kbar

- ZF μSR at P = 24 kbar and T = 270 mK show clear oscillations in the time-spectrum, which is a clear sign of static magnetic order.

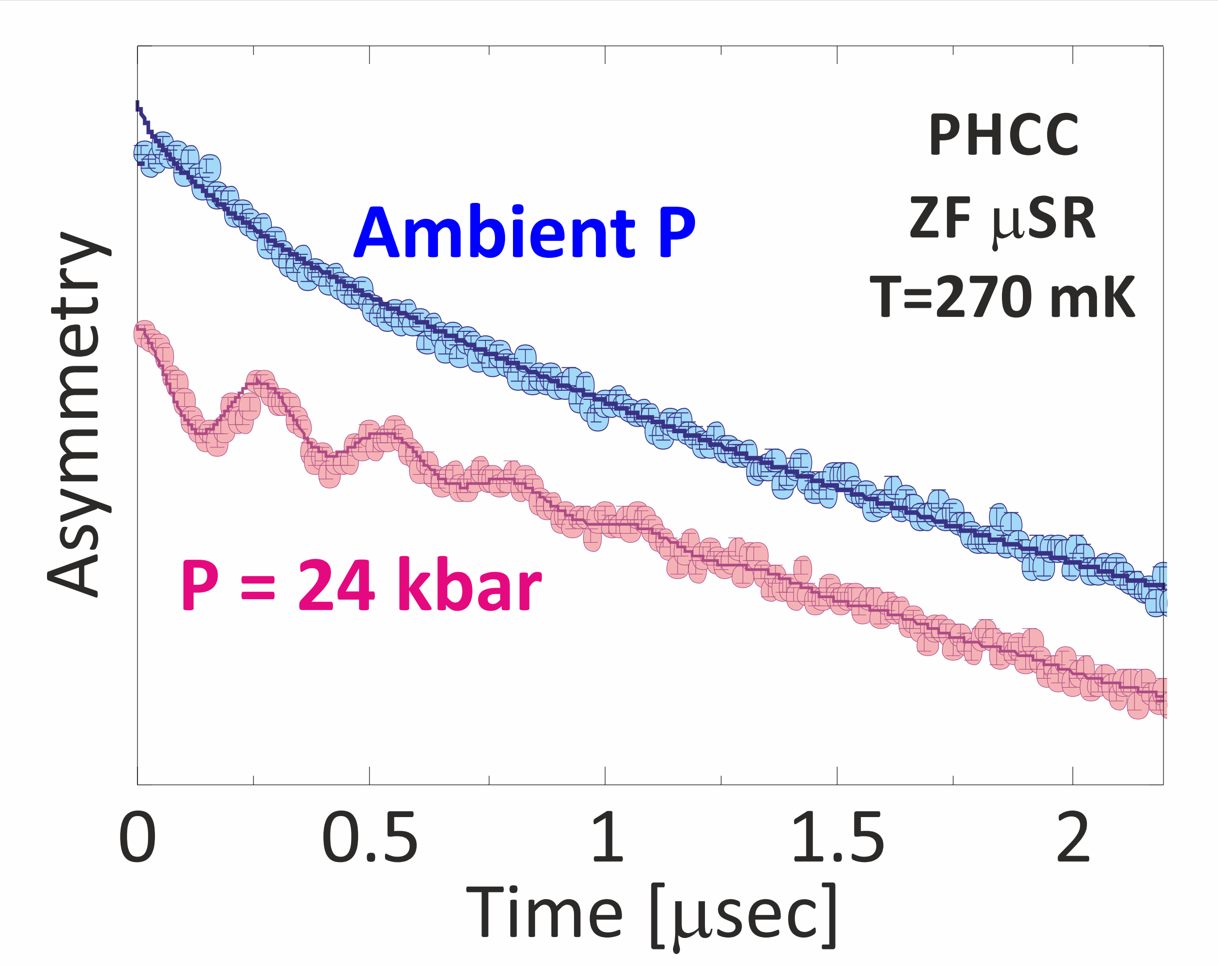

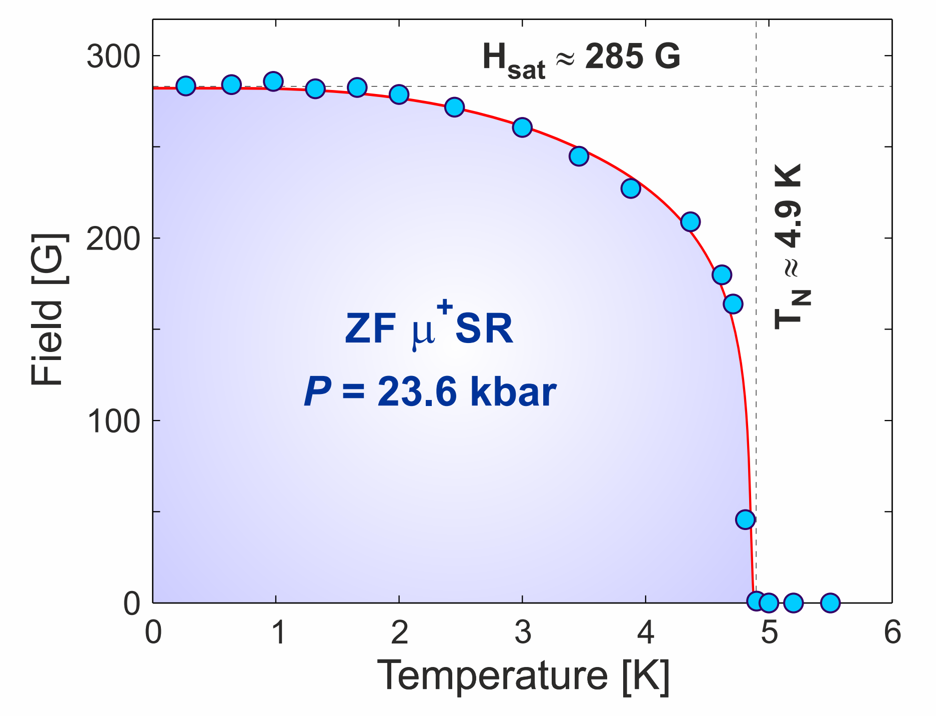

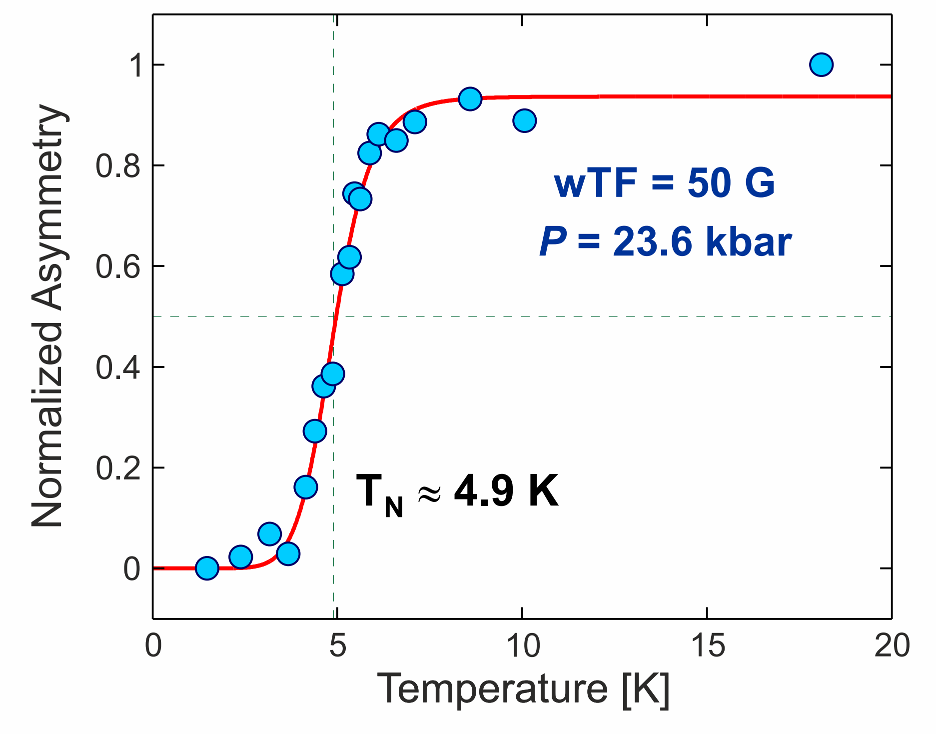

- Temperature dependent ZF data reveal the order parameter indicative of a second order phase-transition.

- ZF and wTF data both clearly show a transition temperature T_N = 4.9 K.

Very first Pressure-induced BEC in PHCC !!!

Systematic P/T Data

- We conducted systematic μ^{+}SR measurements as a function of both P & T.
- Surprisingly (c.f. Tao Hong INS data!!!) we find that magnetic order is already present for P_C > 4.3 kbar.
- ZF data show a strong but 'discontinuous' *P* dependence on the H_{sat} (muon frequency) and T_N.

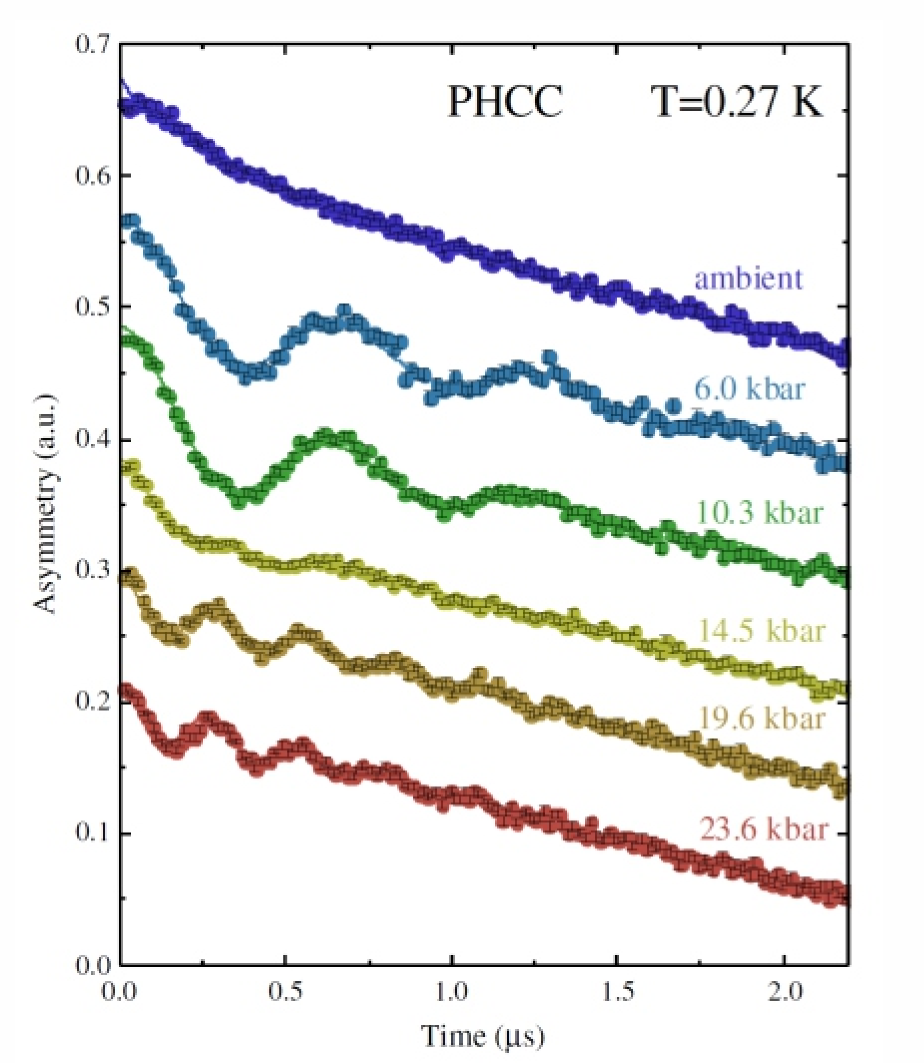

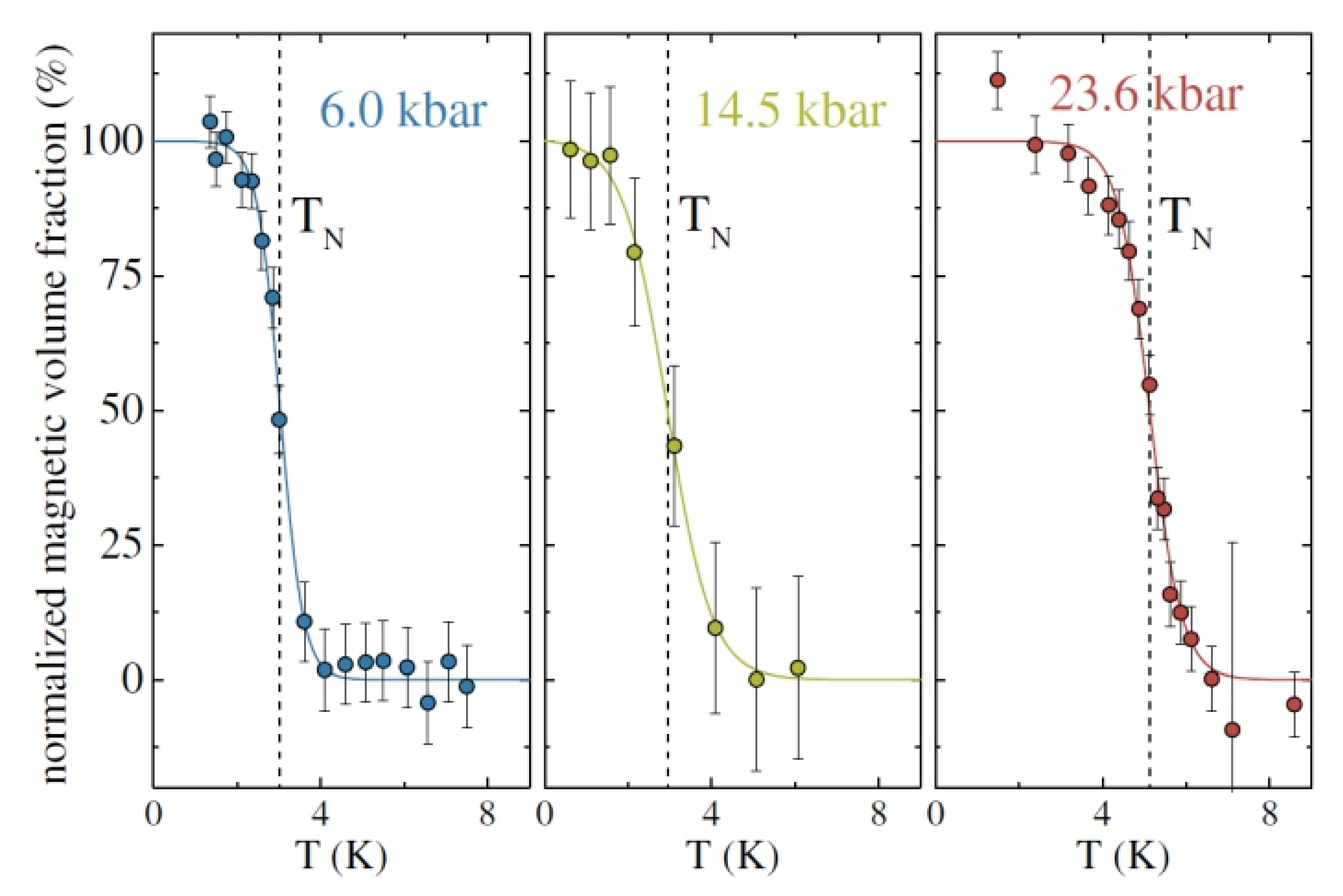

- wTF data supports the pressure dependence of T_N. This allow us to deduce a tentative P/T phase-diagram...

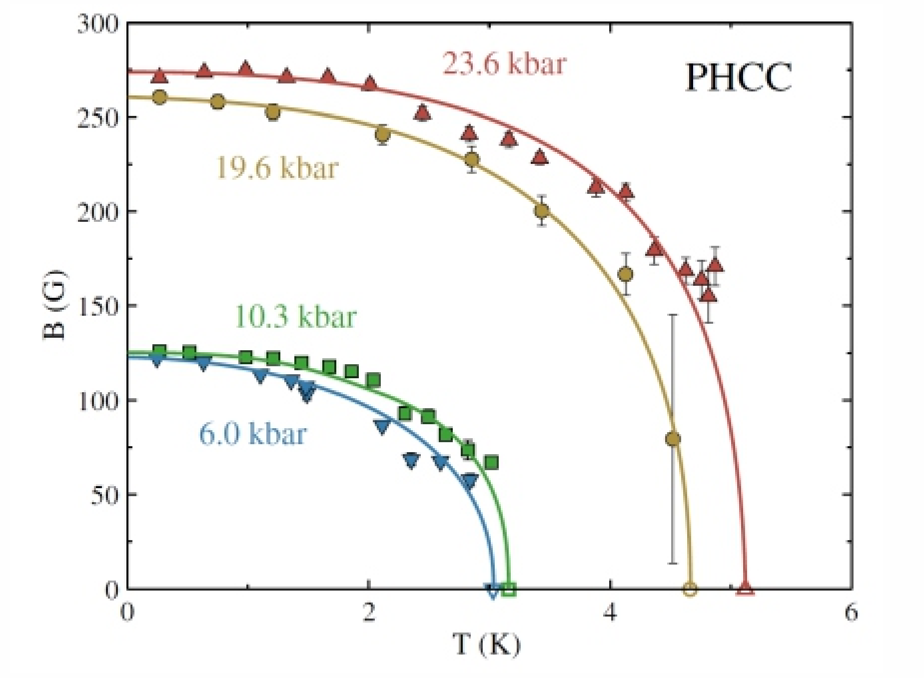

Tentative P/T Phase Diagram

- **Combining ZF and wTF μSR data we can construct a tentative phase diagram.**
- **This clearly highlights the discontinuous behavior in the vicinity of *P* = 14.5 kbar and *T* = 2 K.**
- **Data was reproduced using 3 different pure PHCC sample-batches.**

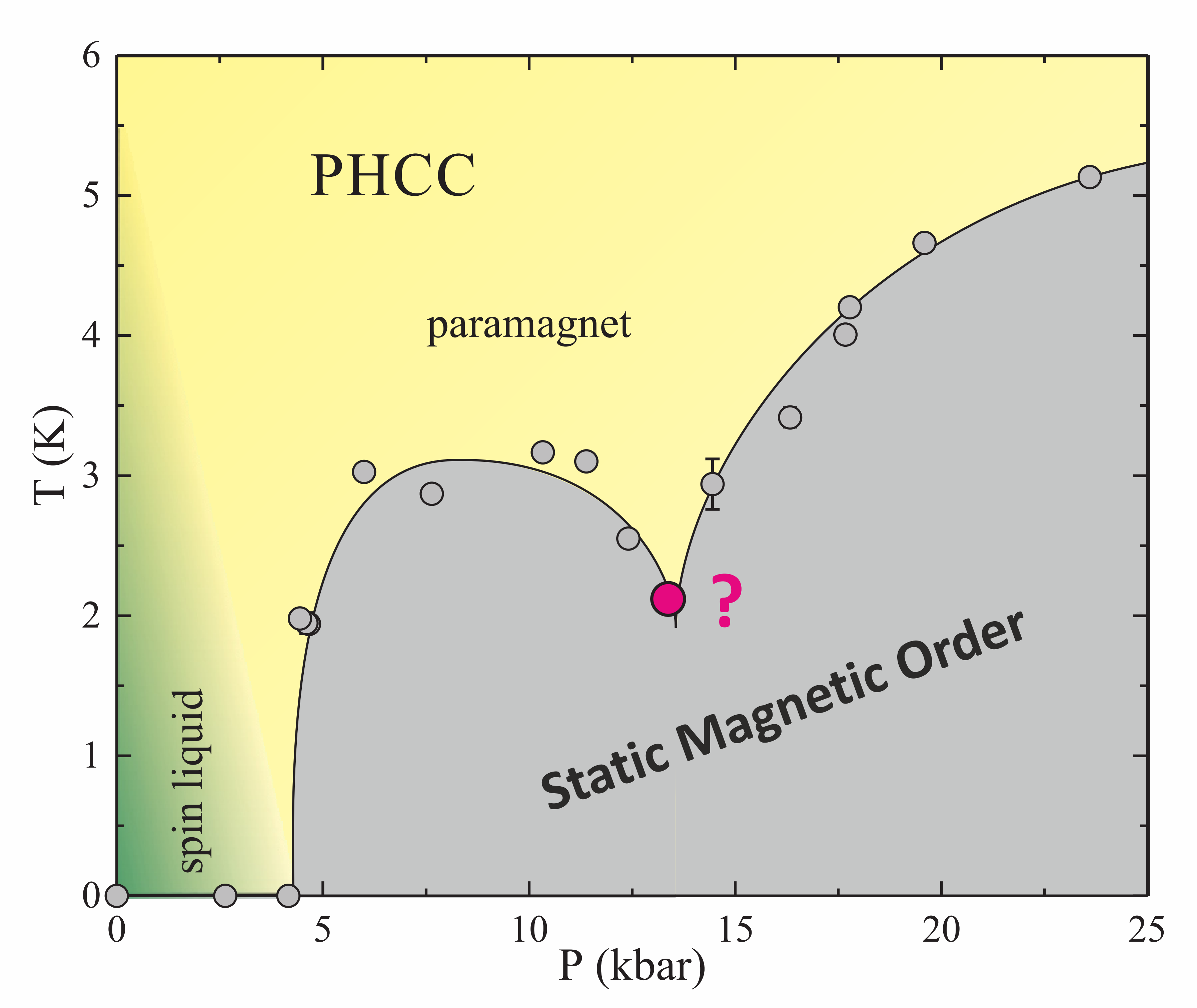

Magnetically Ordered Structure ?

- By looking more in detail at the *P*-dependent ZF μSR data and by careful fitting it is possible to reveal details on the magnetic structure of PHCC.
- From tentative phase diagram it clearly looks like there are 'two parts' separated by the P ≈ 14.5 kbar region.
- Fits for the ZF *P* = 6 kbar and *P* = 19.6 kbar data clearly show a big difference in initial phase (ϕ) of the μSR time spectra.
- For the lower pressure region the phase strongly deviates from zero, which is a clear indication for the presence of an incommensurate magnetic order.
- The 1D nature of the Cu-ions suggest the formation of a helical spin structure.

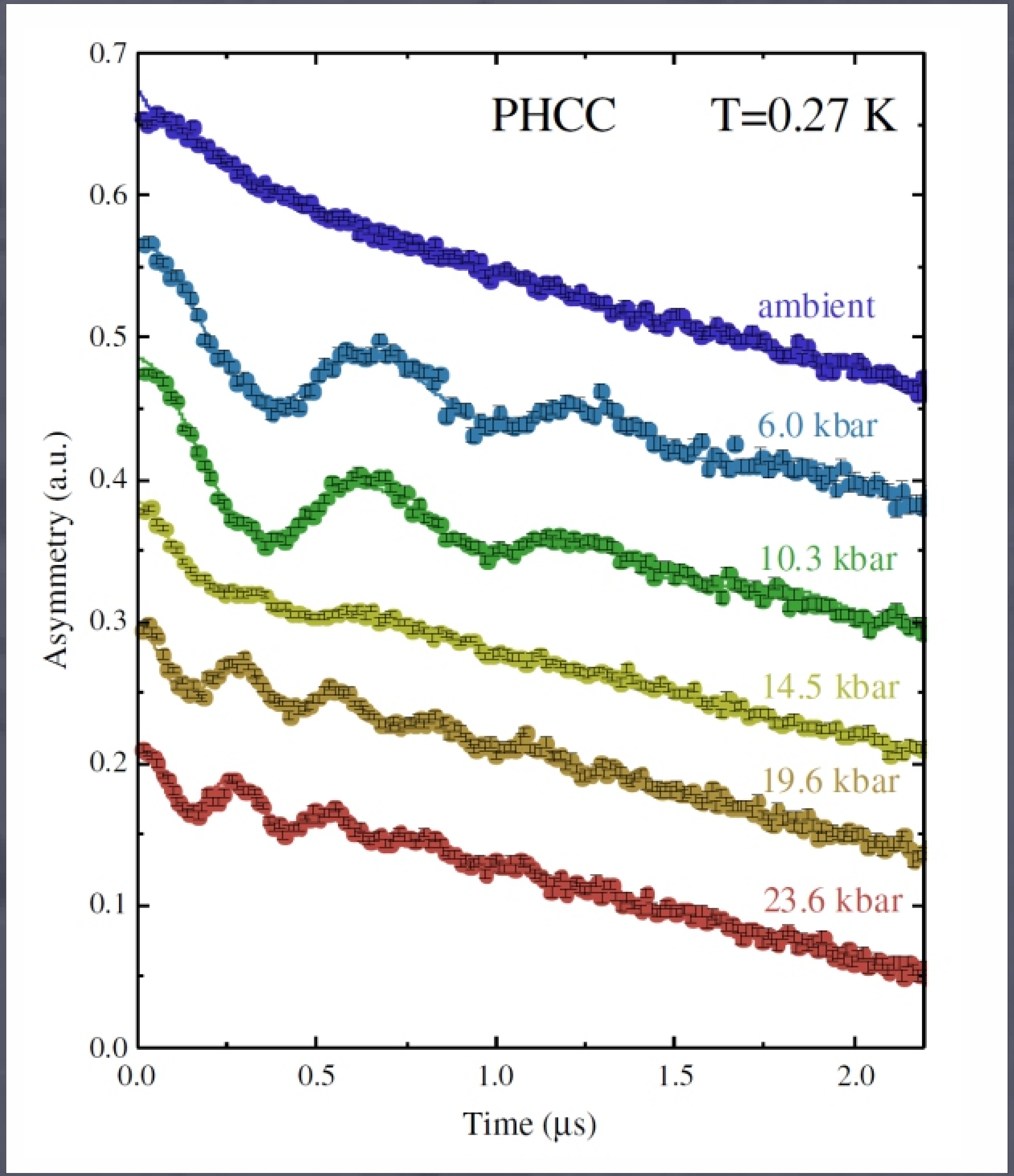

- For pressures above 14.5 kbar ϕ suddently drops to zero and remains so up to the highest investigated pressure (24 kbar).

PHCC: Magnetic P/T Phase Diagram

- We can now construct a more detailed P/T phase diagram for PHCC.
- At P_C = 4.3 kbar a QCP point is present where PHCC goes from being a gapped quantum spin liquid into an incommensurate (IC) helimagnet with max T_N = 3 K.
- At *P* = 13.4 kbar an IC to commensurate (collinear AFM) transition occurs with an associate Lifshitz point at finite temperature. This is a multicritical point where the PM phase meets the two ordered phases.

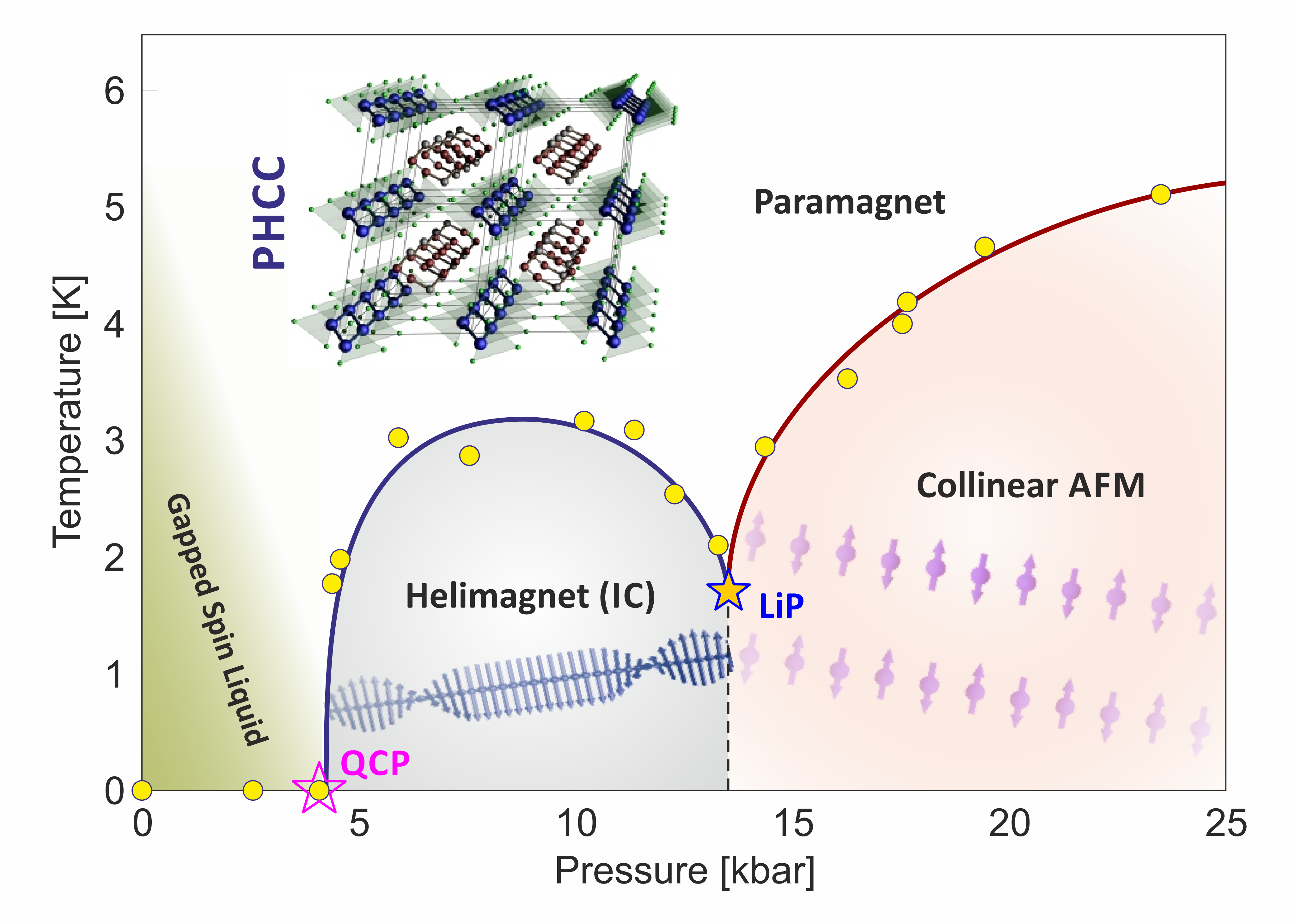

M. Thede, M. Mansson *et al.* Phys. Rev. Lett. 112, 087204 (2014)

μ^{+}SR vs. INS ?!?!

- Obvious question: why is estimate of P_c so different by μSR and INS ???
- μSR show induced incommensurate magnetic order at low-P + μSR is a Q-integrated experimental method.
- The INS data by Tao Hong et al. could have missed a shift in Q of the minimum for the magnon dispersion to an IC position and hereby also missed the actual closing of the gap and the phase transition into a magnetically ordered state.
- This could also explain why the INS intensity disappeared so quickly at low P.

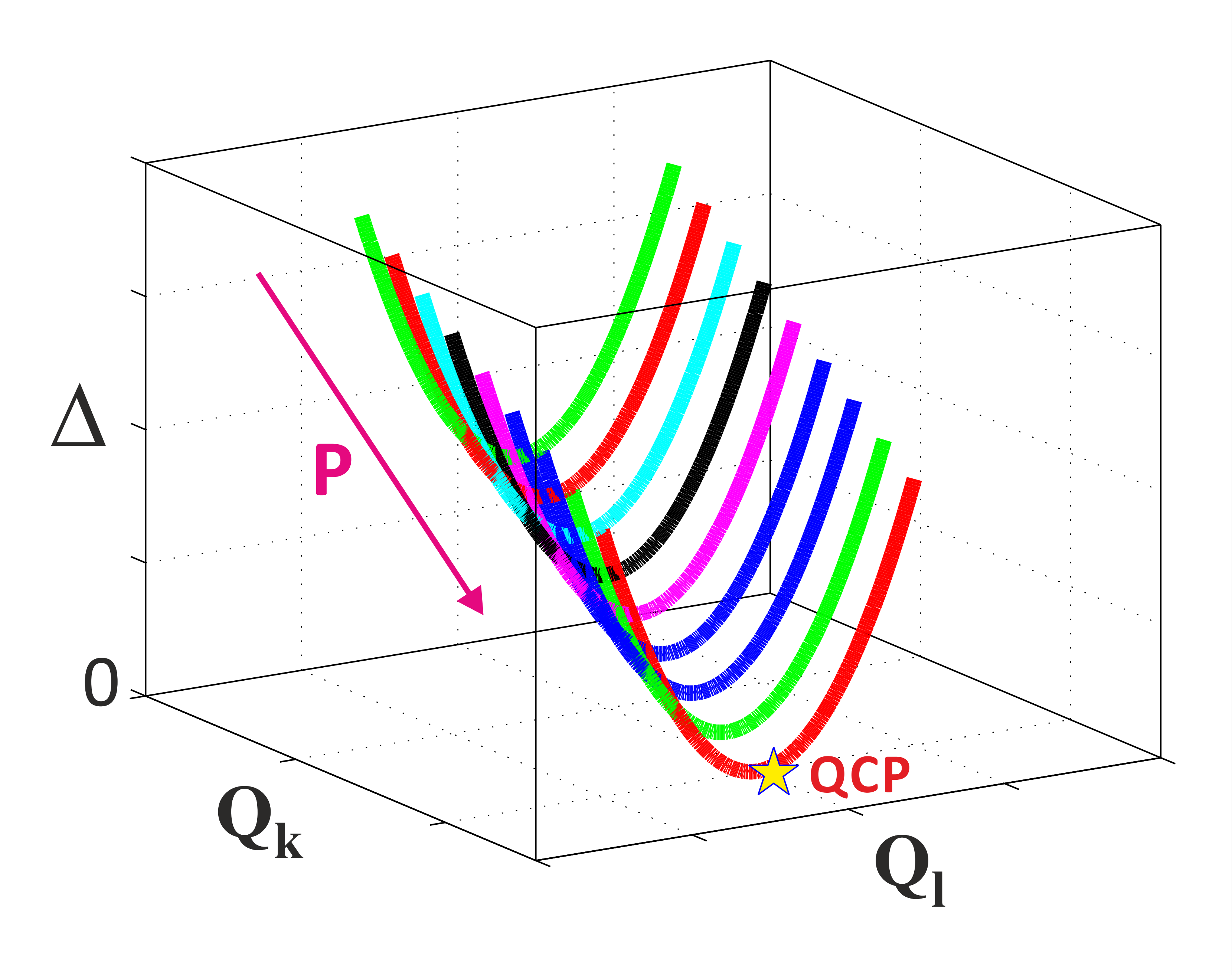

Example #2
Thin Film Superconductor Studied by LEM

LEM: Vortex Protocol

- μ^+SR has a long tradition in studying SC properties of bulk materials by applying a TF through the sample, hereby inducing the vortex state.

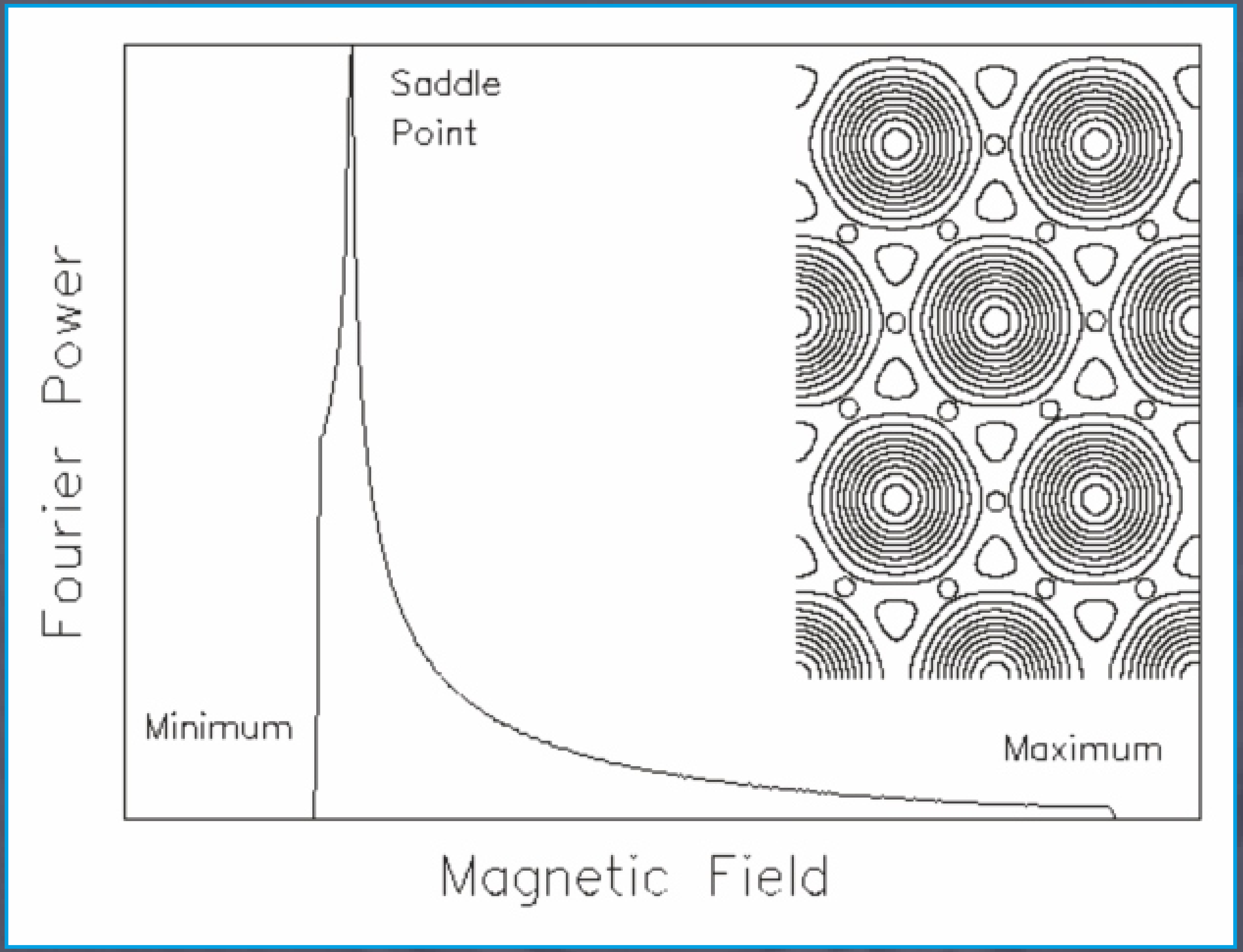

Jeff E. Sonier, PhD Thesis, UBC (1998)

- The vortices result in a non-uniform but "known" field-distribution / σ

- Through T- / H-dependent data it is possible to obtain information on T_c , λ , Δ , ...

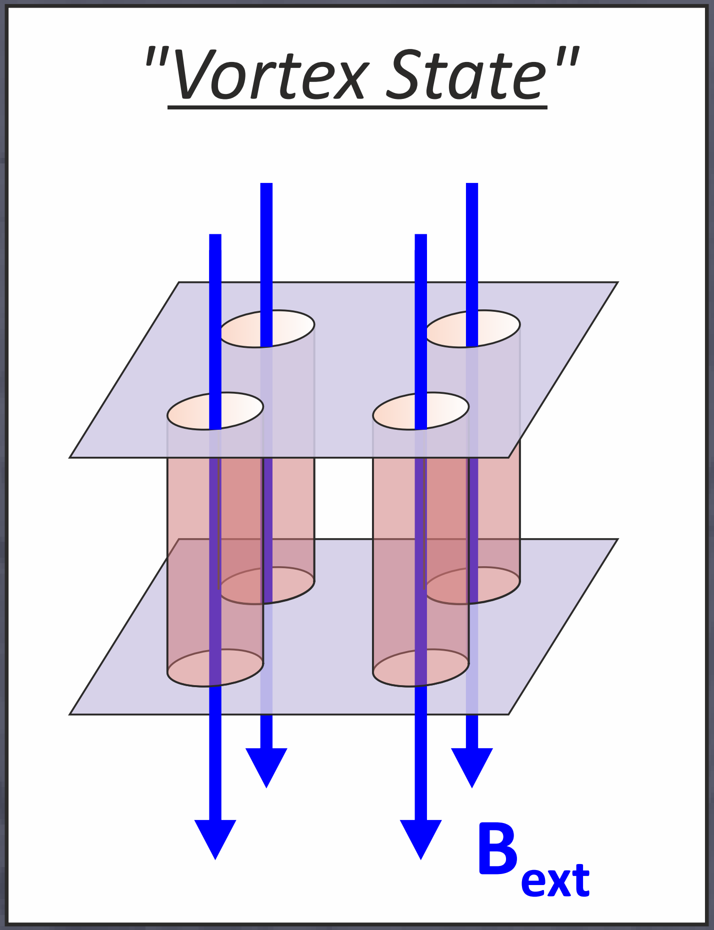

- Vortices "spread out" close to the surface/interface. Such depth (z) dependence is uniquely studied using **LEM @ PSI**

- Soon also available at J-PARC using the Ultra-Slow Muon Microscope

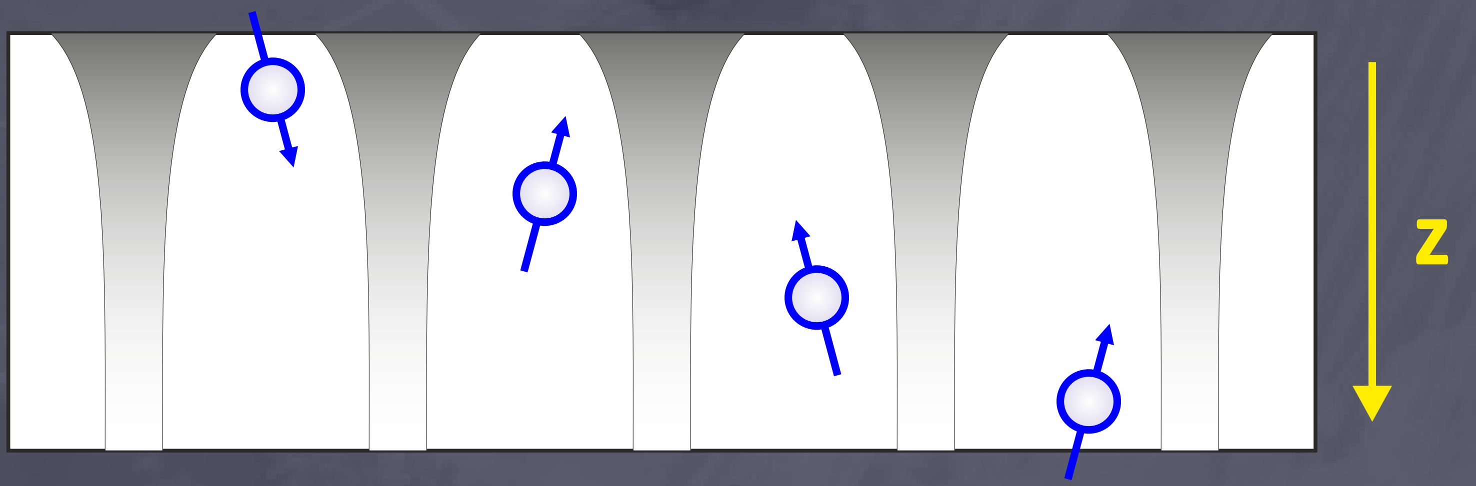

LEM: Meissner Protocol

- **LEM is a unique technique where we can use the the "Meissner" protocol to directly access the SC order parameter (London penetration depth).**

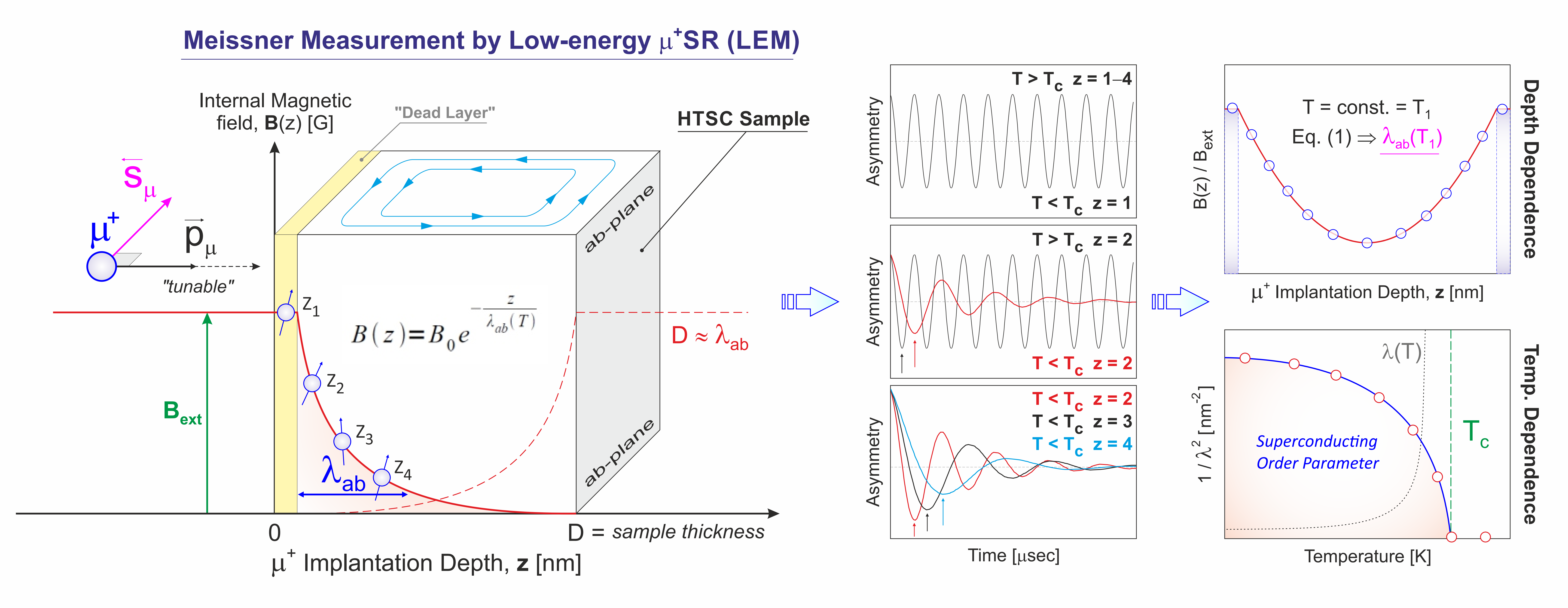

$LiTi_2O_4$

- Lithium titanium oxide (LTO) has a cubic spinel structure.
- LTO has also been shown to be ***the only known spinel oxide superconductor***.
- Bulk samples of LTO display SC below $T_c \approx 12$ K.
- Unfortunately, lack of high-quality single crystals has prevented systematic investigations of LTO's SC properties.

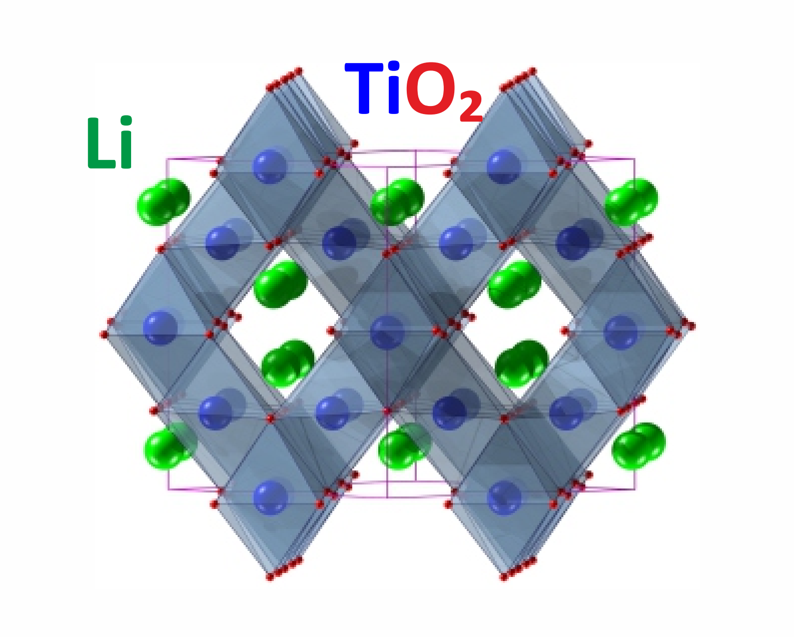

Lithium titanium oxide

"LTO"

$LiTi_2O_4$

Cubic

Fd3m (227)

a = **b** = **c** = 8.41 Å
$\alpha = \beta = \gamma = 90°$
V = 594.72 Å^3
Z = 8
M = 166.70 g/mol
ρ_{theor} = 3.72 g/cm^3

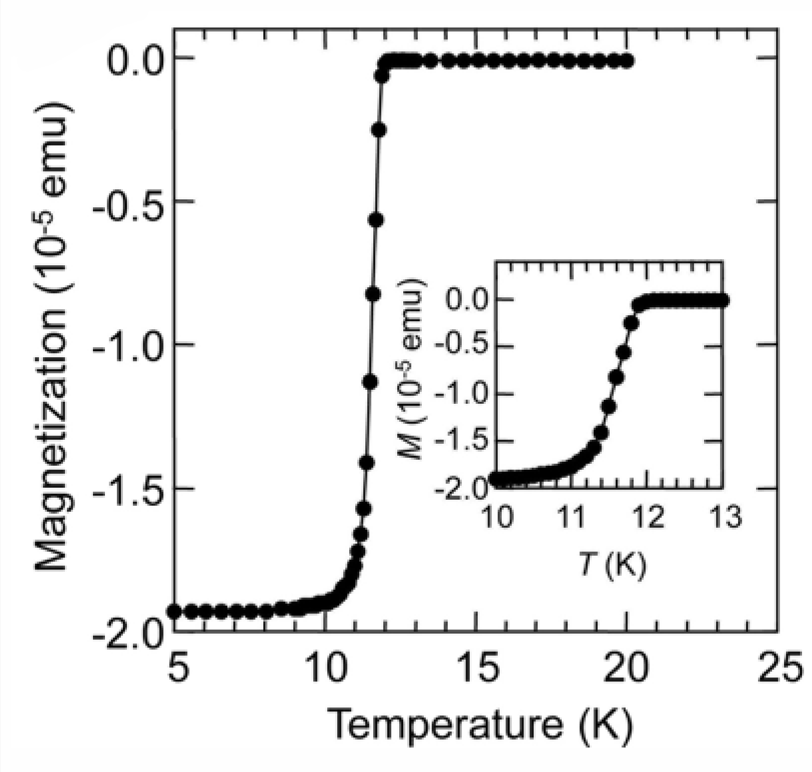

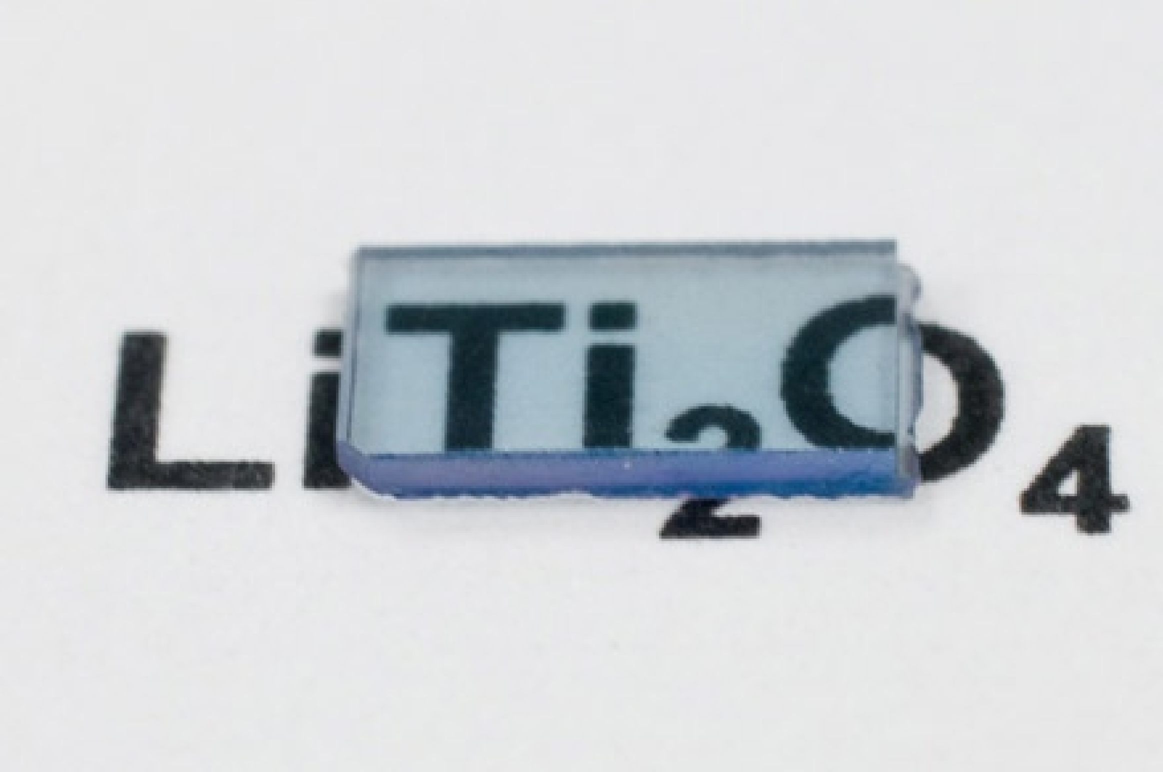

- The solution has been to grow ***thin LTO films*** using mainly PLD.
- Using $MgAl_2O_4$ substrates a small strain is obtained, which stabilizes the film and "increases" T_c as high as 13 K.

Experimental Setup

- These experiments were performed using the **LEM** instrument of **PSI**.
- For this experiment we prepared 4 films covering a total area, $A = 22 \times 22$ mm^2.
- Thickness of all 4 films were carefully calibrated and was nominally d = 220 nm

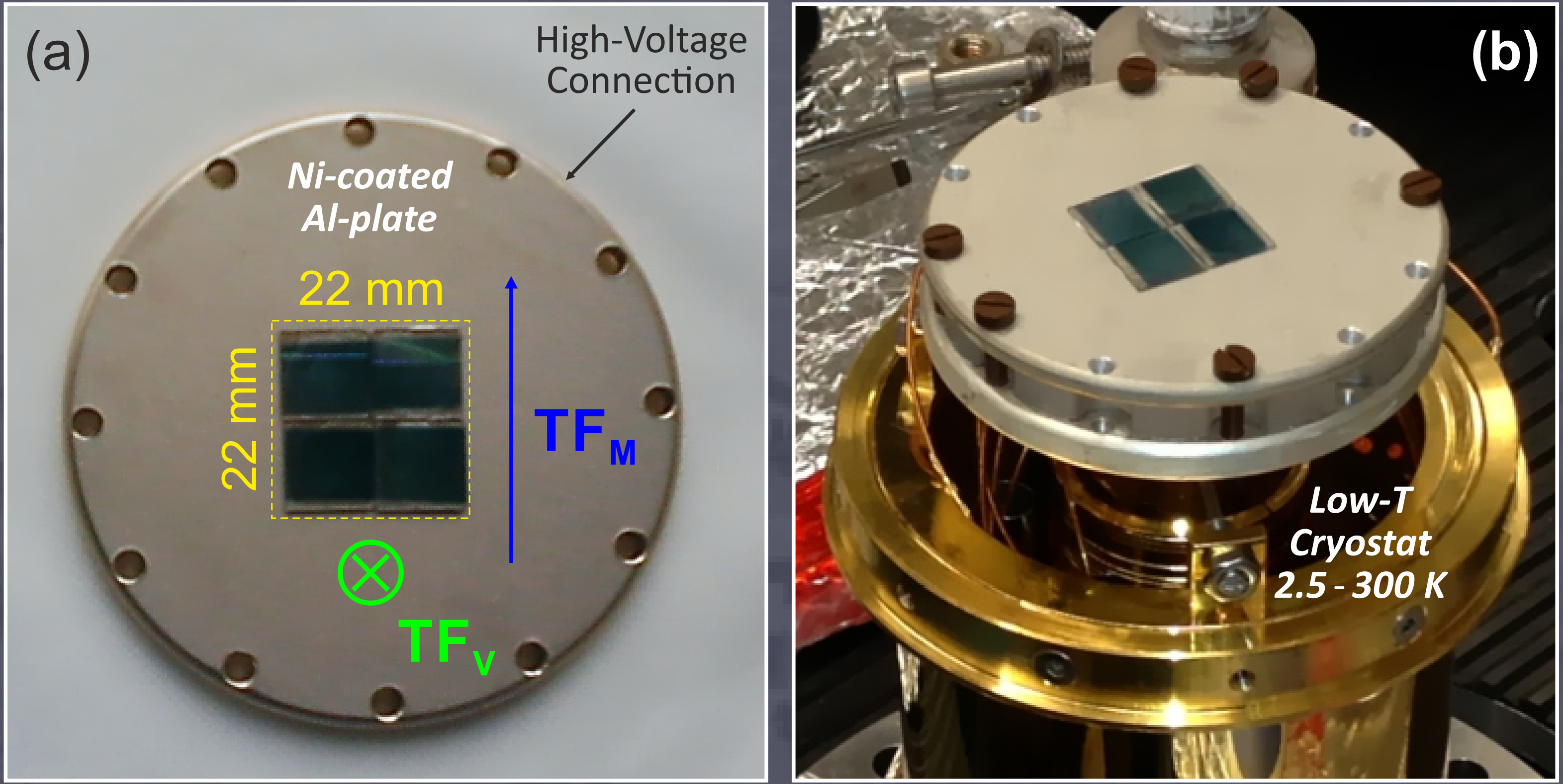

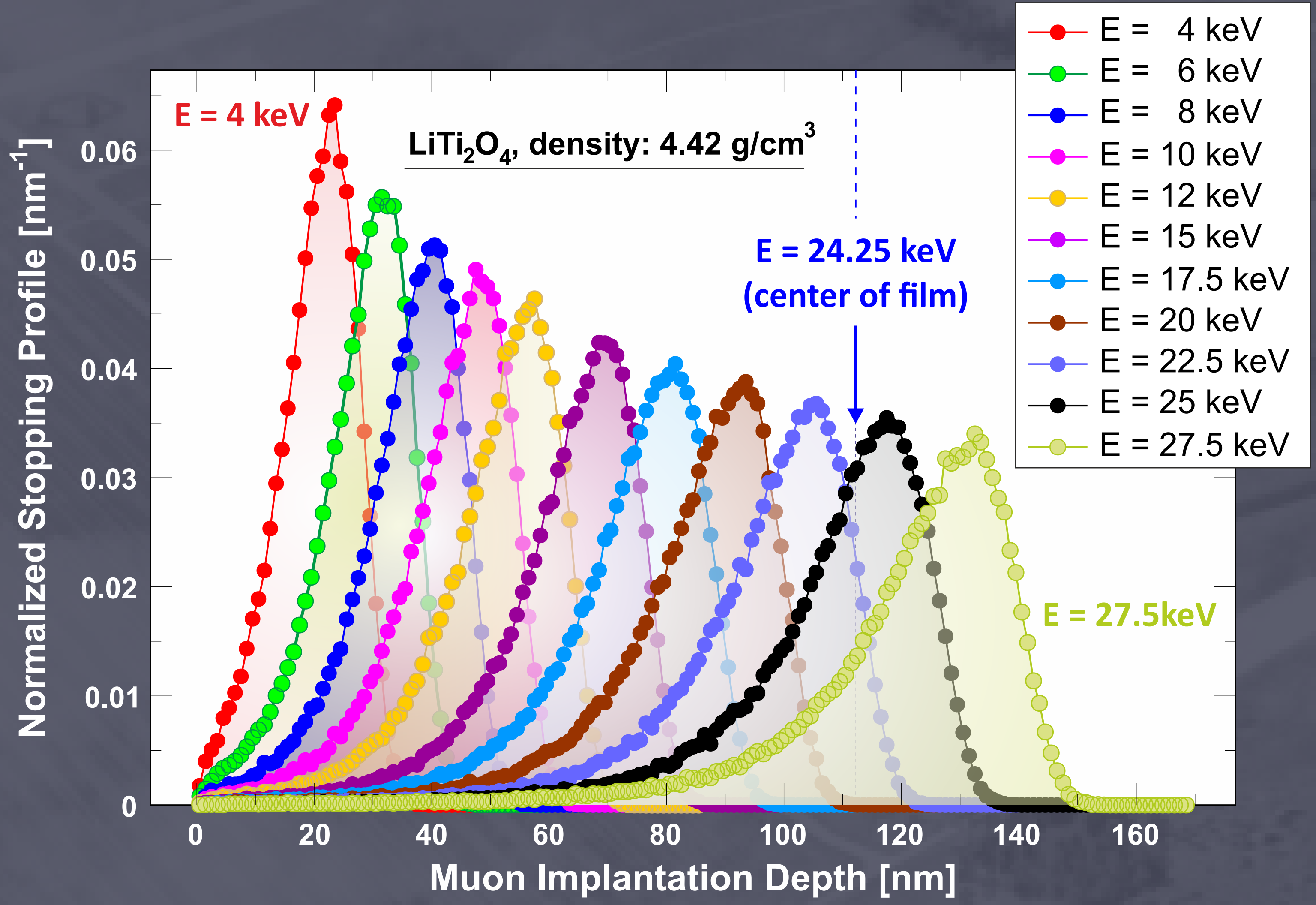

- Films were attached to a Ni-coated Al plate using Ag-paint. Plate was attached to the low-T cryostat.
- *TRIMSP* software was used to calculate the muon stopping profiles. E = 24.25 keV was found to correspond to the center of the film i.e. a muon implantation depth z = 110 nm

$LiTi_2O_4$, Meissner Data

- LEM setup was chosen to collected in the Meissner protocol using TF = 150 G // film surface.

- Depth-resolved scans below T_c (at T = 5 K) clearly show a change in both relaxation rate and frequency.

- Temperature dependent scans were also performed in the center of the film (z = 110 nm) showing expected behaviour.

- Data is extremely clean and can easily be fitted...

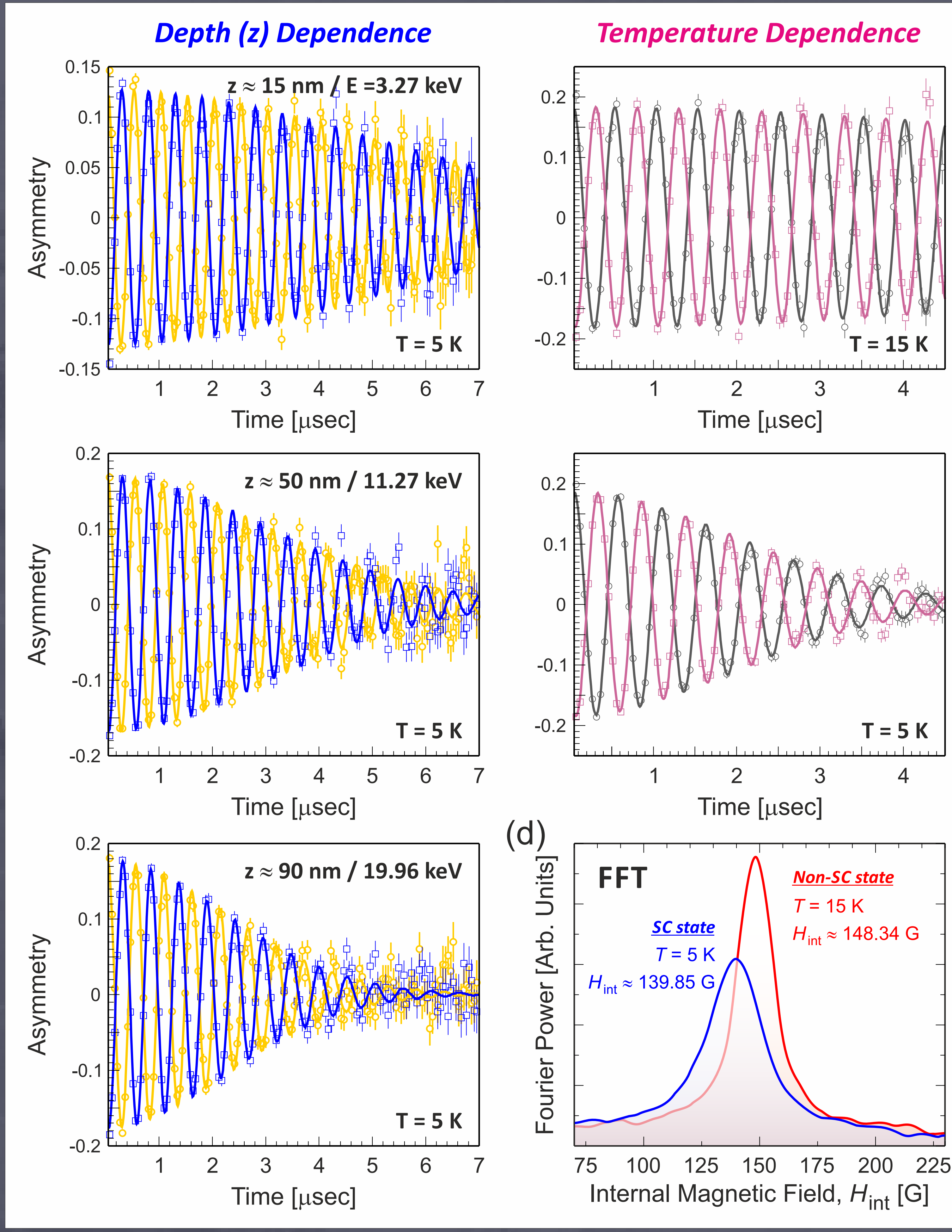

Depth-resolved Results

- **From the fits it is possible to extract the depth-dependent field.**
- **The results clearly show the expected behavior and the London penetration depth (λ) can be extracted.**
- **To obtain a reasonable fit to the data a 10 nm "dead layer" is considered**

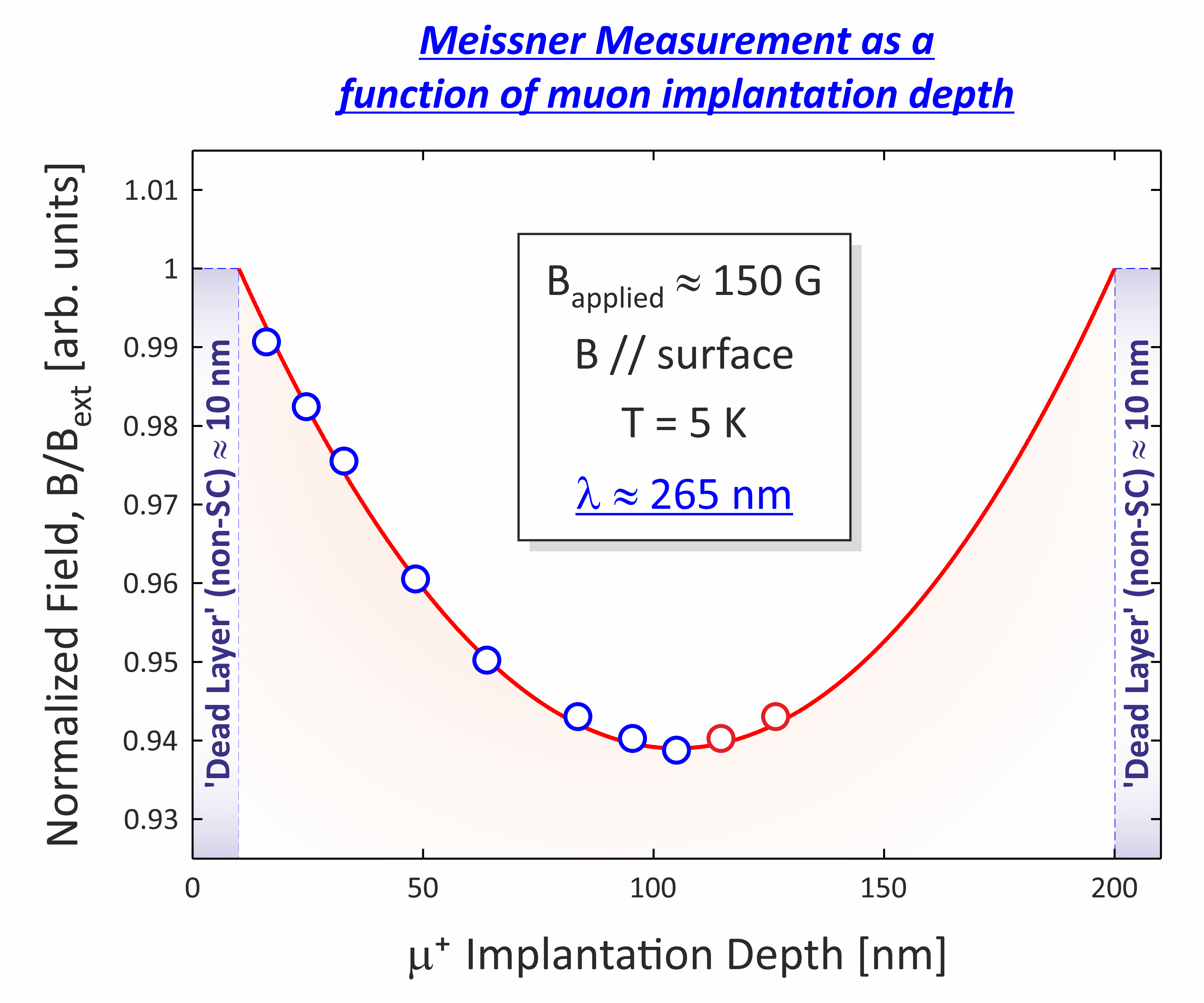

Lenght-/Time-Scales

- For studying dynamics, muons are highly complementary to neutrons !!!

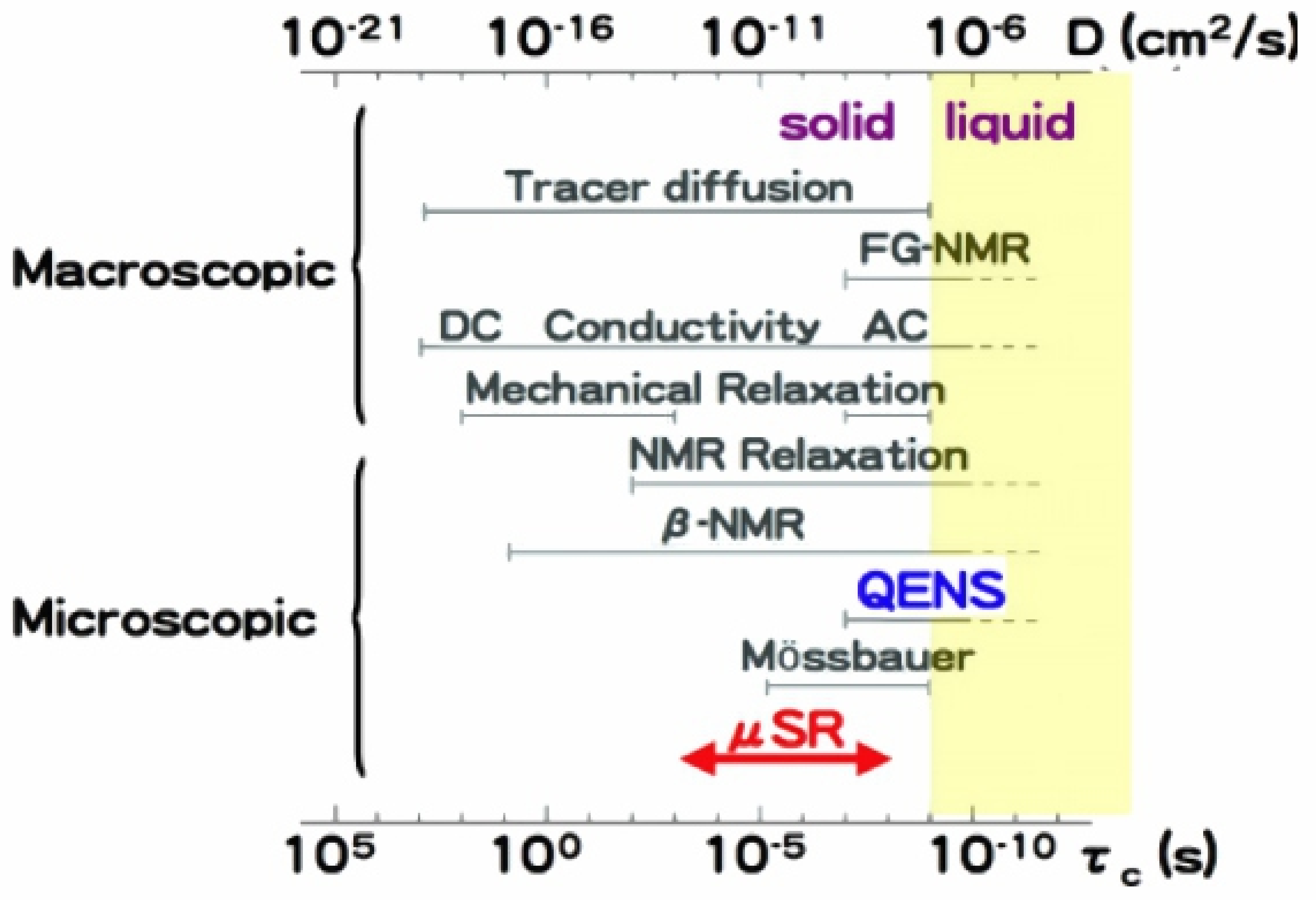

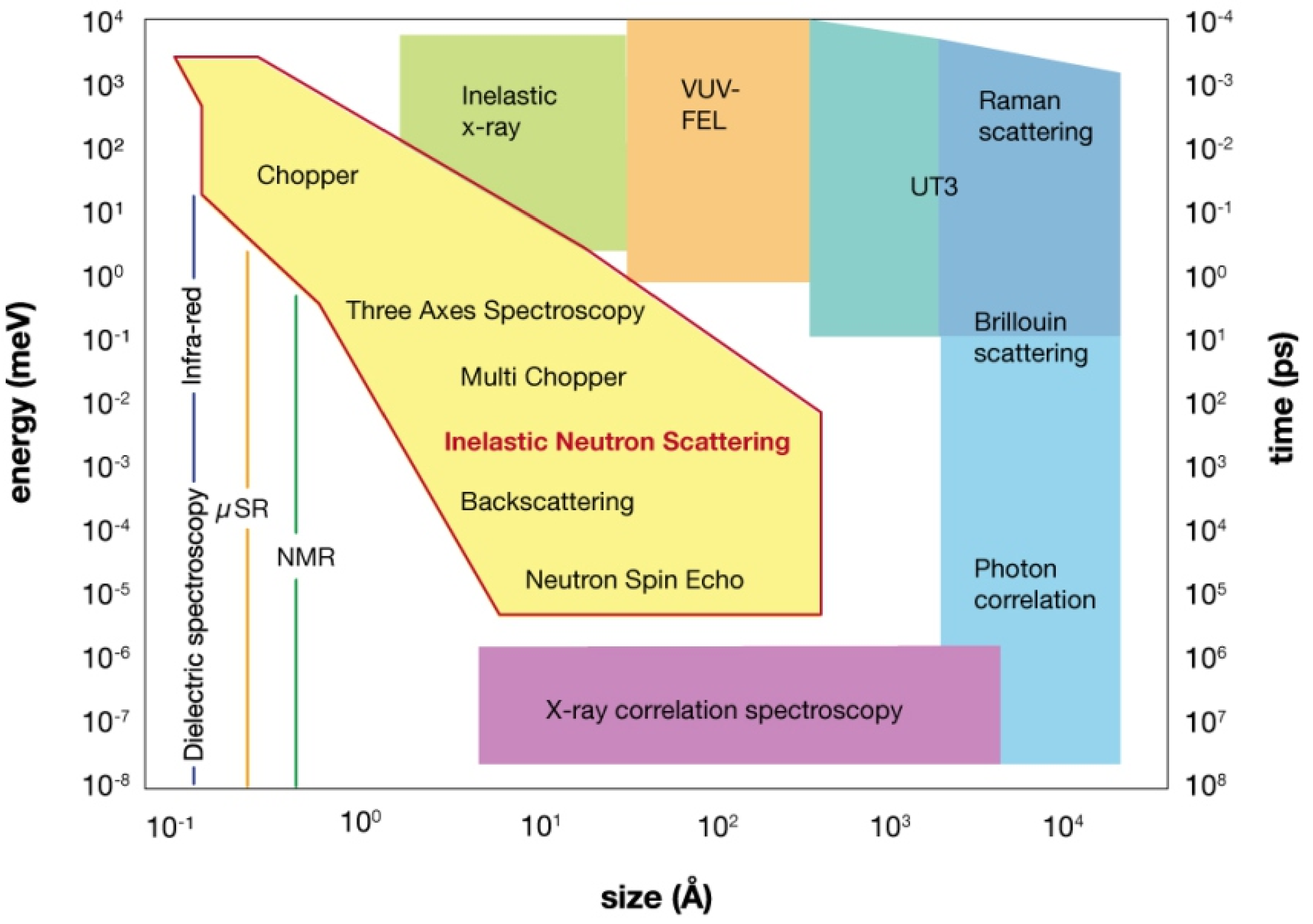

Example #3
Ion Diffusion in a Battery Cathode Material

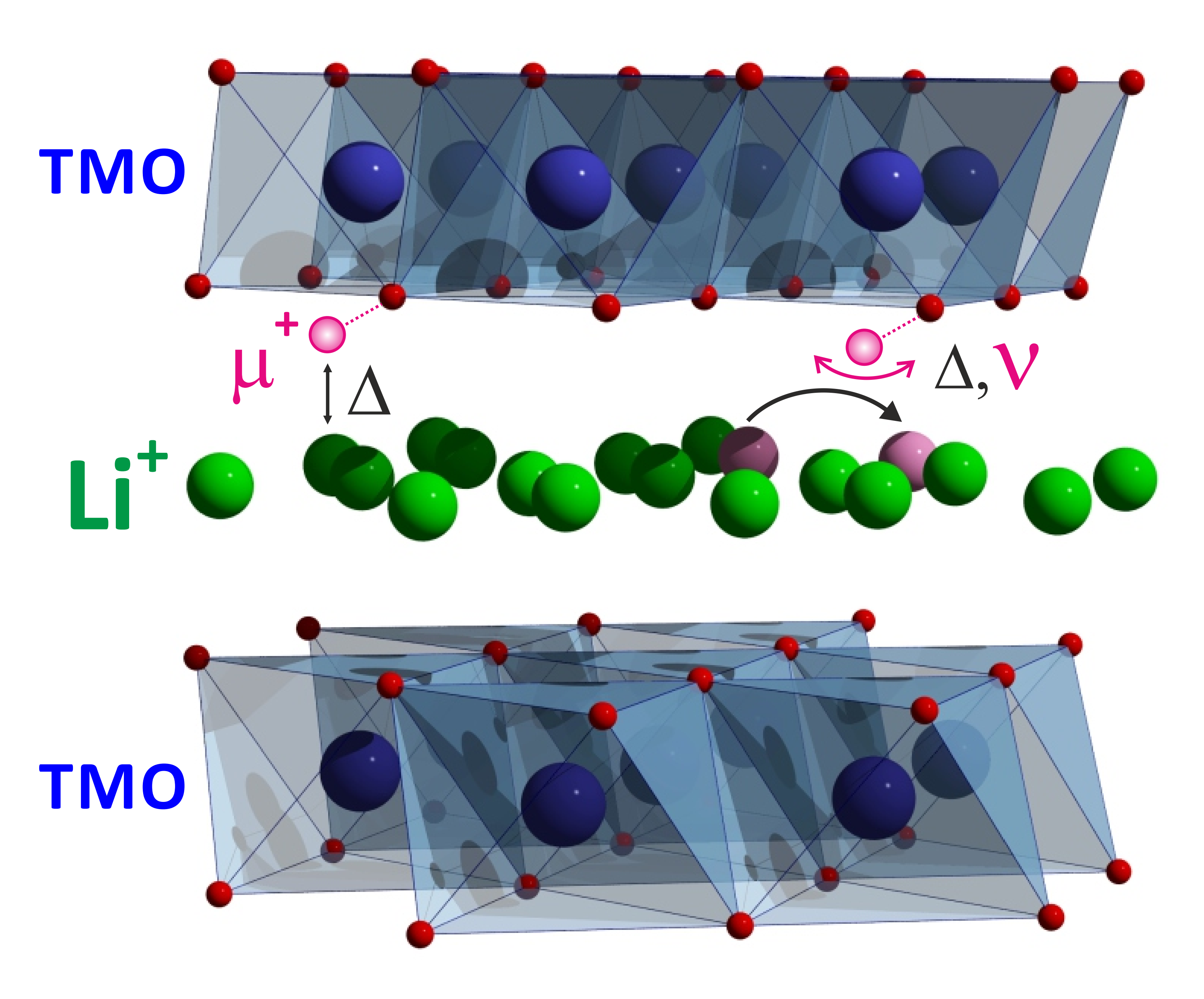

Ion Diffusion by μ^+SR

- Muons are very sensitive probes of local internal fields
- In the paramagnetic state, muons feel mainly the random nuclear dipole fields (of Li) $\rightarrow \Delta$
- Implanted μ^+ bind strongly to O^- within the crystal lattice
- If Li-ions are immobile the mSR time-spectrum is described by a static **Kubo-Toyabe** function

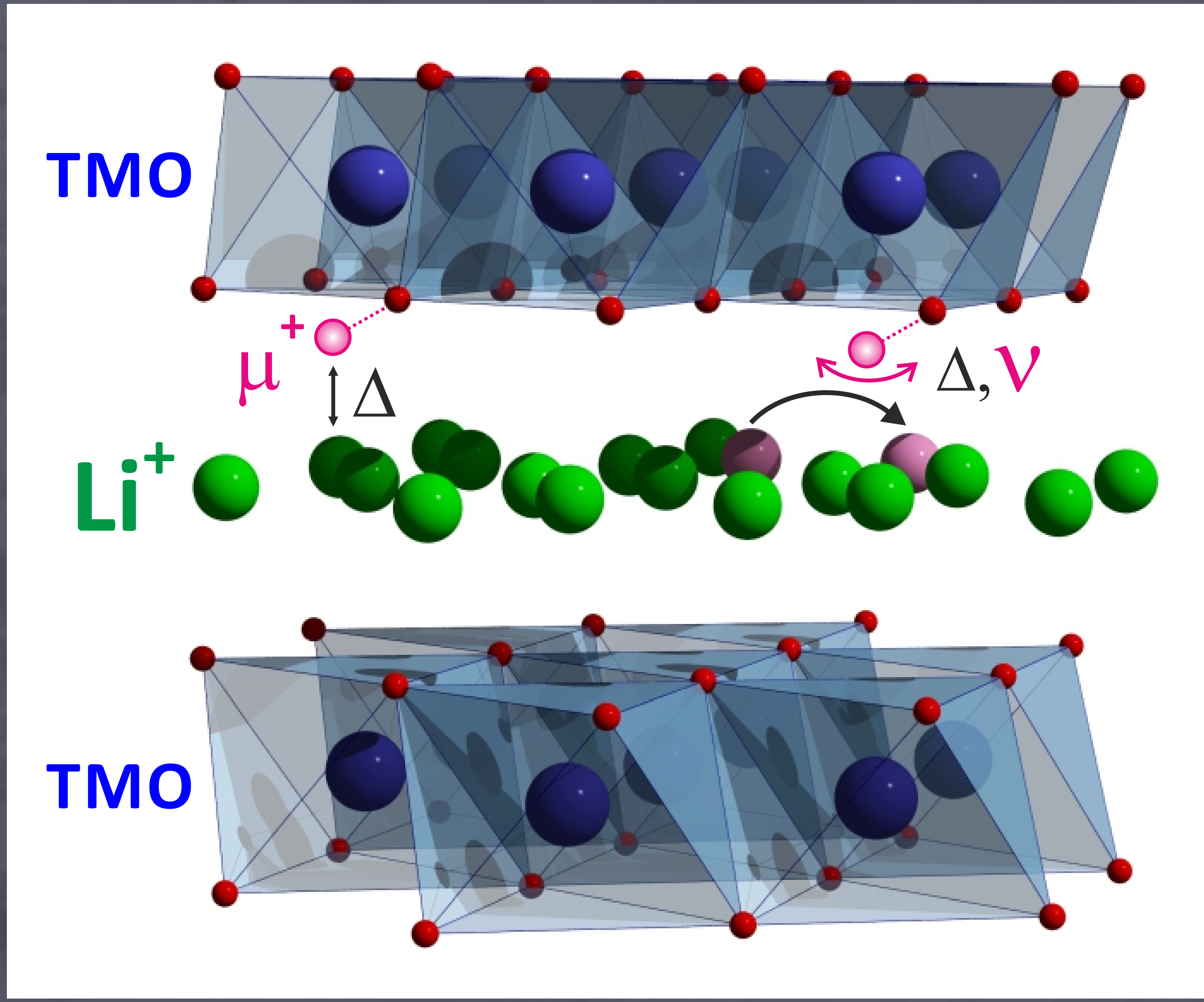

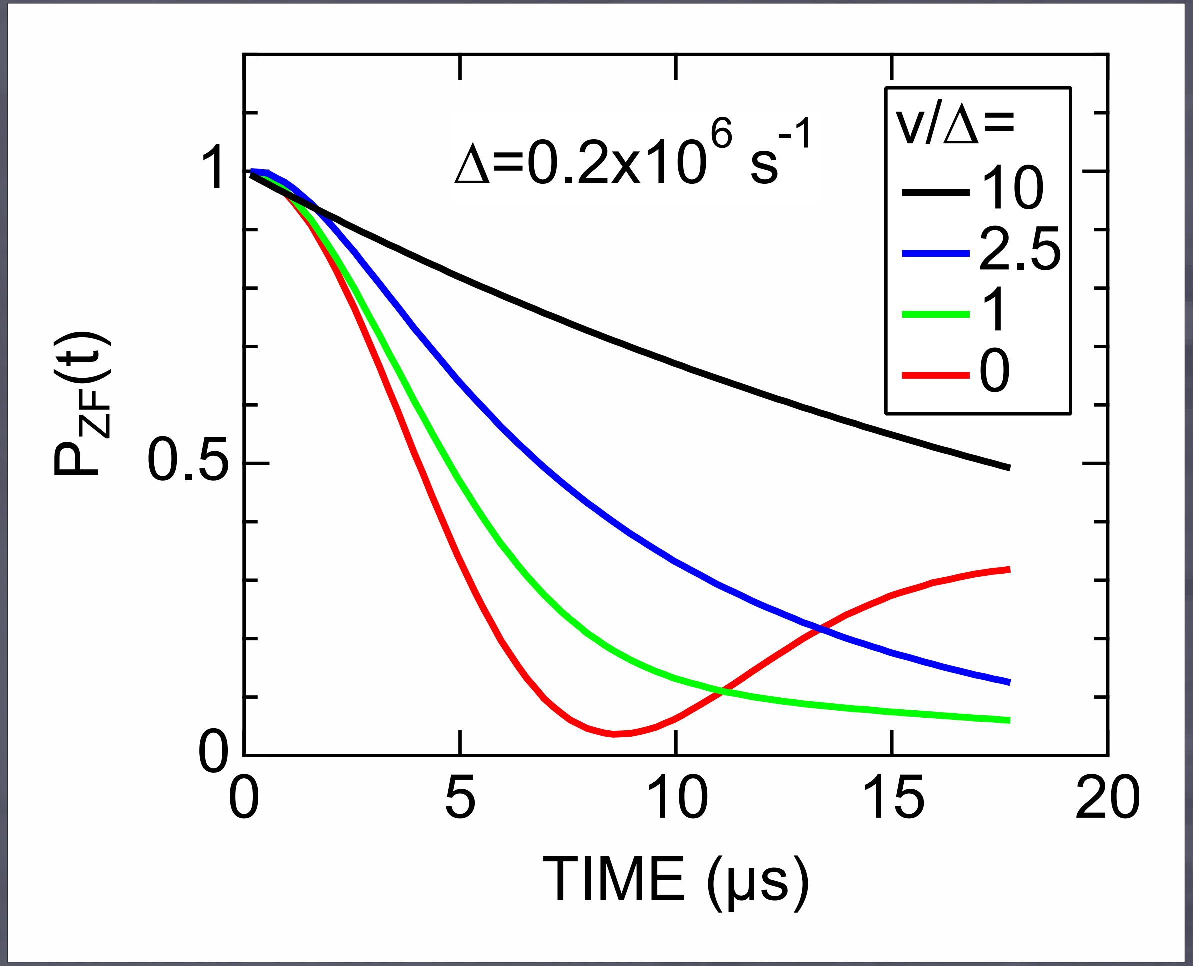

- If ion-diffusion is present, the muons will detect a dynamic contribution to the dipole field.
- Data is now described by a dynamic KT function that includes the parameter field fluctuation rate = **ion hopping rate (ν)**
- From *T*-dependence ν(*T*), the ion self-diffusion coefficient (D_{ion}) can be extracted.

Battery Cathode Materials

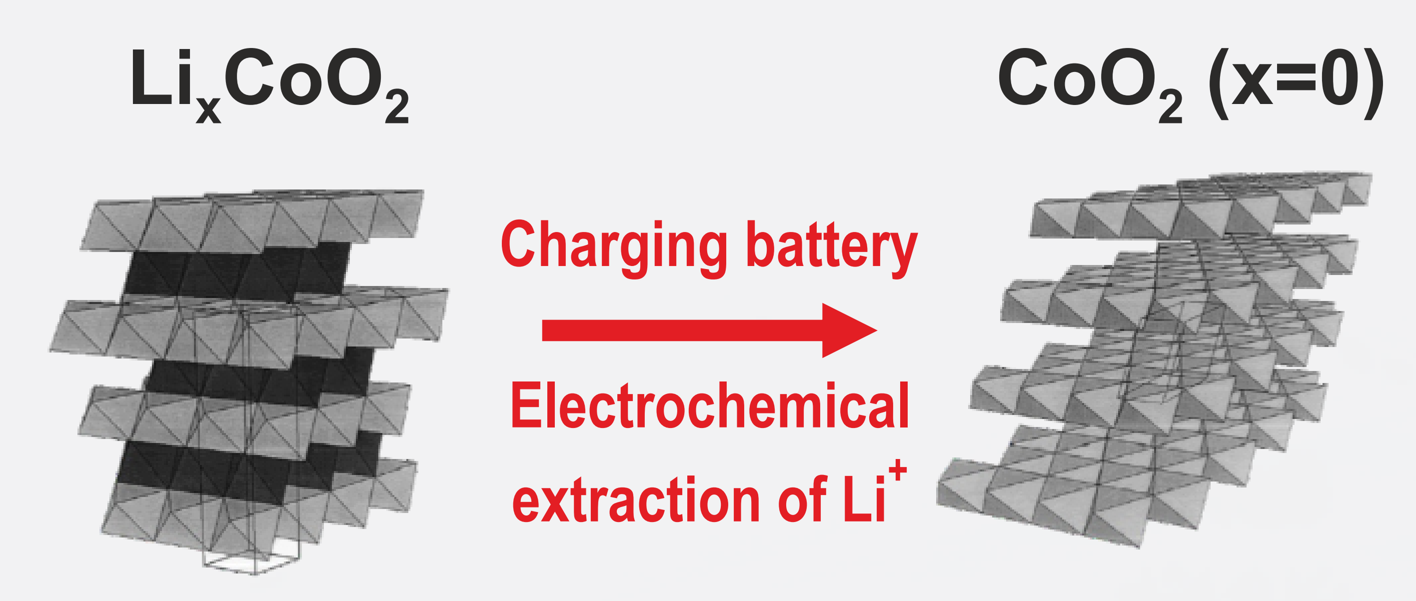

- Cathode materials is a crucial part for battery performance:
  - Low resistivity
  - Safe / 'green'
  - Low cost
  - Stable crystal structure
  - High Li-diffusion rate, D_{Li}
  - High Li-density

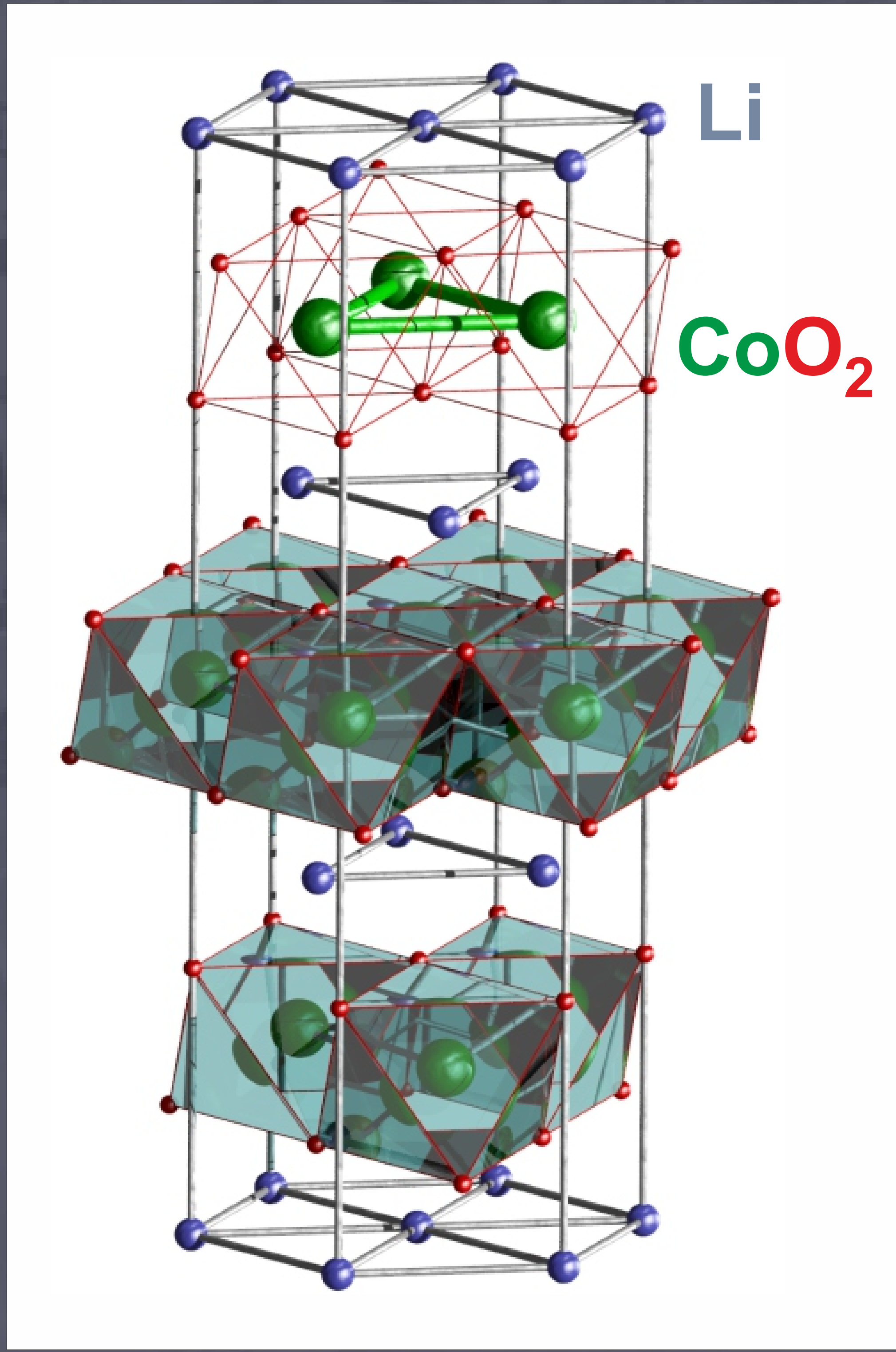

- Layered structure (Li // TMO // Li // ...)
- Archetypical Example: Li_xCoO_2
- 2DT Cobalt lattice + Antiferromagn. interactions = frustrated magnet.
- Tuning of x = tuning of conductionelectrons on the Co 2DTL
- Show no magnetic order for temperatures above T_N = 30 K

Li_xCoO_2

- 2 g $Li_{0.73}CoO_2$ powder sample was pressed into a pellet & sealed in a Ti-cell under He atmosphere
- Using ARGUS instrument at ISIS pulsed muon source we collect zero-field (ZF) + 2 longitudinal-field (LF = 5 and 10 G) μ^+SR spectra.

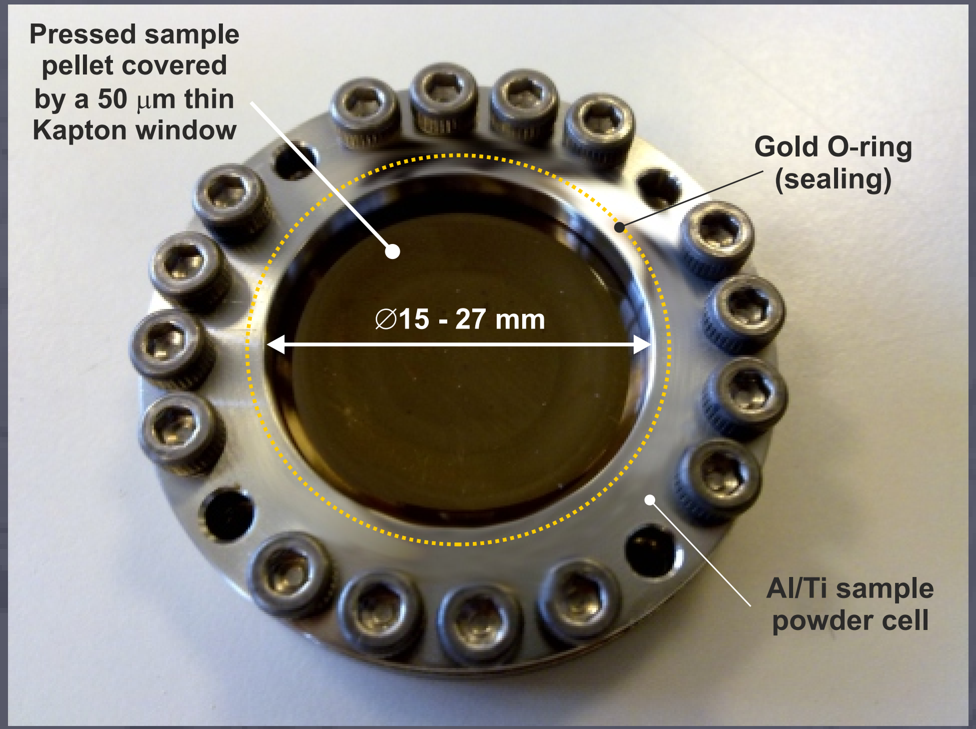

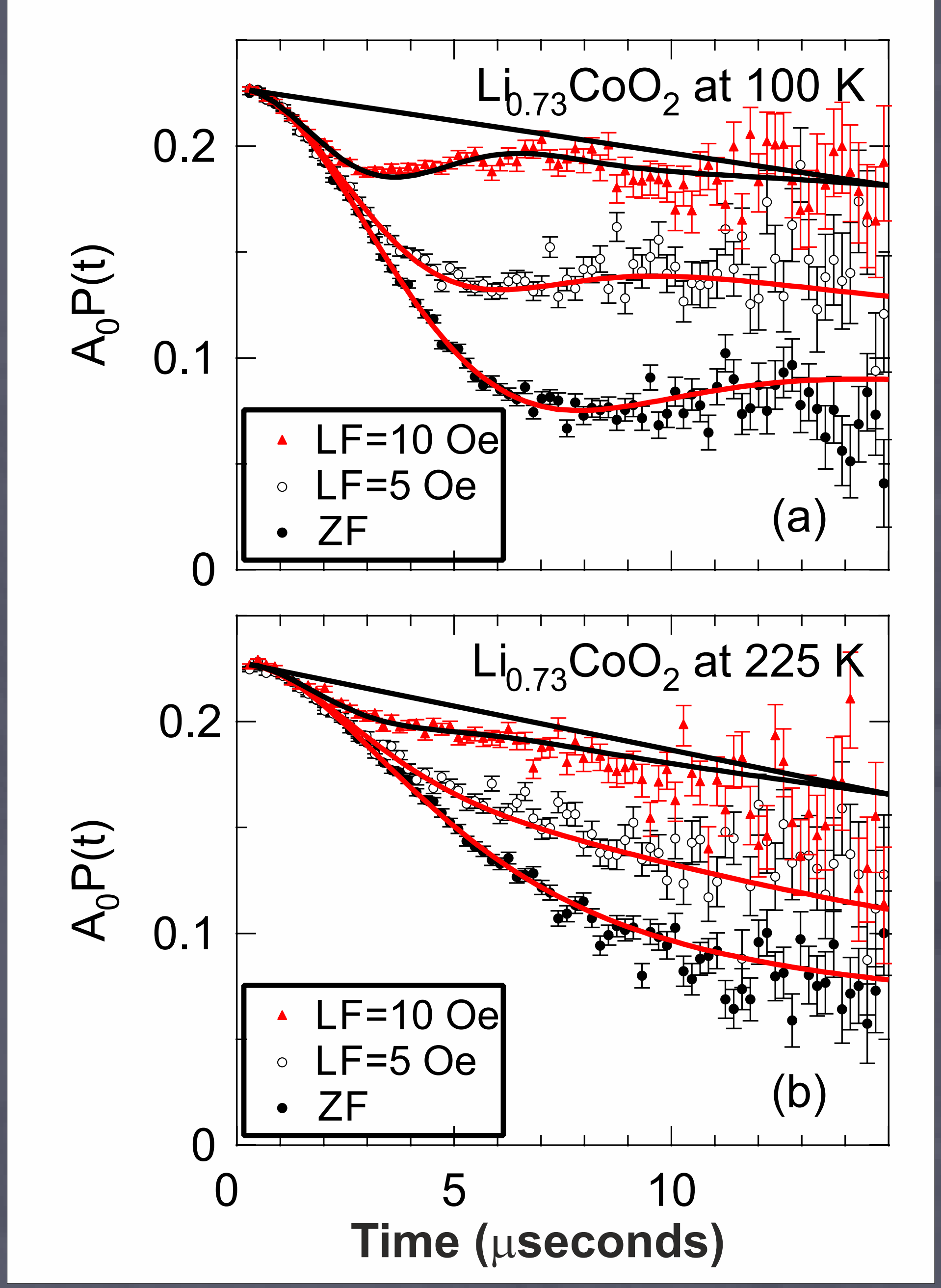

- Data was fitted by a dynamic KT × Exponent. relaxation with 3 parameters:
  - Δ = Field distribution ('STATIC')
  - ν = Hopping-rate ('DYNAMIC')
  - λ = Electronic (PM) relaxation
- Global fit ZF + 2 LF = robust determination of Δ and ν.
- LF allow for separation of the electronic contrib./relaxation (fast PM fluctuations)
- Perform T-dependent ZF/LF measurement and extract $\nu(T)$...

T-dependent Fitting Results

- For T = 160-280 K, ν show a strong exponential increase indicative of a thermally activated process.
- ν(T) fits well to an **Arrhenius type equation**.
- Diffusive motion of either Li-ions or μ
- The activation energy (E_a) can be extracted as **E_a(Li) = 145 meV**.
- Δ is more or less constant in same T-range, i.e. most likely Li-ion diffusion. (μ's create a strong bond to O in these TMO materials)
- Above 280 K ν(T) decreases and remains constant while Δ show a decrease possibly due to "motional narrowing".
- Indicate too fast Li-diffusion or possibly a phase transition or the onset of μ diffusion?

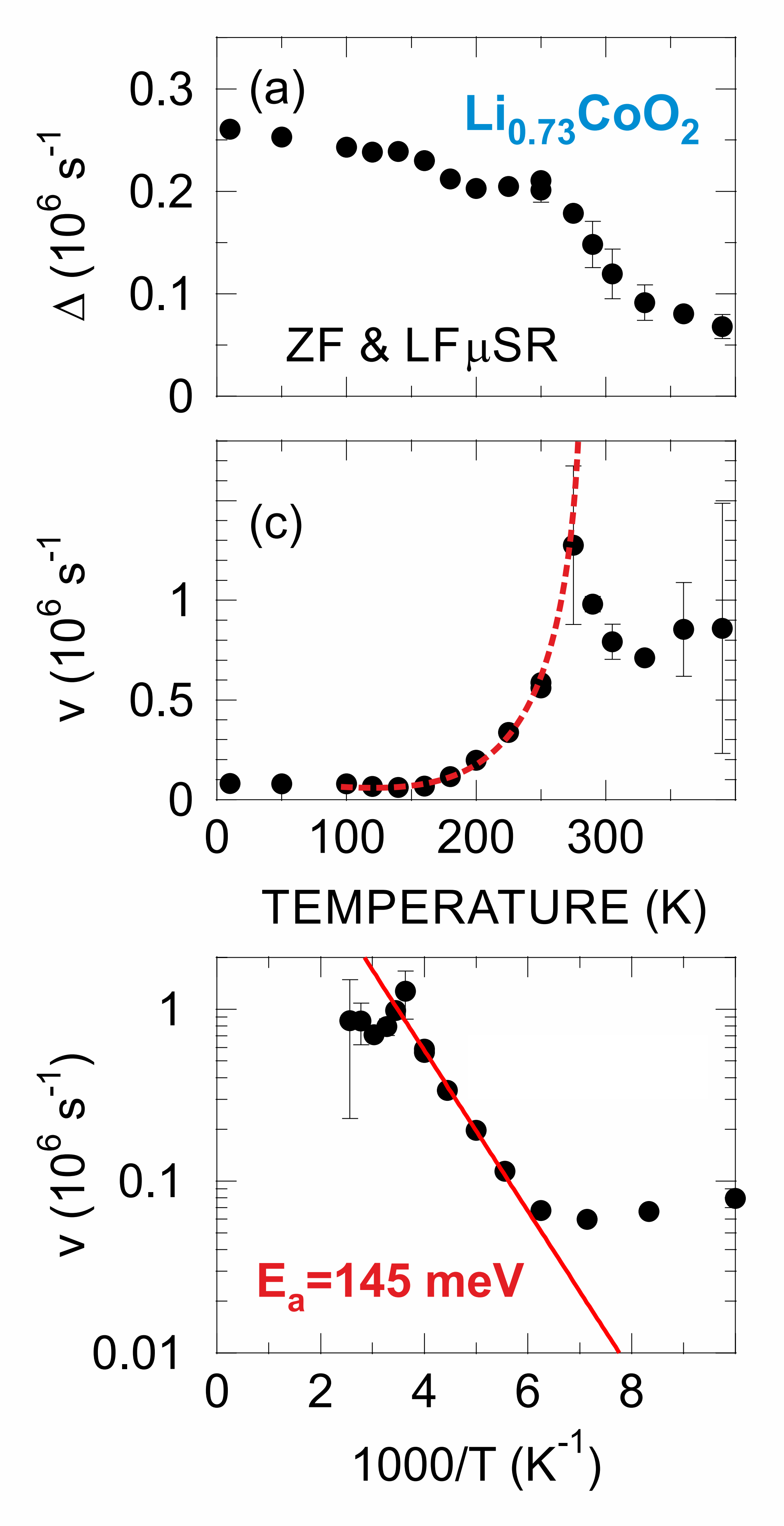

$\nu_{Li} \rightarrow D_{Li}$

- If we assume ν to be direct measure of the jump rate of Li-ions we can express D_{Li} according to (Equation) where N_i are the number of Li jump paths in the *i*:th site, $Z_{v,i}$ is the vacancy fraction and s_i is the jump distance.

$$D_{\mathrm{Li}} = \sum_{i=1}^{n} \frac{1}{N_i} Z_{v,i} s_i^2 \nu,$$

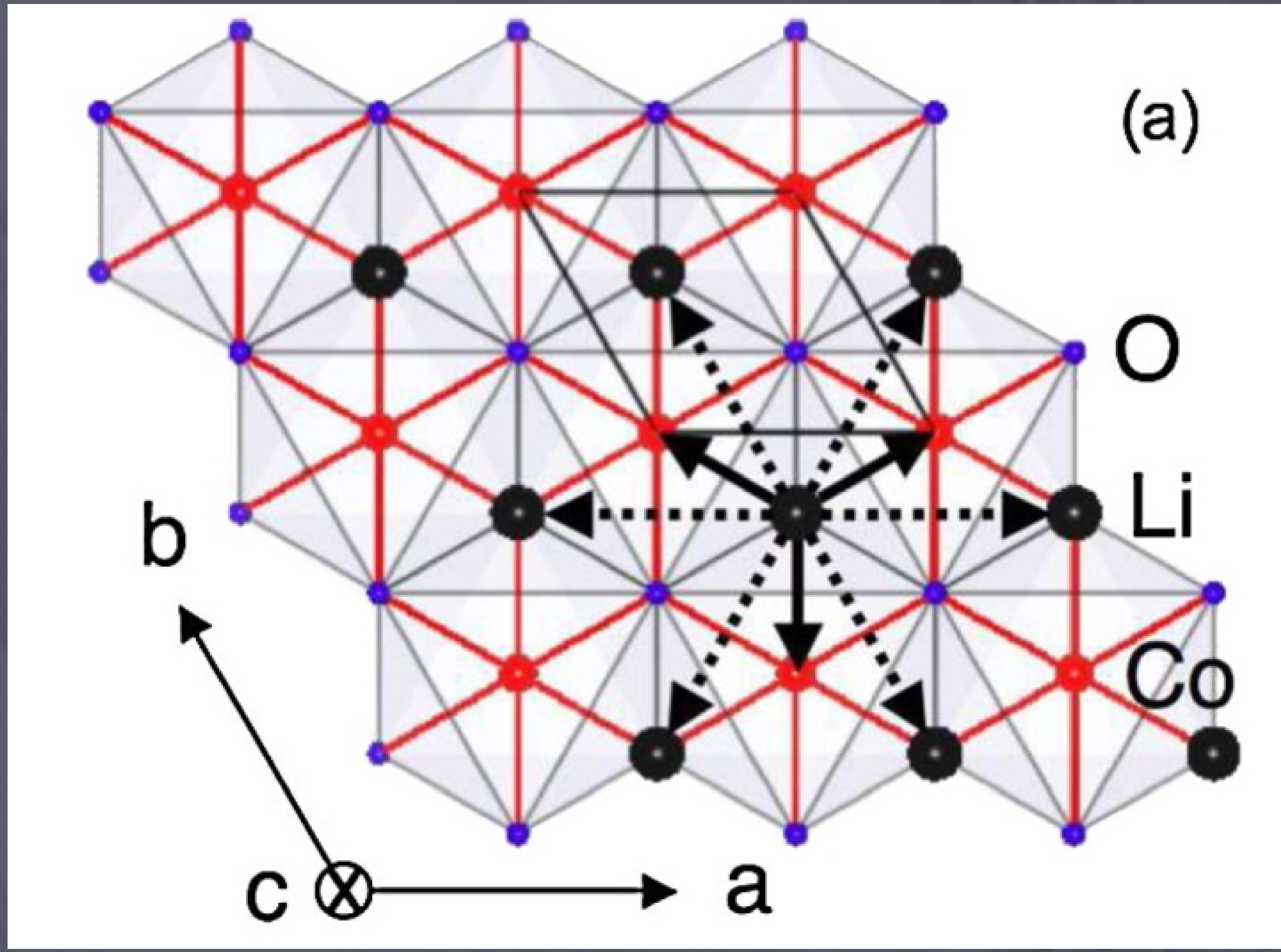

- If we assume the same jump paths as in the first principle calculations of D_{Li} of Li_xCoO_2, each Li has two possible paths within the Li-plane with $N_1 = 6$, $s_1 = a$, $N_2 = 3$ and $s_2 = a/\sqrt{3}$.

- For $Li_{0.73}CoO_2$, $Z_{v,1} = 0.27$ and $Z_{v,2} = 1$, with ν extracted from the μSR data.

- As a result we obtain for $Li_{0.73}CoO_2$ that $D_{Li} = 7\cdot10^{-10}$ cm^2/s at T = 300 K

Li_xCoO_2 Final Results

- Same procedure was been applied to $Li_{0.53}CoO_2$ and $LiCoO_2$ compositions with similar results.
- Obtained results are in excellent agreement with first principle calculations (T = 300 K)

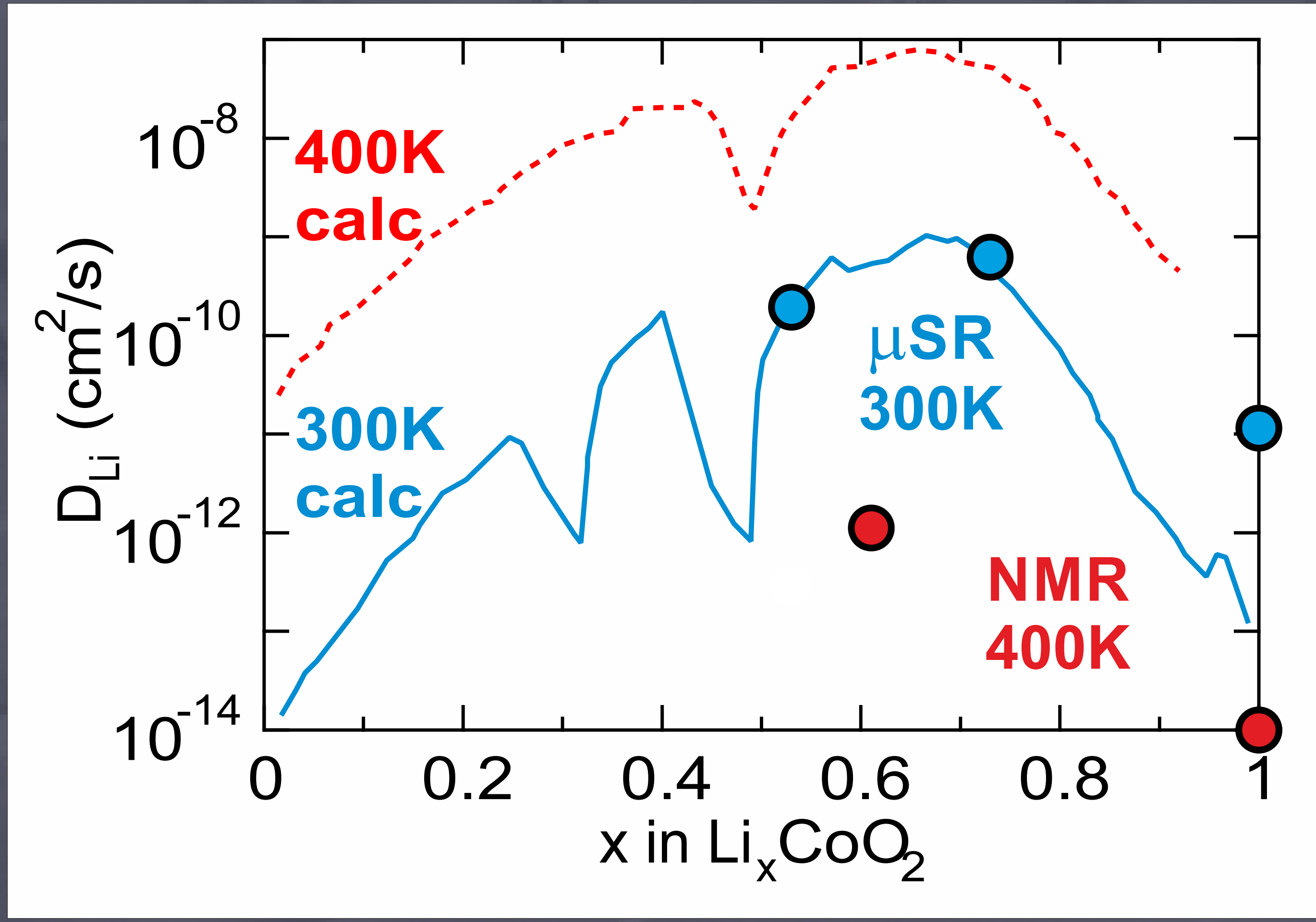

J. Sugiyama, M. Mansson *et al.* Physical Review Letters, 103, 147601 (2009)

We present μ^+SR as a novel and optimal probe for D_{Li} in compounds containing magnetic ions.

Muon Technique Applied to Broad Range of Systems

Battery Cathode Materials

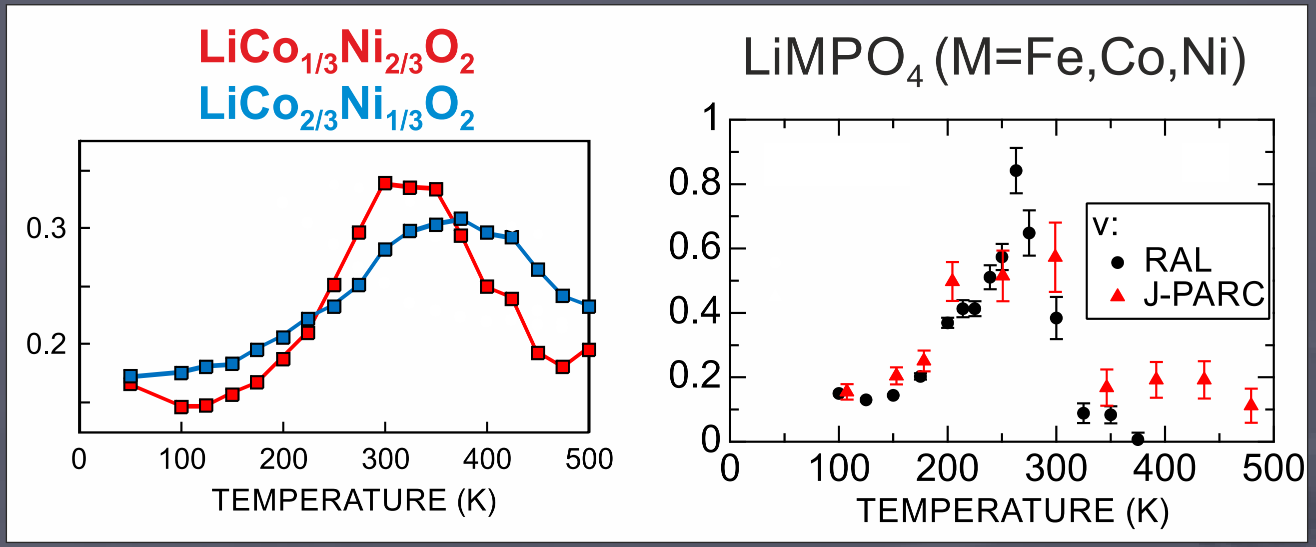

PRB 84, 054430 (2011) - PRB 85, 054111 (2012)

Battery Anode Materials

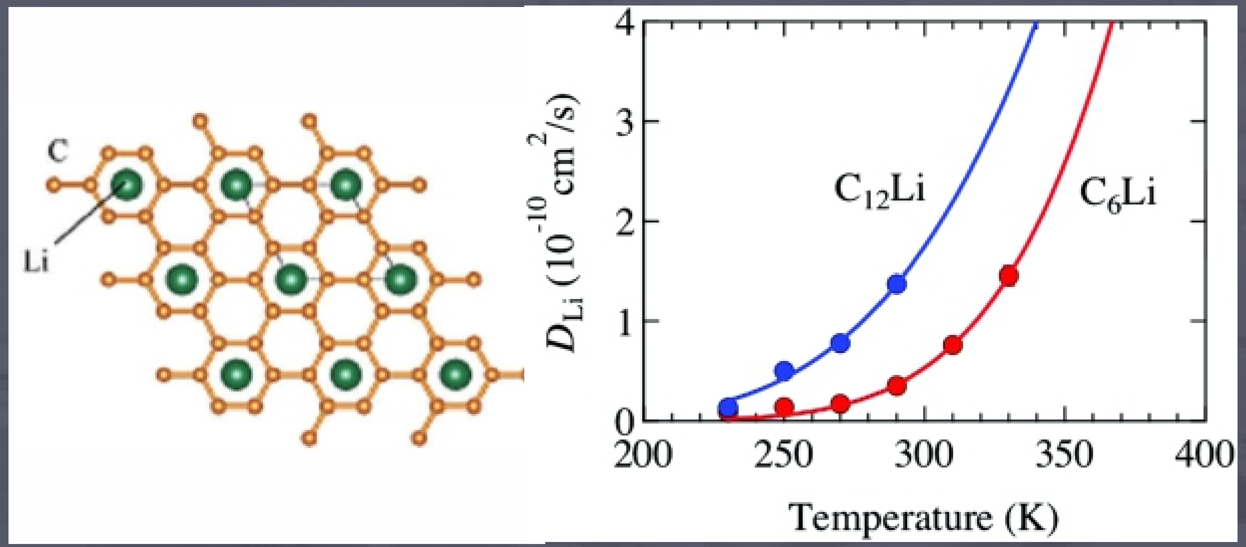

Umegaki, Mansson, Phys. Chem. Chem. Phys. 19, 19058 (2017)

Solid Electrolytes $Li_{10}GeP_2S_{12}$

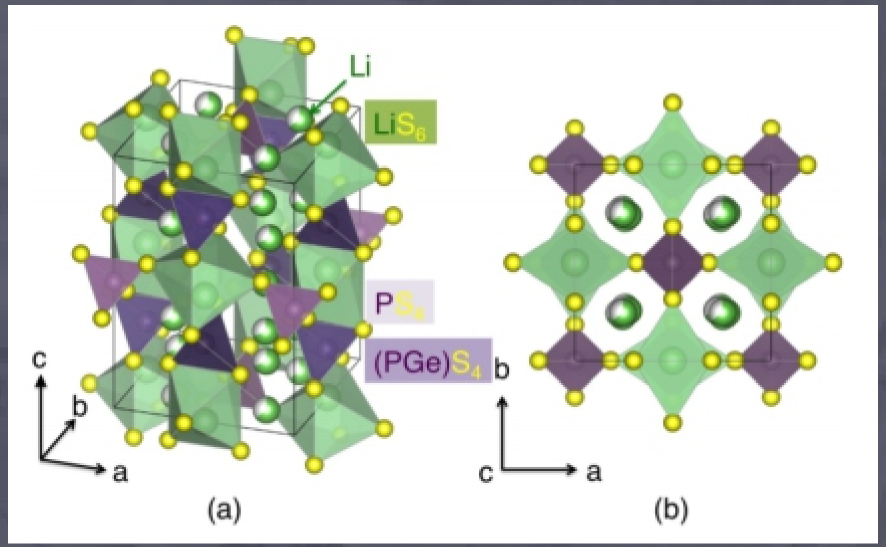

Synthetic Clays for Nuclear Waste Management

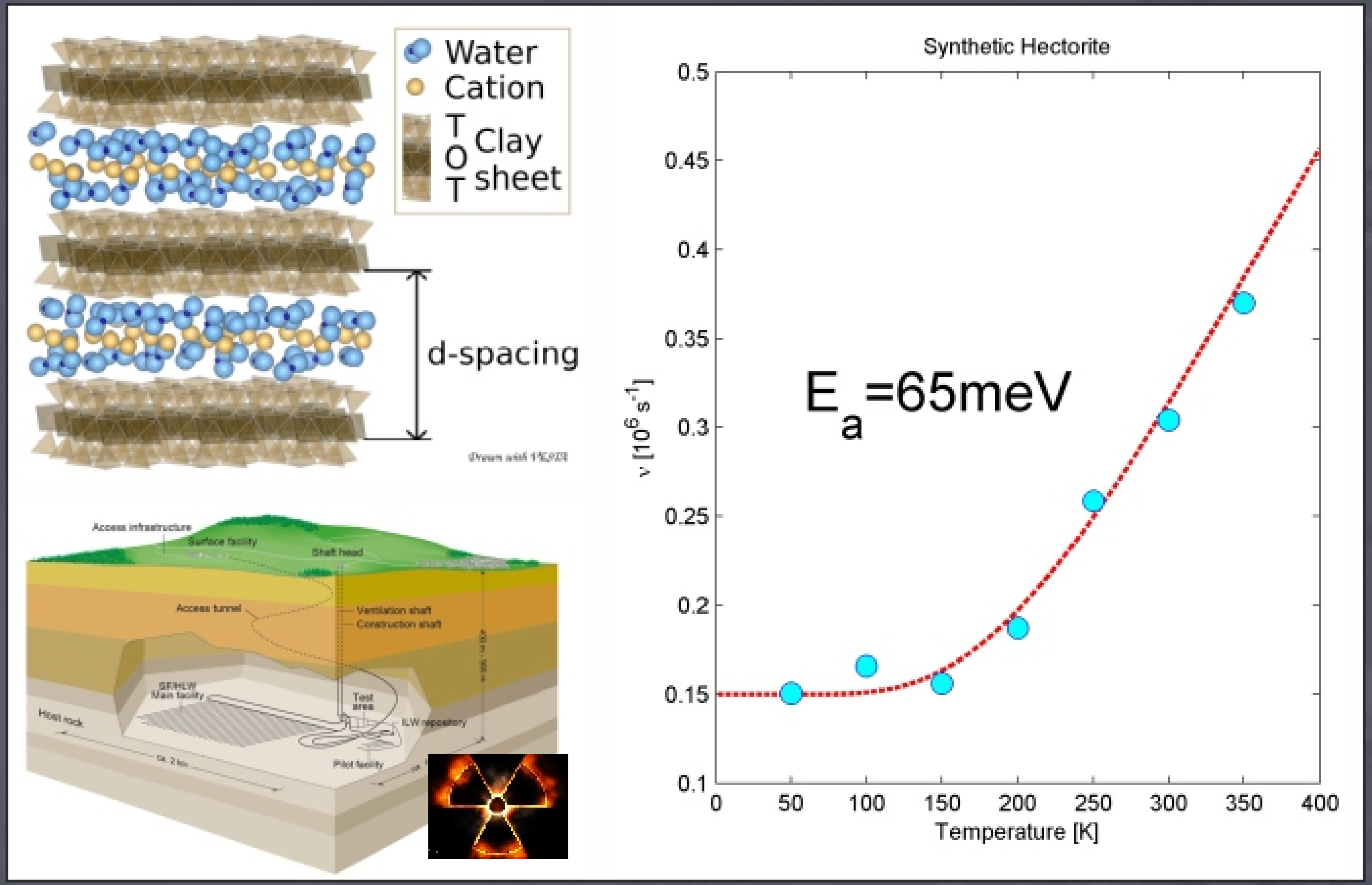

Juranyi, Mansson, *et al.* Manuscript (2019)

Na / Mg Batteries + Oxygen Diffusion

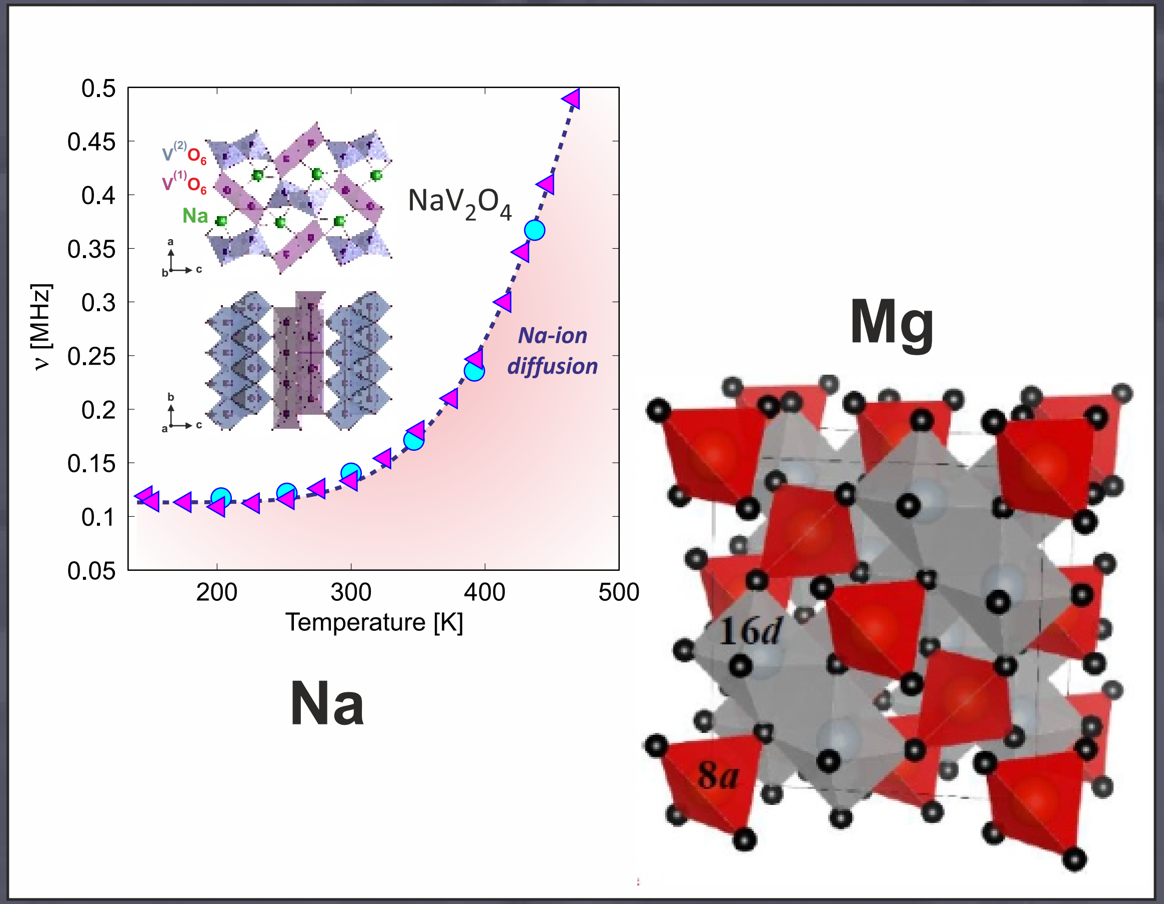

Mansson, *et al.* Unpublished (2019)

H-Storage *in operando* Studies

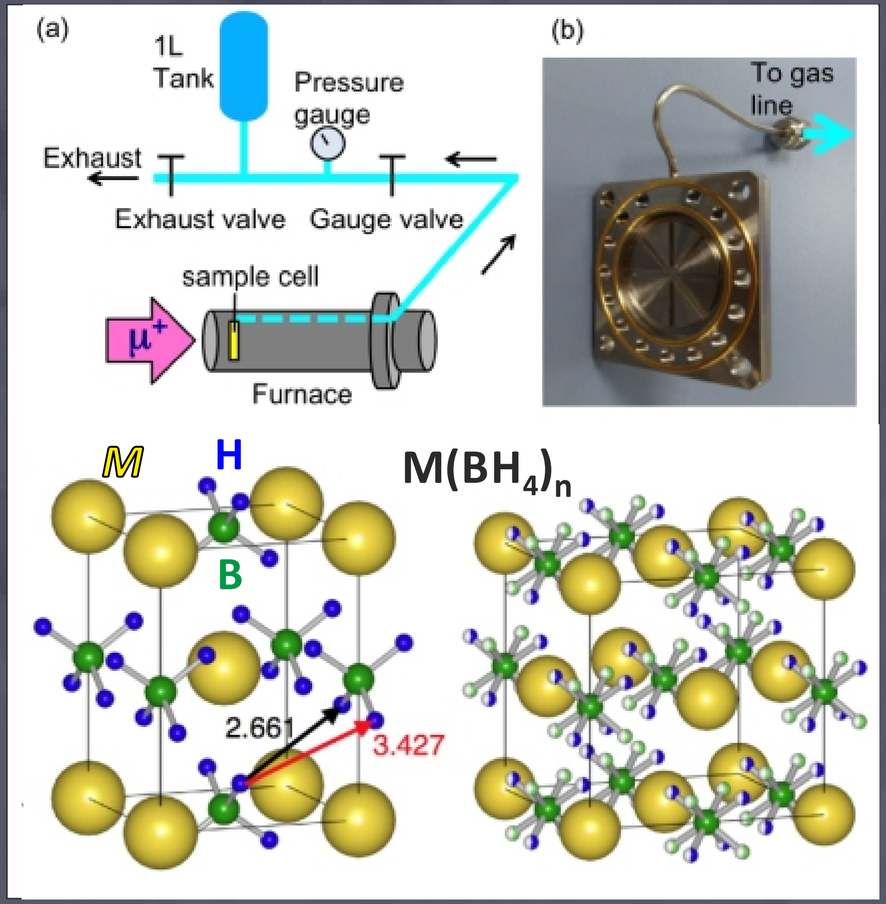

Sugiyama, Mansson, *et al.*
Sustainable Energy Fuels (2019)

Muon Technique Applied to Broad Range of Systems

Journal of Electron Spectroscopy and Related Phenomena 224, 79 (2018)
Physical Review B 97, 024416 (2018)
Inorganic Chemistry (2019) - Accepted for Publication
JPS Conf. Proc. 25, 011009 (2019)
Sustainable Energy & Fuels [RSC] 3, 956 (2019)
Sustainable Energy & Fuels [RSC] 3, 508-513 (2019)
Physica B: Condensed Matter 551 137 (2018)

2017 Sustainable Industrial Processing Summit and Exhibition SIPS 2017 - Volume 8: Surfaces & Interfaces, Composite, Ceramic and Nanomaterials
ISBN: 978-1-987820-75-1

J. Phys. Soc. Japan [JPS Conf. Proc.] 21, 011004 (2018)
J. Phys. Soc. Japan [JPS Conf. Proc.] 21, 011012 (2018)
J. Phys. Soc. Japan [JPS Conf. Proc.] 21, 011012 (2018)
J. Phys. Soc. Japan [JPS Conf. Proc.] 21, 011009 (2018)
J. Phys. Soc. Japan [JPS Conf. Proc.] 21, 011015 (2018)
J. Phys. Soc. Japan [JPS Conf. Proc.] 21, 011018 (2018)
J. Phys. Soc. Japan [JPS Conf. Proc.] 21, 011011 (2018)
J. Phys. Soc. Japan [JPS Conf. Proc.] 21, 011025 (2018)
J. Phys. Soc. Japan [JPS Conf. Proc.] 21, 011005 (2018)
J. Phys. Soc. Japan [JPS Conf. Proc.] 21, 011006 (2018)
J. Phys. Soc. Japan [JPS Conf. Proc.] 21, 011019 (2018)
J. Phys. Soc. Japan [JPS Conf. Proc.] 21, 011010 (2018)
J. Phys. Soc. Japan [JPS Conf. Proc.] 21, 011016 (2018)

Nature Communications (2017)- arXiv:1404.7398
Physical Review B 92, 014417 (2015)
RSC Advances 5, 18531 (2015)
EPJ Web of Conf. 83, 02008 (2015)
Physical Review B 91, 144423 (2015)
Phys. Proc. 75, 868 (2015)
Phys. Proc. 75, 426 (2015)
JPS Conf. Proc. 2, 010303 (2014)
Physical Review B 86, 020402(R) (2014)
Journal of Physics: Conf. Ser. 551 012028 (2014)
Journal of Physics: Conf. Ser. 551 012011 (2014)
Journal of Physics: Conf. Ser. 551 012010 (2014)
Journal of Physics: Conf. Ser. 551 012037 (2014)
Journal of Physics: Conf. Ser. 551 012035 (2014)
Solid State Ionics 262, 901 (2014)
Physical Review Letters 110, 266401 (2013)
Invited Review-article: Phys. Scr. 88 068509 (2013)
RSC Advances 3, 11634 (2013)
Physical Review B 87, 024409 (2013)
Journal of Applied Physics 113, 053904 (2013)
Physical Review B 88, 184417 (2013)
Journal of Physics: Condensed Matter, 25, 286005 (2013)
Physical Review B 85, 214407 (2012)
Physical Review B 85, 054111 (2012)
Phys. Proc. 30, 146 (2012)
Phys. Proc. 30, 142 (2012)
Phys. Proc. 30, 202 (2012)
Phys. Proc. 30, 262 (2012)
Phys. Proc. 30, 105 (2012)
Phys. Proc. 30, 190 (2012)

Phys. Proc. 30, 160 (2012)
Phys. Proc. 30, 117 (2012)
Phys. Proc. 30, 186 (2012)
Phys. Proc. 30, 266 (2012)
Physical Review B 84, 184421 (2011)
Physical Review B 84, 054430 (2011)
Physical Review B 84, 054428 (2011)
Physical Review B 82, 094410 (2010)
Solid State Communications, 150, 307 (2010)
The Journal of Physical Chemistry C, 114, 11320-11327 (2010)
Physical Review B, 82, 214505 (2010)
Physical Review B 82, 224412 (2010)
Physical Review B 81, 184405 (2010)
Physical Review B, 81, 100410(R) (2010)
Physical Review B, 81, 092103 (2010)
Physical Review B, 81, 024404 (2010)
Physica C, 470, S755-S757 (2010)
Journal of Physics: Conference Series 225, 012016 (2010)
Journal of Physics: Conference Series 225, 012017 (2010)
Journal of Physics: Conference Series 225, 012051 (2010)
Journal of Physics: Conference Series 225, 012052 (2010)
Physical Review Letters, 103, 147601 (2009)
Physical Review B, 79, 184411 (2009)
Journal of the Physical Society of Japan, 78, 084715 (2009)
Physica B: Condensed Matter, 404, 607 (2009)

Summary

- Neutron scattering is a very versatile & poweful experimental technique for studying solid state physics, materials science, etc.
- Tell us where atoms are and how spins align (elastic NS)
  Tell us how atoms and spins move / excitations (inelastic NS)
- Muons & Neutrons are covering complementary ranges of time/energy (dynamics) as well as length-scales
- Neutron & Muon sources are co-located making parallel measurements easy
- Muons are in most cases a faster but a 'limited' technique
  BUT: what muons can do, they do REALLY well !!!

Two combined techniques are always better than one :-)
If you need some assistance with μ^+SR, please let me know!

Time for a Coffee Break !!!